AN ABSTRACT OF THE THESIS OF

Michael Kenneth Gaughan (Name) for the Master of Science (Degree)

in Oceanography (Major) presented on 8 June 1973 (Date)

Title: BREAKING WAVES: A REVIEW OF THEORY AND MEASUREMENTS

Abstract approved: Redacted for Privacy

Theoretical breaking criteria for progressive surface gravity waves are examined, and laboratory and field experiments concerned with breaking waves are reviewed with respect to the testing of these breaking criteria. The measurements of Komar and Simmons are presented here for the first time. Only three theoretical breaking criteria have been proposed for maximum steady waves in water of constant depth: (1) the kinematic breaking criterion, in which the horizontal partical velocity at the crest just equals the wave phase velocity, (2) the reversal of the vertical particle velocity near the crest as the ratio of wave height to water depth, H/h, increases, and (3) the reversal of the vertical pressure gradient beneath the crest as H/h increases. Although most theoreticians have applied the kinematic breaking criterion in conjunction with relatively simple wave theories (based on the motion being inviscid, irrotational,

incompressible, surface tension free, and two dimensional), they do not always obtain identical results; for example, theoretical estimates of the particle acceleration at the crest range from zero to g, the gravitational acceleration. For shoaling waves, the kinematic breaking criterion and the presence of a vertical surface are suggested as breaking criteria. Unfortunately, these criteria were applied to the long wave theory which is considered inadequate near the breaking position.

The re-examination of experiments on breaking waves shows that past measurements are not sufficient for testing any of these breaking criteria. In particular, the following improvements should be made: (1) standardize definitions of wave and breaking parameters, (2) apply or design, if necessary, more accurate techniques to measure water particle velocities and accelerations, and (3) monitor the fluid motions from which the breakers cannot be separated (e. g. backwash, solitons, reflected waves, edge waves and rip currents). Studies specifically designed to obtain the necessary measurements for testing the theoretical breaking criteria are needed.

Breaking Waves: A Review of Theory and Measurements

by

Michael Kenneth Gaughan

A THESIS

submitted to

Oregon State University

in partial fulfillment of
the requirements for the
degree of

Master of Science

Completed June 1973

Commencement June 1974

APPROVED:

Redacted for Privacy

Assistant Professor of Oceanography
in charge of major

Redacted for Privacy

Dean of School of Oceanography

Redacted for Privacy

Dean of Graduate School

Date thesis is presented 8 June 1973

Typed by Marjorie Hay for Michael Kenneth Gaughan

ACKNOWLEDGEMENTS

I would especially like to thank Paul Komar for serving as major professor and John Nath, both of whom were patient enough to critically "wade through" the many rewrites of this thesis. Hopefully, it is a readable manuscript. I would also like to thank Margie Hay, who spent some late hours typing my thesis instead of preparing for her vacation trip. The excellent care which my beloved wife, Pam, gave our baby goose also deserves mention.

This research was supported by the Oceanography Section, National Science Foundation, NSF Grant GA-36817.

TABLE OF CONTENTS

Table of Contents, continued

LIST OF TABLES

List of Tables, continued:

LIST OF FIGURES

List of Figures, continued:

LIST OF SYMBOLS

Symbols from the Roman alphabet:

a_r	r-component of water particle acceleration
a_θ	θ-component of water particle acceleration
$A_{(n)}$	Coefficient of stream function
b_1, b_2, b_3	coefficients of complex velocity
B	coefficient of velocity potential
c	wave celerity or phase velocity
c_i	wave celerity at time equal to zero
c_{max}	maximum deep water wave celerity
c_b	wave celerity at the breaking point
c_∞	small amplitude celerity in deep water
D(t)	integration constant with respect to x
e	coefficient of complex velocity
$F_{(t)}$	Bernoulli constant of spacial integration
g	acceleration due to gravity
h	water depth below still water level
h_b	water depth at breaking point
h_i	water depth at intermediate depths
h_∞	water depth in deep water
H	wave height
H_i	wave height in intermediate depth

List of Symbols, continued:

H_∞	wave height in deep water from small amplitude theory
H_b	wave height at breaking point
i	squareroot of minus one
l	coefficient of complex velocity
l_o	horizontal distance from the position of the wave front at t = 0 to the intersection of the still water level with the beach slope
L	wave length
L_∞	wave length in deep water from small amplitude theory
L_s	basin dimension of width or length
m	uniform beach slope
n	summation index
p	fluid pressure
q	two-dimensional complex velocity, -u+iw
q'	radial polar coordinate, Figure 3-1
r	radial polar coordinate, Figure 3-2
s	initial slope of water surface at wave front
s_b	distance wave travels from the time it enters shallow water (h/L_∞ 0.05) until it breaks
t	time
T	wave period
T_s	seiching period of basin
u	x-component of water particle velocity

List of Symbols, continued:

u_i	initial (t = 0) water particle velocity in x-direction
u_r	r-component of water particle velocity
u_θ	θ-component of water particle velocity
$\bar{u}$	water particle velocity vector
v	y-component of water particle velocity
w	z-component of water particle velocity
x	horizontal coordinate in direction of wave advance
x_b	horizontal distance to breaking as measured from the initial position of the wave front
y	horizontal coordinate orthogonal to x direction
Y_b	vertical distance from crest to bottom at the breaking point
z	vertical coordinate, positive up
z_1	vertical distance from crest to still water level at breaking point
z_2	vertical distance from still water level to trough at breaking point

Symbols from the Greek alphabet:

β	dimensionless coefficient from zero to one
Γ	complex velocity potential, $\phi + i\,\Psi$
ε	value of stream function at free surface
η	vertical position of free surface

List of Symbols, continued:

θ	angular polar coordinate, Figure 3-2
ϑ	angular polar coordinate, Figure 3-1
θ_b	one-half of the minimum enclosed crest angle
$\lambda(\Gamma)$	functional factor in complex velocity
μ	dimensionless coefficient from zero to one
ν	two dimensional complex position, $x + iz$
π	pi = 3.14159
ρ	density of water
Σ	summation sign
τ	polar variable, Chapter IV
ϕ	velocity potential
Ψ	stream function

Mathematical Symbols:

$\frac{D}{Dt}$	total derivative, $\frac{\partial}{\partial t} + u\frac{\partial}{\partial x} + v\frac{\partial}{\partial y} + w\frac{\partial}{\partial z}$
$\overline{\nabla f}$	gradient of scalar, f, $\left[\frac{\partial}{\partial x}\hat{x} + \frac{\partial}{\partial y}\hat{y} + \frac{\partial}{\partial z}\hat{z}\right] f$
$\nabla \cdot \bar{u}$	divergence of $\bar{u}$ $\frac{\partial u}{\partial x} + \frac{\partial v}{\partial y} + \frac{\partial w}{\partial z}$
$\nabla x \bar{u}$	curl of $\bar{u}$
$\frac{\partial}{\partial x}$	partial derivative with respect to x
$\nabla^2 f$	divergence of the gradient of f

List of Symbols, continued:

Im	imaginary part of a complex number
Re	real part of complex number
$\|u\|$	absolute value of u
∞	infinity
$\hat{x}$	unit vector in x-direction
$\hat{y}$	unit vector in y-direction
$\hat{z}$	unit vector in z-direction

BREAKING WAVES: A REVIEW OF THEORY AND MEASUREMENTS

CHAPTER I

INTRODUCTION

During storms the phenomenon of wave breaking at the shore is a spectacular event; large storm waves build to larger heights as they approach shore until they crash over, producing a tremendous roar, shaking the ground, and throwing up a great wall of white water which rushes up the beach. Although the more usual, calmer wave conditions which exist along the coast are not nearly so dramatic, these smaller waves also steepen and finally break as they near the shore.

The importance of wave breaking along the coast is also apparent during rough weather. The rapid erosion of valuable shoreline and the destruction of structures along the beach are caused by the large storm waves. Extreme changes may take place in only a few hours time. Less obvious but just as important are the long term changes in the coastline brought about by the calmer wave conditions. In both cases, the breaking waves transfer their energy and momentum to the nearshore zone. Currents are thus generated which may cause sediment transport both in the on-off shore and along shore directions.

Breaking waves along the coast are also of recreational

interest. Surfers are attacked by breakers which will give them an exciting ride; these waves are steep and hollow, allowing the rider just enough time to escape a folding section before it plunges over.

Breaking waves are not limited to the nearshore zone. Primarily during storms, waves may also break far at sea. During these occurrences, breaking is important because it limits the growth of wind generated waves. Not only does breaking occur when the wind bodily carries off the crests of waves, but natural breaking also is present when steep local surface slopes cause water particles to become unstable and break free of the surface. These steep local slopes are due either to the rapid growth of individual waves or to the addition of the many and varied passing waves.

The purpose of this study is to evaluate the present state of knowledge of breaking criteria for progressive surface gravity waves. First, theoretical breaking criteria for waves in deep and in shallow water will be reviewed. Next, both laboratory and ocean observations of shallow water breakers will be reviewed; the laboratory data of breaking waves obtained by P. D. Komar and V. P. Simmons at the Scripps Institute of Oceanography wave facility will be presented here for the first time.

CHAPTER II

SURFACE WATER WAVE THEORIES

In the chapters devoted to theoretical breaking criteria it is necessary to refer to the equations of motion for each of the wave theories being investigated. These equations of motion and other pertinant information are summarized in Table 2-1. All of these wave theories are derived from Euler's equations of motion for incompressible, inviscid, irrotational flow given by

$$(2\text{-}1) \qquad \frac{D\bar{v}}{Dt} = -\frac{1}{\rho}\nabla p - \bar{g}$$

$$(2\text{-}2) \qquad \nabla \cdot \bar{v} = 0$$

$$(2\text{-}3) \qquad \nabla \times \bar{v} = 0$$

where $\bar{v}$ indicates a vector quantity. The variables are defined in the List of Symbols. The appropriate boundary conditions at the free surface defined by $z = \eta(x, y, t)$, Figure 2-1, are

$$(2\text{-}4) \qquad p(x, y, \eta, t) = \text{constant}$$

where

$$(2\text{-}5) \qquad \frac{D}{Dt}\left(\eta_{(x,y,t)} - z\right) = 0$$

or

$$(2\text{-}6) \qquad \frac{\partial \eta}{\partial t} + u\frac{\partial \eta}{\partial x} + v\frac{\partial \eta}{\partial y} - w(x, y, \eta, t) = 0$$

and, the Bernoulli equation on the free surface:

Table 2-1. Nonlinear water wave theories (after LeMehaute, 1961)

Theory:	Stokes	Cnoidal-Solitary	Long	Numerical Stream Function (Dean, 1968)	Biesel (1952)
Relative Wave Height:	$\frac{H}{h} \ll 1$	$\frac{H}{h} < 1$	$\frac{H}{h} \leq 1$	$\frac{H}{h} \leq 1$	$\frac{H}{h} \sim 1$
Ursell Parameter:	$\frac{H}{L}\left(\frac{L}{h}\right)^3 < 10$	$\frac{H}{L}\left(\frac{L}{h}\right)^3 = 1$	$\frac{H}{L}\left(\frac{L}{h}\right)^3 \gg 1$	No limit	$\frac{H}{L}\left(\frac{L}{h}\right)^3 < 10$
Relative Depth:	$\frac{h}{L} > \frac{1}{2}$, deep	$\frac{h}{L} < \frac{1}{10}$	$\frac{h}{L} \ll \frac{1}{20}$	No limit	No limit
	$\frac{1}{20} < \frac{h}{L} < \frac{1}{2}$, finite	shallow	very shallow		
Pressure Distribution:	non-hydrostatic	non-hydrostatic	hydrostatic	non-hydrostatic	non-hydrostatic
Rotationality:	irrotational	irrotational	irrotational	irrotational	irrotational
Friction:	perfect fluid	perfect fluid	perfect fluid	perfect fluid	perfect fluid
Wave Type:	oscillatory	oscillatory, translational	translatory	oscillatory	oscillatory
Mass Transport:	yes, small	yes, small	yes	yes	no

Table 2-1. Nonlinear water wave equations.

1. Stokes

$$\nabla^2\phi = \frac{\partial^2\phi}{\partial x^2} + \frac{\partial^2\phi}{\partial z^2} = 0$$

$$\frac{\partial\phi}{\partial t} + \frac{1}{2}(u^2+w^2) + g\eta = f(t) \qquad w = \frac{\partial\eta}{\partial t} + u\frac{\partial\eta}{\partial x}\Big|_{z=\eta}$$

2. Cnoidal - Solitary ($L \to \infty$)

$$\frac{\partial u}{\partial x} + \frac{\partial w}{\partial z} = 0 \qquad \frac{\partial \bar{v}}{\partial t} + \nabla\left(\frac{\bar{v}^2}{2}\right) = -\nabla p/\rho$$

$$\frac{\partial u}{\partial z} - \frac{\partial w}{\partial x} = 0 \qquad w = \frac{\partial\eta}{\partial t} + u\frac{\partial\eta}{\partial x}\Big|_{z=\eta}$$

3. Long

$$\frac{\partial\eta}{\partial t} + \frac{\partial}{\partial x}(u(h+\eta)) = 0 \qquad \frac{\partial u}{\partial t} + u\frac{\partial u}{\partial x} + g\frac{\partial\eta}{\partial t} = 0$$

4. Numerical Stream Function (Dean, 1968)

$$\nabla^2\psi = 0 \qquad \eta + \frac{1}{2g}((u-c)^2 + w^2) = Q \text{ for } z = \eta$$

$w = o$ for $z = -h$

$$\frac{\partial\eta}{\partial x} = \frac{w}{u-c} \text{ for } z = \eta \qquad \psi = \frac{L}{T}z + \sum_{n=1}^{N} A(n)\sinh\left(\frac{2\pi n}{L}(h+z)\right)\cos\left(\frac{2\pi n}{L}x\right)$$

5. Biesel (1952)

$$\nabla^2\phi = 0$$

$w - mh = 0$ for $z = -h$

$$\frac{1}{g}\frac{\partial^2\phi}{\partial t^2} + \frac{\partial\phi}{\partial z} = 0 \text{ for } z = 0$$

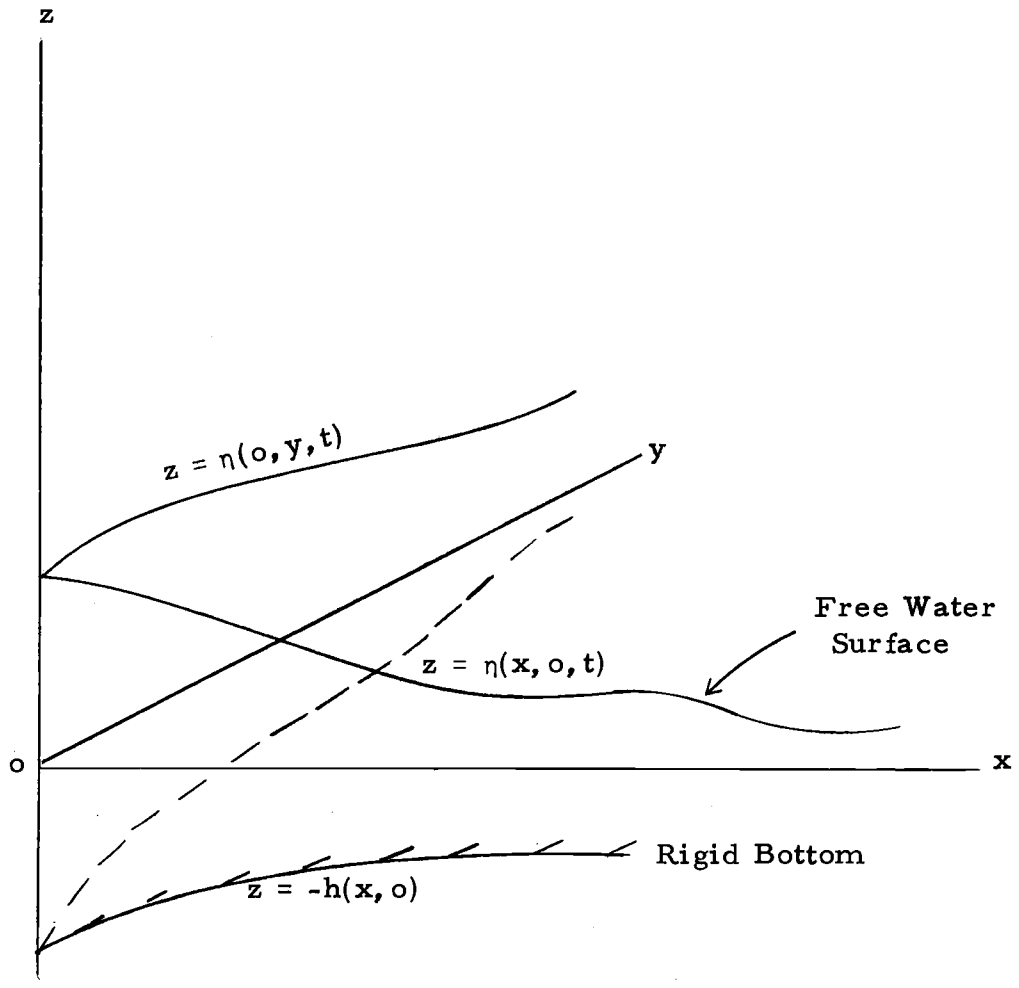

Figure 2-1. Coordinate System

$$(2\text{-}7) \qquad \frac{\partial \phi}{\partial t} + \tfrac{1}{2}(u^2 + v^2 + w^2) + \frac{1}{\rho} p + g \eta = 0.$$

The boundary condition at the fixed bottom defined by $z = -h(x, y)$ requires that there be no flow through the bottom

$$(2\text{-}8) \qquad u\frac{\partial h}{\partial x} + v\frac{\partial h}{\partial y} - w(x, y, -h, t) = 0$$

For inviscid, incompressible flow, the wave equations are often reformulated in terms of the complex velocity potential (which is the complex formulation of the velocity potential, ϕ, and the stream function, Ψ) in order to simplify their solution (Chappelear, 1959; Stokes, 1880; Davies, 1952; Michell, 1893; Packham, 1952; Lenau, 1966; and McCowan, 1894). The velocity potential ϕ is defined as

$$(2\text{-}9) \qquad u = -\frac{\partial \phi}{\partial x}, \quad v = -\frac{\partial \phi}{\partial y}, \quad w = -\frac{\partial \phi}{\partial z}$$

so that equation (2-2) becomes LaPlace's equation

$$(2\text{-}10) \qquad \nabla^2 \phi = 0.$$

Integration of the Euler equation, equation (2-1), along the component directions results in the Bernoulli equation for constant density

$$(2\text{-}11) \qquad \frac{\partial \phi}{\partial t} + \tfrac{1}{2}(u^2 + v^2 + w^2) + \frac{1}{\rho} p + g z = F(t).$$

Since the fluid motion is affected only by pressure gradients, and the gradients are not affected by F(t), then F(t) can be incorporated into the definition of the velocity potential. Equation (2-11) then becomes

$$(2\text{-}12) \quad \frac{\partial \phi}{\partial t} + \tfrac{1}{2}(u^2 + v^2 + w^2) + \frac{1}{\rho} p + g z = 0.$$

The stream function Ψ, for the case of two dimensional motion, can be defined as

$$(2\text{-}13) \quad u = -\frac{\partial \Psi}{\partial z}, \quad w = \frac{\partial \Psi}{\partial x}$$

so that equation (2-3) becomes LaPlace's equation

$$(2\text{-}14) \quad \nabla^2 \Psi = 0.$$

The flow can now be represented by the complex velocity potential Γ as a function of the complex position ν as

$$(2\text{-}15) \quad \Gamma(\nu) = \phi + i \Psi$$

where

$$(2\text{-}16) \quad \nu = x + i z$$

This also results in a complex velocity q given by

$$(2\text{-}17) \quad q = +u - i w$$

If a coordinate system moving with the wave propagation velocity is used, the motion may become steady, and the free surface is then a streamline. Identifying the free surface with $\Psi(x, \eta) = \varepsilon$ and the bottom with $\Psi(x, -h) = 0$, the boundary condition for a horizontal bottom is

$$(2\text{-}18) \quad \text{Im } q(x, -h) = 0$$

where Im is the imaginary part, $w(x, z, t)$, of the complex velocity. In terms of the complex velocity the Bernoulli equation, (2-7), on

the free surface becomes

$$(2\text{-}19) \quad \tfrac{1}{2}|q|^2 + g\,\mathrm{Im}\,\nu = \text{constant.}$$

CHAPTER III

THEORETICAL DEEP WATER WAVE BREAKING CRITERIA

In order to review theoretical breaking criteria for deep water waves, an examination of the properties of the 'highest' steady waves is essential because these properties are upper limits to wave growth. Theoretical attempts to predict the properties of the 'highest' wave are all based on the kinematic breaking criterion, which is a limiting value of the water particle velocity at the crest (Stokes, 1880; Michell, 1893; Havelock, 1918; Davies, 1952; Yamada, 1957; Chappelear, 1959; Dean, 1968). These properties include the wave steepness, the enclosed crest angle, and the water particle acceleration at the crest. A review will be made of the mathematical techniques developed to derive the properties of the 'highest' wave, and comparisons will be made between the various properties derived.

The Kinematic Breaking Criterion

There has been only one limiting value proposed for the water particle velocity at the wave crest, the wave phase velocity. This

criterion was first utilized by Rankine (1864). It is a plausible criterion since if the particle velocity exceeds the phase velocity, the particles at the crest will advance forward faster than the wave and become separated from it.

In determining the properties of a wave so limited, all of the studies reviewed employed a coordinate system which traveled with the wave phase velocity so that the wave motion was steady or independent of time. Viewed from this reference frame, the kinematic criterion requires that the particle velocity at the crest be zero.

Methods do differ in the way in which the kinematic breaking criterion is satisfied. Descriptions of two of these methods applied by Davies (1952) and Chappelear (1959) follow. These two methods were chosen because each is an important contribution to the theory of the 'highest' wave.

Davies (1952) transforms the particle velocity components in cartesian coordinates u, w to polar coordinates q', θ', Figure 3-1, and also introduces a new variable τ defined by

$$(3\text{-}1) \qquad q' e^{i\theta'} = c e^{\tau + i\theta'}$$

where c is the wave phase velocity. Equation 3-1 determines the relationship between q' and τ as

$$(3\text{-}2) \qquad q' e^{i\theta'} = c e^{\tau + i\theta'} = c\, e^{\tau} e^{i\theta'}$$

so that

$$(3\text{-}3) \qquad q' = c e^{\tau}$$

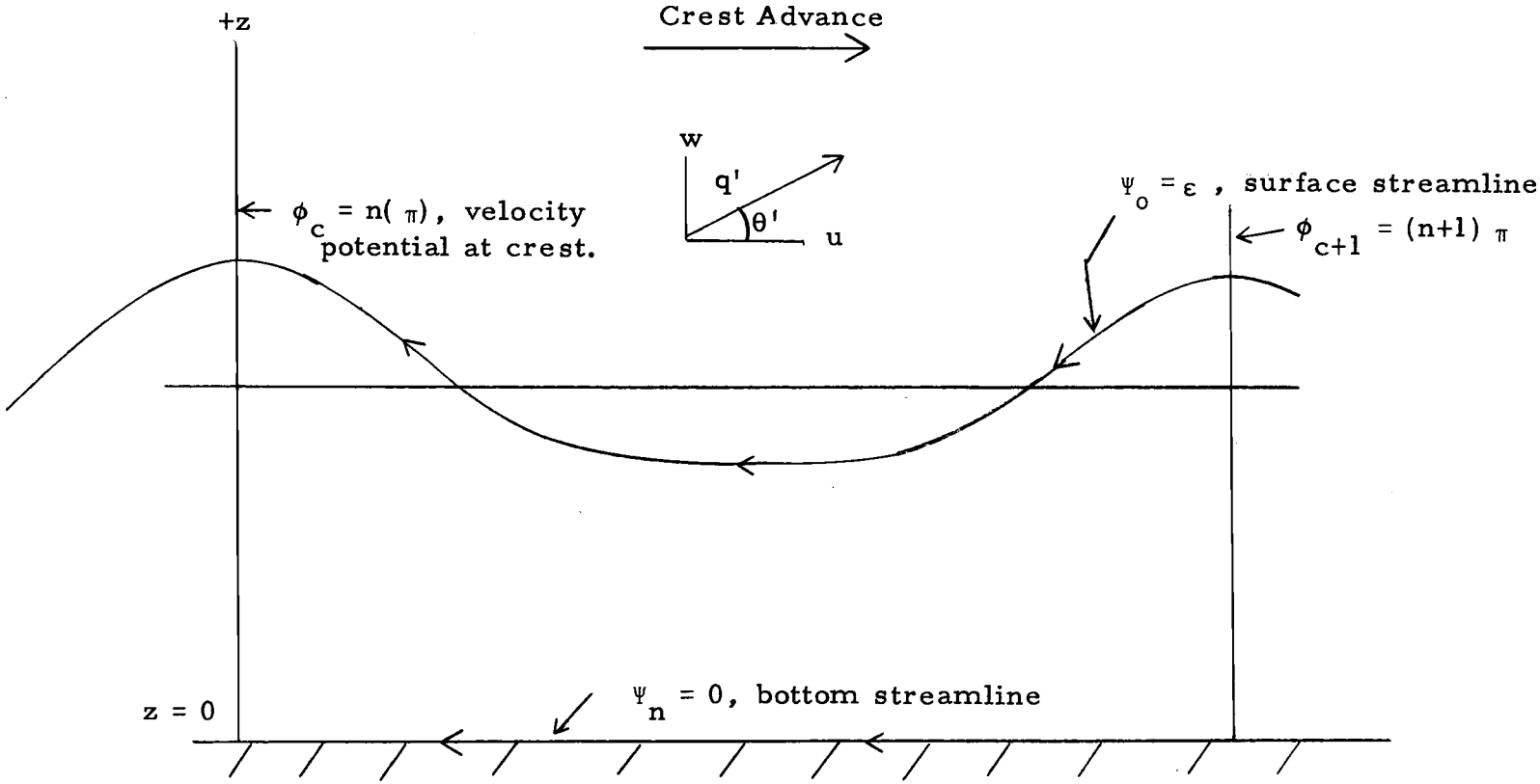

Figure 3-1. Coordinate System.
(Chappelear, 1959 and Davis, 1952).

To summarize, Davies has transformed u, w according to

u, w (Cartesian) $\rightarrow$ q' θ' (polar) $\rightarrow$ c, τ , θ' (polar).

In terms of the new variables τ and θ', the kinematic breaking criterion requires that

(3-4) $\tau \rightarrow -\infty$ at the crest.

This simple change of variables is very important because it enabled Davies to obtain a solution which satisfied a non-linear surface boundary condition exactly. This non-linear boundary condition is used as an approximation to the Bernoulli equation (equation 2-12) on the free surface. It is obtained by differentiating the Bernoulli equation with respect to arc length and substituting τ and θ' for q' and z. The resulting boundary condition is

$$(3\text{-}5) \qquad \frac{\partial \theta'}{\partial \Psi} = \frac{g}{c^3} e^{-3\tau} \operatorname{Sin} \theta', \quad \Psi = \epsilon$$

where $\Psi = \epsilon$ is the surface streamline.

The second important contribution is that of Chappelear (1959). Chappelear, after studying the functional form of the complex velocity given by finite amplitude wave theories, followed a suggestion of Michell (1893) and chose the complex velocity given by (Figure 3-1)

$$(3\text{-}6) \qquad q(\Gamma) = \frac{\lambda^{1/3}(\Gamma)}{2} \left(1 + 2b_1 e^{-2\epsilon} \operatorname{Cos} 2\Gamma + 2b_2 e^{-4\epsilon} \operatorname{Cos} 4\Gamma + 2b_3 e^{-6\epsilon} \operatorname{Cos} 6\Gamma \right)$$

where

$$(3\text{-}7) \qquad \Gamma = \phi + i\,\psi$$

and

$$(3\text{-}8) \qquad \lambda(\Gamma) = 1 + 2 \sum_{n=1}^{\infty} (-1)^n e^{-2n^2\epsilon} \cos(2n\Gamma).$$

The satisfactory characteristic about this form of the complex velocity is that it is zero at the crest positions defined by $\psi = \epsilon$, $\phi = n\pi$, and so satisfies the kinematic breaking criterion.

Chappelear's contribution is that the results are valid for the 'highest' wave in any depth of water.

These two examples illustrate two important theoretical contributions to utilizing the kinematic breaking criterion.

Derived Breaking Criteria

A review of the derived wave properties of the kinematically limited wave is desired because it will make readily available the essential portions of the complex proofs found in the original papers. It is hoped that workers who intend to use certain properties of the limiting wave in their own studies may find this review helpful.

Crest Angle

One of the most widely quoted properties of the limiting wave is that the enclosed crest angle is 120 degrees (Figure 3-2). Stokes (1880) was the first to derive this value, and it has since been

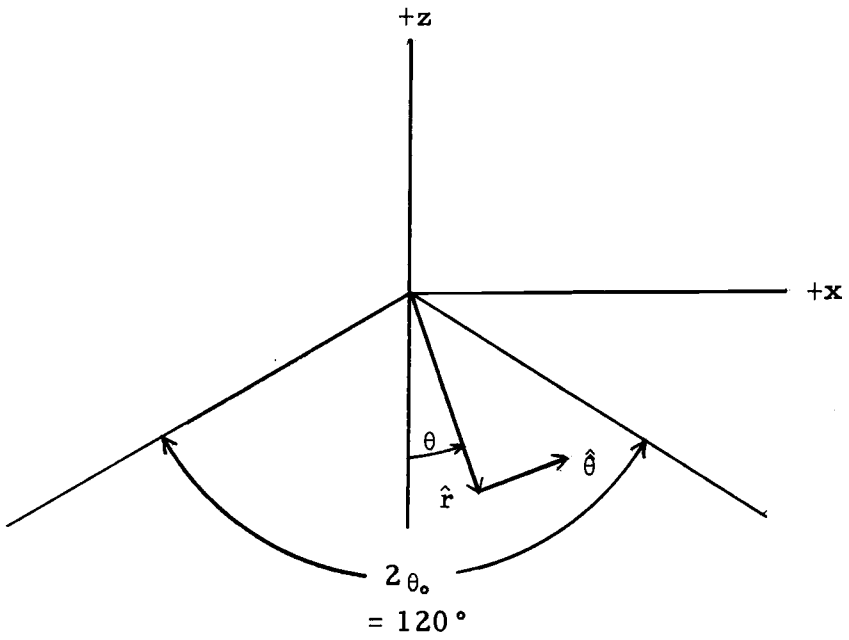

Figure 3-2. Enclosed crest angle for kinematically limited wave.

verified theoretically by Michell (1893), Miche (1944), and Chappelear (1959). Since Stokes omitted much of the detail of this important derivation, it is presented here in full. Kinsman (1965, page 272) gives a similar proof but one that is dependent on assigning the special value of zero to the surface streamline.

There are three initial assumptions germane to this proof: (1) the kinematic breaking criterion is satisfied, (2) the crest is formed by two intersecting straight lines which are the tangents to the real water surface curvature, and (3) the velocity potential in the region of the crest can be approximated by

$$(3\text{-}9) \qquad \phi(r,\theta) = B\, r^{n} \operatorname{Sin}(n\,\theta)$$

where B and n are coefficients to be evaluated, and r and θ are polar coordinates (Figure 3-2). To evaluate n, the fact that the surface is a streamline is used. Since the velocity is tangent to the surface streamline, there is no velocity component normal to the surface. This condition is

$$(3\text{-}10) \qquad u_{\theta} = -\frac{1}{r}\, \partial\phi/\partial\theta = 0$$

or

$$(3\text{-}11) \qquad \frac{\partial\phi}{\partial\theta} = \operatorname{Cos}(n\theta_{o}) = 0.$$

For equation 3-11 to be zero, the argument of the cosine must be $\pi/2$

$$(3\text{-}12) \qquad n\theta_{o} = \pi/2.$$

Assuming the pressure on the free surface is zero, the Bernoulli equation (equation 2-7) near the crest is

$$(3\text{-}13) \quad gz + \tfrac{1}{2}(u_r^2 + u_\theta^2) = 0.$$

Calculating z, u_r, and u_θ according to

$$(3\text{-}14) \quad z = -r\,\mathrm{Cos}(\theta_o) \ ,$$

$$(3\text{-}15) \quad u_r = -\,\partial\phi/\partial r \quad \text{and} \quad u = -\frac{1}{r}\,\frac{\partial\phi}{\partial\theta}$$

and substituting into equation (3-12), yields, on the free surface,

$$(3\text{-}16) \quad -gr\mathrm{Cos}(\theta_o) + \tfrac{1}{2}n^2B^2r^{2(n-1)}\mathrm{Sin}^2(n\,\theta_o) + \tfrac{1}{2}n^2B^2r^{2(n-1)} \mathrm{Cos}^2(n\theta_o) = 0$$

or

$$(3\text{-}17) \quad \tfrac{1}{2}n^2B^2r^{2(n-1)} = gr\mathrm{Cos}(\theta_o)$$

or

$$(3\text{-}18) \quad \tfrac{1}{2}n^2B^2r^{2\,n-3} = g\mathrm{Cos}(\theta_o) = \text{constant.}$$

Since the right-hand-side of equation (3-18) is a constant, the exponent of r must be zero. This gives

$$(3\text{-}19) \quad 2n-3 = 0$$

or

$$(3\text{-}20) \quad n = 3/2.$$

From equation 3-12, the enclosed crest angle $2\,\theta_o$ becomes

$$(3\text{-}21) \quad 2\,\theta_o = 2\,\pi/3$$

or 120 degrees. The coefficient B in equation (3-9) is determined by

substitution of n into equation (3-17) and yields

$$(3\text{-}22) \quad B = 2\, g^{\frac{1}{2}} /3.$$

For these values of n and B, the velocity potential of equation 3-9 becomes

$$(3\text{-}23) \quad \phi(r,\theta) = \frac{2}{3}\, g^{\frac{1}{2}}\, r^{3/2} \operatorname{Sin}(3/2\,\theta).$$

The particle velocity components are

$$(3\text{-}24) \quad u_r = -\frac{\partial \phi}{\partial r} = -\, g^{\frac{1}{2}}\, r^{\frac{1}{2}} \operatorname{Sin}(3/2\theta)$$

and

$$(3\text{-}25) \quad u_\theta = -\frac{1}{r}\,\frac{\partial \phi}{\partial \theta} = -\, g^{\frac{1}{2}}\, r^{\frac{1}{2}} \operatorname{Cos}(3/2\,\theta).$$

Thus the velocity components tend to zero as r approaches zero, satisfying the kinematic breaking criterion. The second assumption, that the crest is formed by two intersecting straight lines, involved the identification of the free surface by the constant polar angle θ_o.

Wave Steepness

Another commonly quoted property of the 'highest' wave is the wave steepness, a wave height to length ratio of 0.142. Usually this is expressed as "the wave height is one-seventh of the wave length." When examining the values obtained theoretically (see Table 3-1) this quote is observed to be very accurate. However, since nearly all of these approaches utilized the kinematic breaking criterion and a

Table 3-1. Derived wave steepness for kinematically limited deep water waves.

Investigator	Maximum Wave Steepness	Breaking Criterion	Sharp Crest	c/c_∞
(1)	(2)	(3)	(4)	(5)
Michell, J. H. (1893)	0.142	u = c	yes	1.10
Havelock, T. H. (1918)	0.1418	u = c	yes	1.10
Davies, T. V. (1951)	0.1443	u = c	yes	1.08
Yamada, H. (1957)	0.1412	u = c	yes	1.09
Chappelear, J. E. (1959)	0.1428	u = c	yes	1.10
Dean, R. G. (1968)	0.1723	u = 0.985c	no	--

sharp crested wave, the similarity of their results is not surprising.

This consistent result indicates that the essential ideas of this 'classical' approach may be acquired by examining just one of the studies shown in Table 3-1. Since Chappelear (1959) was introduced earlier in connection with the application of the kinematic breaking criterion, his approach will also be reviewed here. A second reason for continuing with Chappelear's derivation is that the results are good for all water depths.

To determine the enclosed crest angle, it was seen that a velocity potential valid only in the immediate vicinity of the crest was sufficient. But now, to evaluate the wave steepness, a solution is required over the entire wave length. Beginning with equation (3-6) to represent the complex velocity, Chappelear utilized the Bernoulli equation at the free surface (equation 2-19) to find the unknown b_i coefficients. The terms in equation (3-6) with these coefficients represent the first three terms of the Fourier series expansion of the complex velocity along the bottom where the velocity is real. The expansion variable is the complex velocity potential, $\Gamma = \phi + i\,\Psi$.

First, the Bernoulli equation is transformed to the complex form

$$(3\text{-}26) \quad \frac{\partial}{\partial \phi} \left| q(\phi + i\varepsilon) \right|^4 = 4g\,\mathrm{Im}\, q(\phi + i\varepsilon)$$

by taking the partial derivative of equation (2-19) with respect to the velocity potential ϕ. Since this expression is being evaluated at the free surface, the stream function Ψ is constant. Next, the left- and right-hand sides of equation (3-26) are separately expanded in Fourier series in terms of the velocity potential ϕ, and the coefficients of the respective cosines with identical arguments are set equal and solved for the b_i's. Since these calculations are very lengthy, they are omitted here.

The complex velocity is now completely evaluated, and hence, the wave steepness can be calculated. For deep water, Chappelear obtained a wave steepness to four decimal places as 0.1428.

The only alternative approach to the 'classical' method of evaluating the wave steepness for the highest wave was that carried out by Dean (1968), employing a numerical solution for the stream function. A wave steepness of 0.1723 was obtained, twenty percent higher than the commonly quoted value 0.142. Dean formulates the wave problem (see Table 2-1) in terms of a stream function, Ψ, which must satisfy LaPlace's equation, and is given by

$$(3\text{-}27) \qquad \Psi(x,z) = \frac{L}{T} z + \sum_{n=1}^{N} A(n) \operatorname{Sinh}\left(\frac{2\pi n}{L} [h+z] \right) \operatorname{Cos} \frac{2\pi h}{L} x$$

where the unknown coefficients L and A(n) are evaluated from the boundary conditions. Since this formulation is applicable for all

wave conditions, Dean solved for the coefficients numerically for a constant wave period and water depth as a function of increasing wave height. For a water depth of 1000 feet, a wave period of 10.0 seconds, and a wave height of 105.7 feet, Dean obtained a wave length of 613.8 feet for a wave whose particle velocity at the crest is equal to 98.5% of the wave phase velocity. The wave steepness is then equal to 105.7/613.8 = 0.1723.

In the following section on the water particle acceleration at the crest, the disagreement between the 'classical' approach and the numerical stream function approach arises again. A discussion on the disagreement between the two approaches is included at the end of this chapter.

Water Particle Acceleration

Theoretical estimates of the water particle acceleration near the crest range from zero to g, the gravitational acceleration. Kinsman (1965, page 273) states that for a wave with a crest angle of 120 degrees, the water particle acceleration is g. However, using the water particle velocities (equations 3-24 and 3-25) developed from the velocity potential for the wave with a 120 degree crest angle, it will be shown that the water particle acceleration near the crest is $\frac{1}{2}$g.

The particle acceleration in polar coordinates is given by

$$(3\text{-}28) \quad a_r = \frac{Du_r}{Dt} = \frac{\partial u_r}{\partial t} + u_r \frac{\partial u_r}{\partial r} + \frac{u_\theta}{r} \frac{\partial u_r}{\partial \theta} - \frac{u_\theta^2}{r}$$

and

$$(3\text{-}29) \quad a_\theta = \frac{Du_\theta}{Dt} = \frac{\partial u_\theta}{\partial t} + u_r \frac{\partial u_\theta}{\partial r} + \frac{u_\theta}{r} \frac{\partial u_\theta}{\partial \theta} + \frac{u_r u_\theta}{r}$$

Since the coordinate system is moving with the wave phase velocity, the motion is steady, and the $\frac{\partial u_r}{\partial t}$ and $\frac{\partial u_\theta}{\partial t}$ terms are zero. Using equations (3-24) and (3-25) to calculate the remaining terms of equation (3-29) it is found that $a_\theta = 0$. Substituting for u_r and u_θ, a_r becomes

$$(3\text{-}30) \quad a_r = \tfrac{1}{2} g \, \mathrm{Sin}^2 (\tfrac{3}{2}\theta) + \tfrac{3}{2} g \mathrm{Cos}^2 (\tfrac{3}{2}\theta) - g \, \mathrm{Cos}^2 (\tfrac{3}{2}\theta)$$

or

$$(3\text{-}31) \quad a_r = \tfrac{1}{2} g.$$

Thus, the particle acceleration near the crest is directed radially downward from the crest with a magnitude $\frac{1}{2}g$. This result conforms with that obtained by Longuet-Higgins (1963) who carried out a similar calculation.

The numerical stream function approach (Dean, 1968) is again in disagreement with the classical approach, yielding an estimate of zero for the particle acceleration near the crest. Figure (3-3) shows the particle velocity and acceleration near the crest as a function of increasing wave height determined by the numerical approach. In this example, the wave period is 10.0 seconds, and the water depth

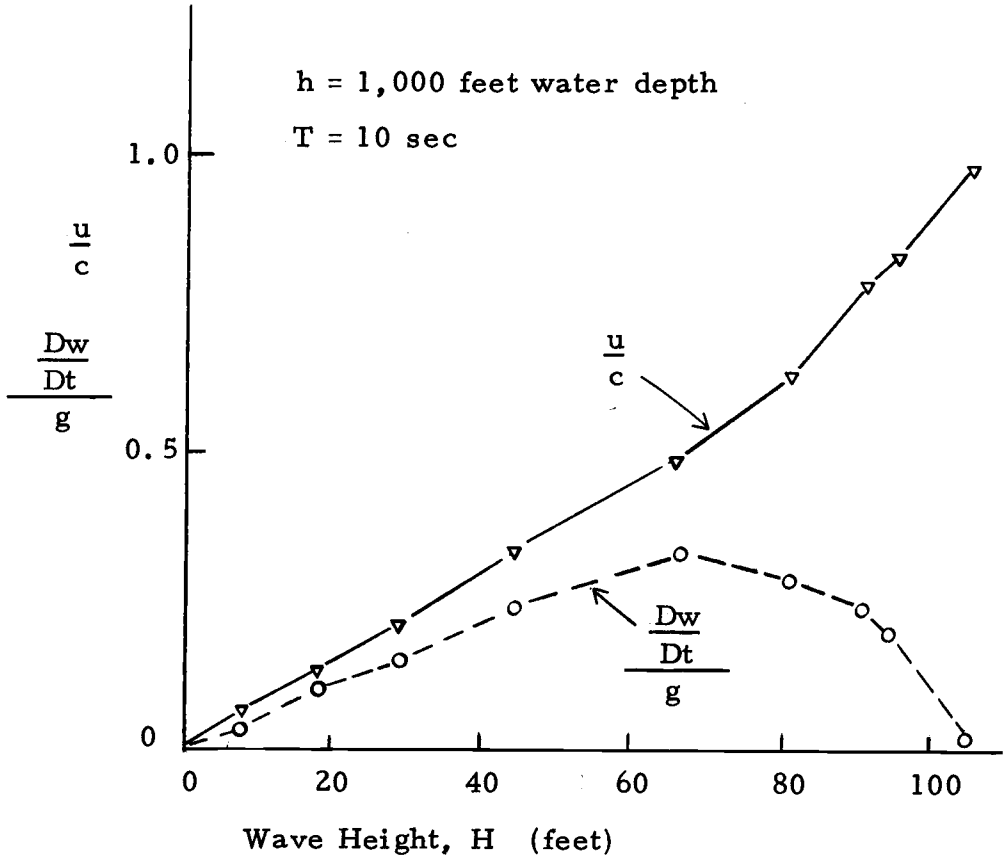

Figure 3-3. Particle velocity and acceleration near the crest as a function of wave height for a deep water wave (Dean, 1968).

is 1000 feet. As the wave height increases, the particle velocity increases in an approximately linear fashion, while the vertical particle acceleration shows a more complex behavior. First, the acceleration increases to a maximum of about $\frac{1}{4}g$ at a wave height of 65 feet and then decreases to zero at a wave height of 105 feet. At the latter point, the horizontal particle velocity is nearly equal to the wave phase velocity, the point at which the wave should break.

Other Properties of the 'Highest' Wave

Some properties of the highest wave which have not found much application are the wave profile, the wave phase velocity, and the kinetic to potential energy ratio. These properties are briefly reviewed.

Figure 3-4 shows the deep water wave profile plotted from tables of numerical values given in Chappelear (1959). This profile is identical to that obtained by Michell (1893) who likewise used the classical approach. Also shown in Figure 3-4 is the wave profile obtained from the numerical stream function example discussed in the previous section. This latter profile is steeper near the crest, indicating that it has a slightly smaller enclosed crest angle. However, due to the scarcity of points in the crest region, it is not possible to determine the enclosed crest angle accurately for either wave profile.

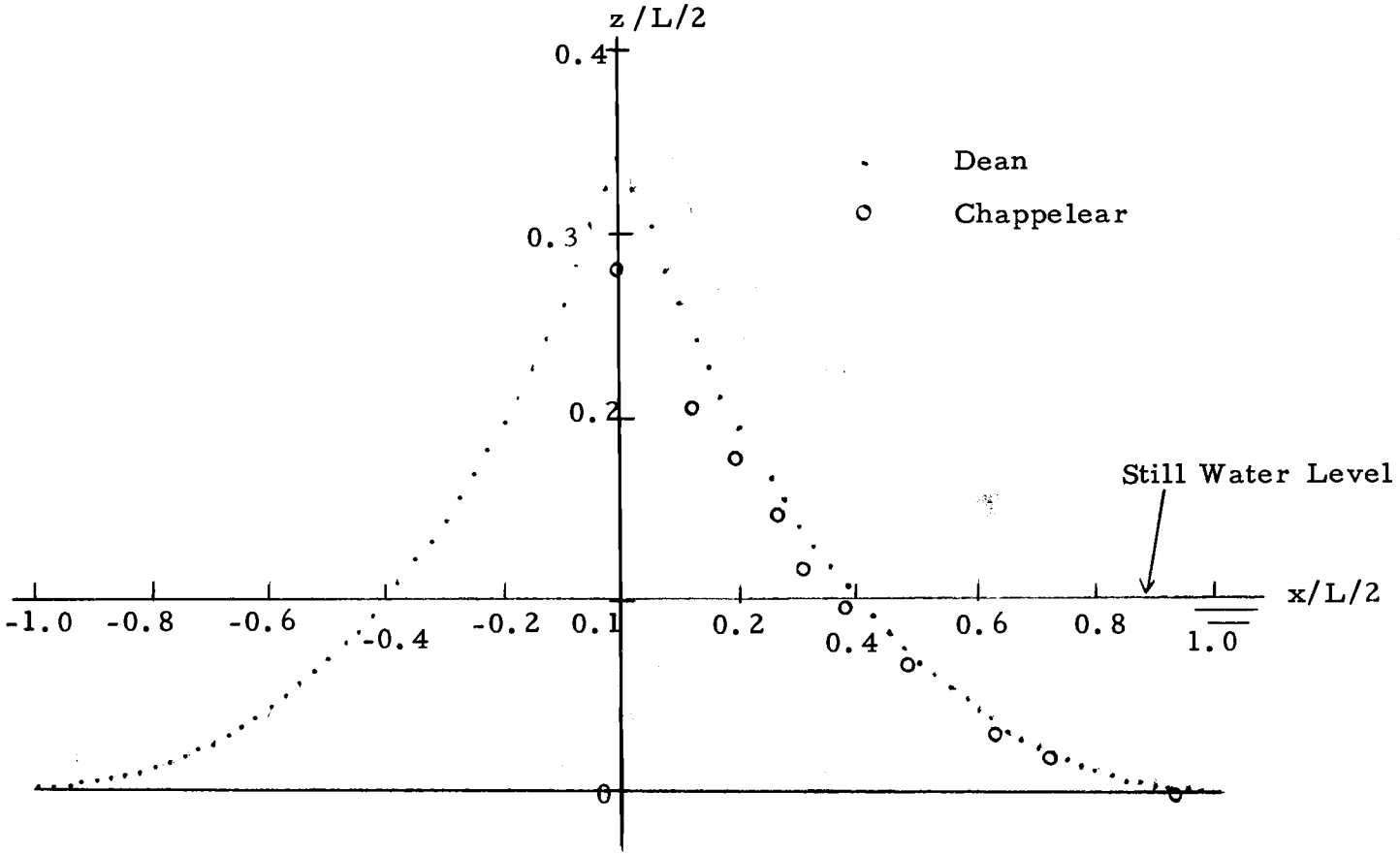

Figure 3-4. Surface profiles of kinematically limited deep water waves. (Chappelear, 1959; Dean, 1968)

Table 3-1 contains several estimates of the ratio of the wave phase velocity for the highest wave to the wave phase velocity for the small amplitude wave. Using the expression for the square of the wave phase velocity for a Stokes finite amplitude wave to third order given by

$$(3\text{-}32) \quad c^2 = c_\infty^2 \left(1 + (\pi H/L)^2 \right)$$

and H/L equal to 0.142, Kinsman (1965) obtained $c/c_\infty = 1.1$, which is in good agreement with the accepted estimates in Table 3-1.

As a sidenote, Michell (1893, page 437) made an error when he stated that the ratio of the maximum wave speed to the small amplitude wave speed was 1.20; he meant the square of this ratio was 1.20.

A final property of the kinematically limited wave is the ratio of the kinetic to potential energy. Davies (1952) obtained a value of 1.1 for this ratio. For comparison, this ratio is 1.0 for the small amplitude deep water wave, indicating that kinetic energy may increase at a greater rate than potential energy as the wave approaches its upper limit.

Discussion and Conclusions

Only one breaking criterion has been proposed for deep water waves; the kinematic breaking criterion in which the horizontal particle velocity just exceeds the wave phase velocity. The

'classical' approach introduced by Rankine (1864) and Stokes (1880) assumed that the highest steady wave had a sharp crest with the horizontal particle velocity at the crest equal to the wave phase velocity. The only alternative approach is that of Dean (1968). Utilizing a numerical stream function, Dean computed the horizontal particle velocity and the vertical particle acceleration at the wave crest as a function of increasing wave height to determine which attained a limiting value first. The results were that the horizontal particle velocity approaches the wave phase velocity, and the vertical particle acceleration approaches zero as the wave height increases. Dean concluded that the kinematic breaking criterion is a more suitable breaking criterion than a limiting value of the vertical particle acceleration at the crest.

Although these two approaches agree that the kinematic breaking criterion is appropriate for deep water waves, the derived wave properties for the highest steady wave are not in agreement. The derived value of the vertical particle acceleration at the crest was $\frac{1}{2}g$ for the classical approach and zero for the numerical stream function approach. The derived wave steepness was 0.14 for the classical approach and 0.17 for the numerical approach. The wave profiles are compared in Figure 3-4.

The largest discrepancy of the two approaches is the different estimates of the vertical particle acceleration at the crest. Dean

(1968) explained this difference by examining the vertical particle acceleration given by

$$(3\text{-}33) \quad \frac{Dw}{Dt} = (u-c)\frac{\partial w}{\partial x} + w\frac{\partial w}{\partial z}$$

At the crest, w is zero, and equation (3-32) becomes

$$(3\text{-}34) \quad \frac{Dw}{Dt} = (u-c)\frac{\partial w}{\partial x}$$

At breaking (u-c) is zero and Dw/Dt must be zero unless $\frac{\partial w}{\partial x}$ is infinite. Dean stated that if the peak were assumed sharp crested then the surface slope would be infinite at the crest and that $\frac{\partial w}{\partial x}$ would also be infinite, accounting for the differing results.

Another explanation of this argument may be given. A particle on the free surface must conform to the boundary condition that it stay on the surface. This condition is given by

$$(3\text{-}35) \quad \frac{\partial \eta}{\partial x} = w/(u-c) , \qquad z = \eta .$$

Solving for w

$$(3\text{-}36) \quad w = (u-c)\frac{\partial \eta}{\partial x}$$

and substituting for w in equation (3-34) yields

$$(3\text{-}37) \quad \frac{Dw}{Dt} = (u-c)\frac{\partial u}{\partial x} \cdot \frac{\partial \eta}{\partial x} + (u-c)^2 \frac{\partial^2 \eta}{\partial x^2}$$

For a sharp crest wave with an enclosed crest angle of 120 degrees, $\frac{\partial^2 \eta}{\partial x^2}$ must be infinite at the crest because $\frac{\partial \eta}{\partial x}$ changes from $+(3)^{-\frac{1}{2}}$ to $-(3)^{-\frac{1}{2}}$. Hence, Dw/Dt may be non-zero at the crest of a

wave with a sharp peak.

Although it remains for observations to determine which approach most closely approximates actual water waves, one comment seems appropriate. Both of these approaches have neglected surface tension forces which may become locally important if the surface curvature is large. With a sharp crest, the curvature is very large, so that it may not be neglected in the neighborhood of the crest. The effect of the large surface tension forces would be to generate capillary waves at the crest, as first shown theoretically by Longuet-Higgins (1963). Thus, the highest steady wave with a sharp crest may not be a physical possibility.

It is also apparent from this review that several aspects of breaking waves in deep water have not been studied; (1) wave breaking by a progressive wave, which overtakes and passes through a second slower wave, (2) wave breaking in a random sea, and (3) the details of the breaking process and the restabilization of the broken wave.

CHAPTER IV

THEORETICAL SHALLOW WATER BREAKING CRITERIA

One of the conclusions of the preceding chapter, which reviewed deep water wave breaking criteria, was that the theoretical breaking criteria were based on the physical properties of the highest steady wave, and that these criteria limited wave growth. For the shallow water wave, where the bottom is important to the breaking process, an additional class of wave breaking occurs. This class consists of waves which deform as they shoal, eventually becoming unstable and toppling forward.

For the case of the highest steady wave, the kinematic breaking criterion, the limiting vertical particle velocity near the crest, and the limiting vertical pressure gradient near the crest are reviewed as factors limiting shallow water wave growth.

For waves which deform as they travel, the local surface slope and the kinematic breaking criterion are reviewed as breaking criteria for the theory of long waves.

The equations of motion for solitary, cnoidal, and Stokes wave theories are given in Table 2-1. These equations are utilized throughout this chapter.

1. Theoretical Breaking Criteria

Kinematic Breaking Criterion

The kinematic breaking criterion has been applied to two types of shallow water waves, (1) the highest steady wave in water of constant depth, and (2) the shoaling wave which deforms as it travels into water of decreasing depth. The mathematical techniques employed to determine the properties of the highest steady wave in water of constant but arbitrary depth do not depend on the depth; Chapter III reviewed many of these techniques. For the case of the shoaling wave, the kinematic breaking criterion applies only at the instant the horizontal particle velocity at the crest is equal to the wave phase velocity.

One unsteady wave theory to which the kinematic breaking criterion has been applied is the long wave theory (Ayyar, 1970). Long waves with positive amplitudes (i.e., all the water surface is above the still water level) which are propagating into quiescent water are considered. To determine the breaking position, the concept of a wave front is introduced. The wave front is defined to be the position at which a discontinuity in the surface slope occurs, with the surface slope zero ahead of the wave front and negative at the wave front (Figure 4-1a). Also, the surface elevation is zero ahead of the wave front and positive behind the front.

Defining η as the vertical elevation of the free surface above the still water level, u as the horizontal particle velocity (constant with respect to depth), and x as the horizontal distance from the origin in the direction of wave advance, Ayyar obtained the surface slope at the wave front as

$$(4\text{-}1) \qquad \frac{\partial \eta}{\partial x} = (1 - t(2\sqrt{l_o/mg})^{-1})(l_o m/g)^{\frac{1}{2}} \frac{\partial u}{\partial x}$$

where l_o is the horizontal distance from the position of the wave front at t = 0 to the intersection of the still water level with the beach slope, m the uniform beach slope, g the acceleration of gravity, and t time. Here it is assumed that at time t = 0 the wave front passes the position x = 0 (Figure 4-1a).

Integrating equation (4-1) with respect to x, the relation

$$(4\text{-}2) \qquad \eta(x,t) = (1 - t(2\sqrt{l_o/mg})^{-1})(l_o m/g)^{\frac{1}{2}} u(x,t) + D(t).$$

is obtained, where D(t) results from the integration. Ayyar (1970) made use of the kinematic breaking criterion to substitute the wave phase velocity c for the horizontal particle velocity u in equation (4-2) yielding

$$(4\text{-}3) \qquad \eta(x,t) = (1 - t(2\sqrt{l_o/mg})^{-1})(l_o m/g)^{\frac{1}{2}} c(x,t) + D(t).$$

This relationship is important because it represents the first application of the kinematic breaking criterion to deforming waves. In addition, Ayyar utilized this relationship and the geometry of a plunging breaker to derive a limiting ratio of 2.0 for the height of the

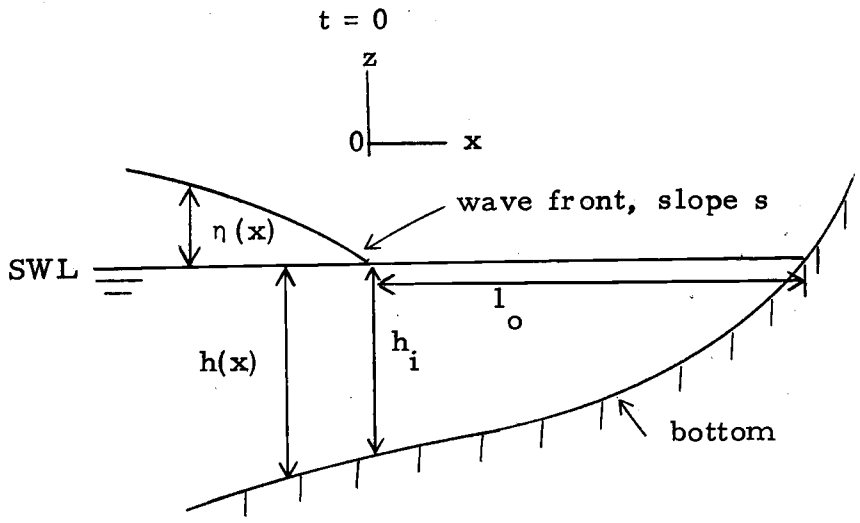

Figure 4-1a. Wave front at initial position.

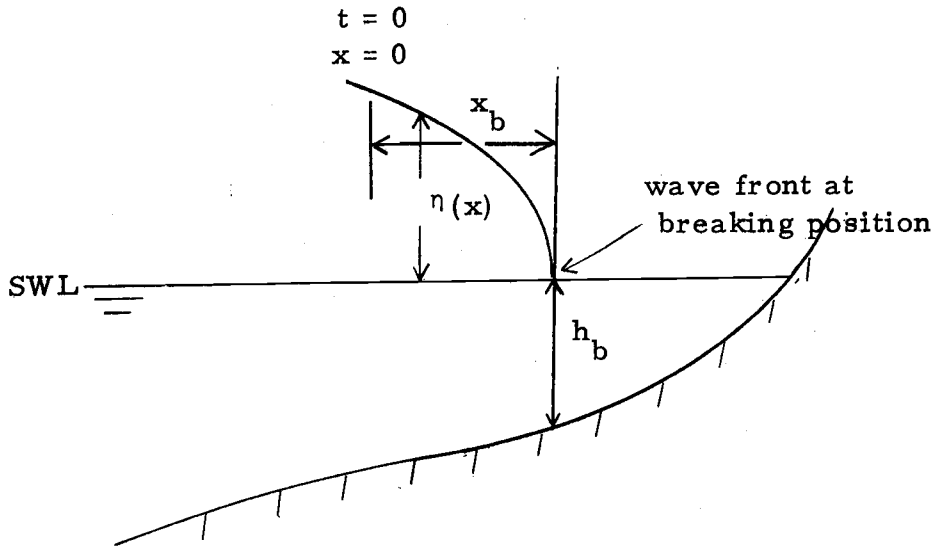

Figure 4-1b. Wave front at breaking position.

breaker crest above the bottom to the depth of breaking below the still water level, Y_b/h_b (Figure 4-2). Unfortunately, he did not present the derivation.

On the other hand, a significant limitation of Ayyar's approach is the use of the long wave theory (Table 2-1). In the long wave theory, the horizontal particle velocity is assumed constant along the vertical, and it may be considered as a vertically averaged velocity. This means that Ayyar has equated a mean horizontal particle velocity to the wave phase velocity as the criterion for breaking. From observations it is known that the horizontal particle velocity is maximum at the surface. Thus, the limiting velocity will occur first at the surface.

Vertical Surface Slope

Another assumed breaking criterion is that where the slope of the water surface approaches a limiting value. Beyond this value, the wave is unstable, and water particles along the steep surface fall forward ahead of the wave. This breaking criterion has been applied to the long wave theory (Table 2-1) in which the shoaling wave is continually steepening on its shoreward face (Stoker, 1949, 1957; Greenspan, 1958; Burger, 1967). The limiting value of the surface slope is assumed to be infinity; that is, the surface is vertical.

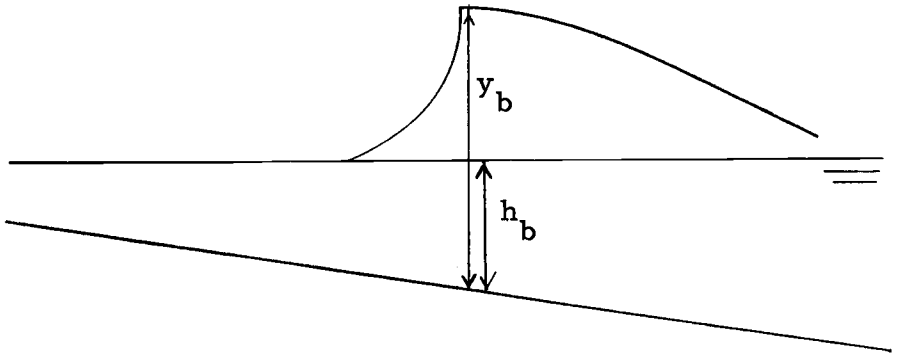

Figure 4-2. Sketch of breaking wave.

Stoker (1957) proved that long waves with positive amplitudes always attain this vertical slope even if the bottom is horizontal. Although he did this by using the method of characteristics to numerically solve for the surface elevation as a function of time and horizontal position, the important physical concept of why the surface slope becomes vertical is easily demonstrated. This is accomplished by examining the expression of the local speed of propagation of small disturbances relative to the moving stream given by Stoker (1957) as

$$c(x,t) = \left(g(h + \eta) \right)^{\frac{1}{2}} \qquad (4\text{-}4)$$

where h is the still water depth and η the height of the surface above the still water level. According to equation (4-4), each small disturbance travels at a speed depending on the square root of the height of the water surface above the bottom. Since the crest is the highest surface elevation, it moves faster than the wave trough ahead of it. This causes the forward face of the crest to steepen, and eventually the surface slope becomes vertical.

Stoker's numerical methods are seldom used because the entire solution must be recalculated each time the initial conditions are changed. Choosing to follow the changing surface slope at the wave front as the wave advances, Greenspan (1958) and Burger (1967) related the bottom slope and the initial surface slope at the wave front to the horizontal distance the wave front travels until the

surface slope is vertical at the wave front. These relationships are reviewed in a following section.

Vertical Water Particle Velocity

Rather than use the kinematic criterion to determine the properties of the highest steady wave in shallow water of constant depth, Laitone (1963) analyzed series relationships for the vertical velocity. For solitary wave theory, he obtained a value of the series expansion parameter that yielded vertical velocities that could not physically occur.

Using a coordinate system moving with the steady wave phase velocity (Figure 4-3), Laitone derived the vertical velocity to be

$$(4\text{-}5) \qquad w(x, z) = \sqrt{gh}\ \sqrt{3(H/h)^3}\ (1 + \frac{z}{h})\ \mathrm{Sech}^2\, \alpha X \tanh \alpha X,$$

where

$$(4\text{-}6) \qquad \alpha X = \sqrt{\frac{3}{4}\frac{H}{h}}\ (1 - \frac{5}{8}\frac{H}{h})\frac{x}{h}\ .$$

Terms of order $(H/h)^2$ and higher have been omitted on the assumption that H/h is much less than unity. Equation (4-5) shows that the vertical velocity increases with increasing z without limit, and that there is no limiting height for a solitary wave to this order of H/h. But to the next order of approximation $(0(H/h)^3)$, w(x, z) is given by Laitone (1963) as

$$(4\text{-}7) \qquad w = \sqrt{gh}\ \sqrt{3(H/h)^3}\ (1 + \frac{z}{h})(1 - \frac{11}{8}\frac{H}{h}) \tanh \alpha X$$

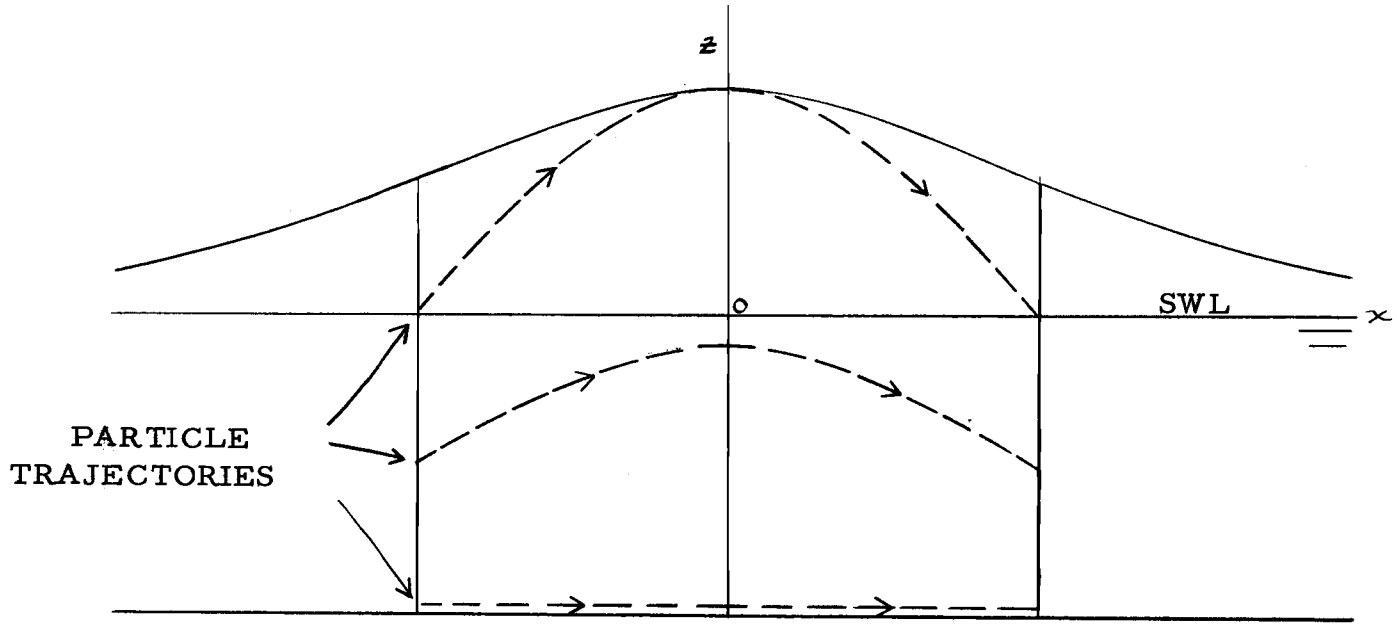

Figure 4-3. Particle trajectories produced by the passage of a solitary wave.

$$\text{for} \quad |x| \approx 0 \qquad z \geq 0$$

for the region near the wave crest. From equation (4-7), the vertical velocity increases with increasing z only if H/h is less than 8/11. If H/h = 8/11, the vertical velocity is zero for all z. When the vertical velocity in the region near the crest ceases to be an increasing function of z for constant H/h, the maximum value of H/h is obtained. The physical meaning of this criterion may be understood by investigating the water particle motion at a position fixed relative to the crest as H/h is increased.

Figure 4-3 schematically shows the particle trajectories produced by the passage of solitary wave. As the solitary wave advances into still water, the water particles rise to a maximum elevation at the crest, and then, as the wave passes, the water particles fall back to their initial horizontal level. Hence, for positions just in front of the wave crest, the vertical particle velocity should be upward, and for positions just behind the crest, the water particle velocity should be downward. If H/h is less than 8/11, the particle trajectories will be correct. For H/h = 8/11, the veritcal velocity is zero everywhere, and for H/h greater than 8/11, equation (4-7) predicts that the vertical velocity reverses its direction. Thus, a particle just in front of the advancing wave crest would have a downward motion, a physical impossibility.

As a final estimate of the limiting value of H/h, Laitone solved

for the vertical velocity to the next higher order in H/h ($0(H/h)^4$). To this order, w ceases to increase with increasing z when

$$(4\text{-}8) \qquad H/h = \sqrt{3} - 1 = 0.7321 ,$$

which is close to the previous estimate of 8/11 (0.7272).

Laitone (1963) extended the vertical velocity criterion to the cnoidal wave theory which is an oscillatory wave theory (Table 2-1). Solving for the vertical velocity to order $0(H/h)^3$, he obtained the maximum value of H/h to be

$$(4\text{-}9) \qquad H/h = \frac{8\beta}{9\beta + 2}$$

where $\frac{1}{2} < \beta \leq 1$. As β approaches 1.0, the cnoidal wave approaches the solitary wave, and equation (4-9) gives $(H/h)_{max} = 8/11$, as it should. As β decreases below 1.0, H/h from equation (4-9) also decreases. As β approaches $\frac{1}{2}$, it is not clear from Laitone if his series relations are valid. (As β approaches zero, these expressions for $(H/h)_{max}$ are not meaningful because the cnoidal wave becomes the small amplitude Airy wave.)

Vertical Pressure Gradient

Laitone (1963) also examined his series solutions for the vertical pressure gradient, attempting to detect a limiting value of H/h. The prediction of a vertical pressure gradient equal to zero beneath the crest (x = 0) was chosen as the limiting physical

condition.

For cnoidal wave theory, the vertical pressure gradient beneath the crest is given to order $0(H/h)^3$ by Laitone as

$$(4\text{-}10) \quad \frac{\partial p}{\partial z} = -\rho g \left(-1 + (H/h)^2 (3/2\,\beta)(1 + z/h) \right)$$

Near the crest, z is the same order as H, and the term $(H/h)^2(z/h)$ is of order $(H/h)^3$ and must be omitted. Equation (4-10) becomes

$$(4\text{-}11) \quad \partial p / \partial z = -\rho g \left(-1 + (H/h)^2 (3/2\beta)\right)$$

If $H/h = (2\beta/3)^{\frac{1}{2}}$, the vertical pressure gradient is zero, and, if H/h is greater than $(2\beta/3)^{\frac{1}{2}}$, the vertical pressure gradient reverses its algebraic sign, which is physically impossible.

The maximum limiting wave height for cnoidal waves occurs when $\beta = 1.0$, and the cnoidal wave with its periodic wave form becomes the solitary wave with the surface elevation approaching the still water level very far from the crest. Equation (4-11) yields $H/h = (2/3)^{\frac{1}{2}} = 0.812$ for $\beta = 1.0$. This value of H/h differs significantly from the estimates of $(H/h)_{max}$ (i.e., 0.7272 & 0.7321) predicted from the vertical velocity criterion, but the cause of this discrepancy could not be resolved by this writer.

2. Properties of Waves Limited by Theoretical Breaking Criteria

Vertical Water Particle Acceleration

In Chapter III, it was demonstrated that a discrepancy existed between theoretical estimates of the vertical particle acceleration near the crest for deep water waves. The 'classical' approach of Stokes, which assumed the wave had a sharp crest, yielded a vertical acceleration of $\frac{1}{2}$ g. The numerical stream function approach of Dean (1968) predicted a vertical particle acceleration of zero. In both cases, the kinematic breaking criterion was the limiting physical test. For steady state waves in shallow water of constant depth, these same estimates are obtained. Thus, the discrepancy also exists for the shallow water condition of constant depth.

Long Wave Breaker Properties

Using the breaking criterion of a vertical surface at the wave front (wave front defined on page 31), Burger (1967) derived a general relation for the horizontal distance the wave front propagates to reach the breaking position. More explicitly, this horizontal distance is the distance between the position where the initial (t = 0) surface slope at the wave front is specified and the position where the surface at the wave front is vertical. Figure 4-1a shows the wave front for t = 0, and Figure 4-1b shows the wave front at a later time at the breaking position. Here it is assumed that at t = 0, the wave front

passes the position x = 0.

For a variable beach slope, the horizontal distance to breaking, x_b, is given by Burger (1967) as

$$(4\text{-}12) \quad \int_0^{x_b} \left(\frac{h(x)}{h_b}\right)^{-7/4} dx = \frac{2}{3} \frac{h_i}{s} ,$$

in which s is the initial surface slope at the wave front, h_i the initial water depth, and h_b the depth at the breaking position. For a constant beach slope, m, $h(x) = h_i - mx$, and equation (4-12) becomes

$$(4\text{-}13) \quad x_b = \frac{h_i}{m} \left(1 - \frac{2s}{s+m}\right)^{4/3} ,$$

which is identical to the relation derived by Greenspan (1958) for this particular case. As would be expected, equation (4-13) predicts that x_b increases with an increase in h_i, a decrease in m, and a decrease in s.

There are several limitations to Burger's and Greenspan's theoretical calculations. First, since the changing surface slope behind the wave front is not examined, a vertical surface may occur earlier here than at the wave front, such as at the crest of the wave. This will depend on the initial specification of the surface elevation. Second, this approach does not predict the wave height at breaking, an important breaker property. Finally, the long wave theory is not strictly applicable for waves near the breaking position. As has been pointed out by Price (1971), Peregrine (1972) and others, the

horizontal particle velocity cannot be assumed to be constant with depth, nor can be the vertical pressure gradient be assumed to be hydrostatic for breaking waves. Wave theories which account for these complications are needed for a better prediction of breaker properties.

Limiting Wave Height to Depth Ratio

Table 4-1 shows the theoretical maximum wave height to depth ratios estimated for several shallow water wave theories. The waves being considered are the highest steady waves which can occur for the criterion specified in Table 4-1. For the solitary wave limited by the kinematic criterion, theoretical estimates of $(H/h)_{max}$ range from 0.73 to 1.03. Although the cause of the varying estimates probably lies in the approximate fits of the complex velocity potential to the free surface boundary conditions, it was not possible to verify this opinion. Additional causes of the variance in the estimates of $(H/h)_{max}$ may be due to the numerical calculations which include truncation of infinite series (e.g., Laitone, 1963; etc.) necessary to obtain each value.

Laitone estimated $(H/h)_{max}$ for solitary waves using two new physical criteria (page 37). These values are also within the range noted above. In addition, he obtained the first theoretical estimates of $(H/h)_{max}$ for cnoidal waves. These values have the solitary wave

Table 4-1. Derived maximum ratio of wave height to water depth for shallow water waves with specified limiting condition.

Investigator	$(H/h)_{max}$	Limiting Condition	Wave Theory	Sharp Crest
Boussinesq 1871	0.73	u = c	solitary	?
Lord Rayleigh 1876	1.0	u = c	solitary	?
McCowan 1894	0.78	u = c	solitary	yes
Gwyther 1900	0.83	u = c	solitary	?
Packham 1952	1.03	u = c	solitary	yes
Davies 1952	0.83	u = c	solitary	yes
Yamada 1957	0.83	u = c	solitary	yes
Lenau 1966	0.83	u = c	solitary	yes
Laitone 1963	0.73	w = 0	solitary	no
Laitone 1963	$8\beta/(2+9\beta)$, $\frac{1}{2}<\beta\leq 1$	w = 0	cnoidal	no
Laitone 1963	0.81	$\nabla_z p$ reversal	solitary	no
Laitone 1963	$\sqrt{2\beta/3}$, $\frac{1}{2}<\beta\leq 1$	$\nabla_z p$ reversal	cnoidal	no
Chappelear 1959	0.87	u = c	Stokes	yes
Dean 1968	1.0	u = c	stream f.	no

$(H/h)_{max}$ as upper limits, as would be expected.

The two estimates of $(H/h)_{max}$ by Dean (1968) and Cahppelear (1959) for oscillatory wave theory are also within the range given for the solitary wave.

Limiting Wave Steepness

Maximum wave steepness (H/L) values have been derived for oscillatory waves in water of constant but arbitrary depth limited by the kinematic breaking criterion. Miche (1944) obtained numerical estimates of $(H/L)_{max}$ from theoretical considerations that are approximated very well by the function

$$(4\text{-}14) \quad (H/L)_{max} = 0.14 \tanh\left(\frac{2\pi h}{L}\right) ,$$

although an error in Miche's derivation was recently discovered by Madsen (1971). However, equation (4-14) also fits the theoretical numerical results of Chappelear (1959) quite closely as shown in Figure 4-4.

Wave Profile

Essentially two types of wave profiles occur in the theoretical studies of the highest steady wave in shallow water of constant depth. Figure 4-5 shows a representative profile for those derivations that assumed a sharp crested wave. This particular profile was obtained

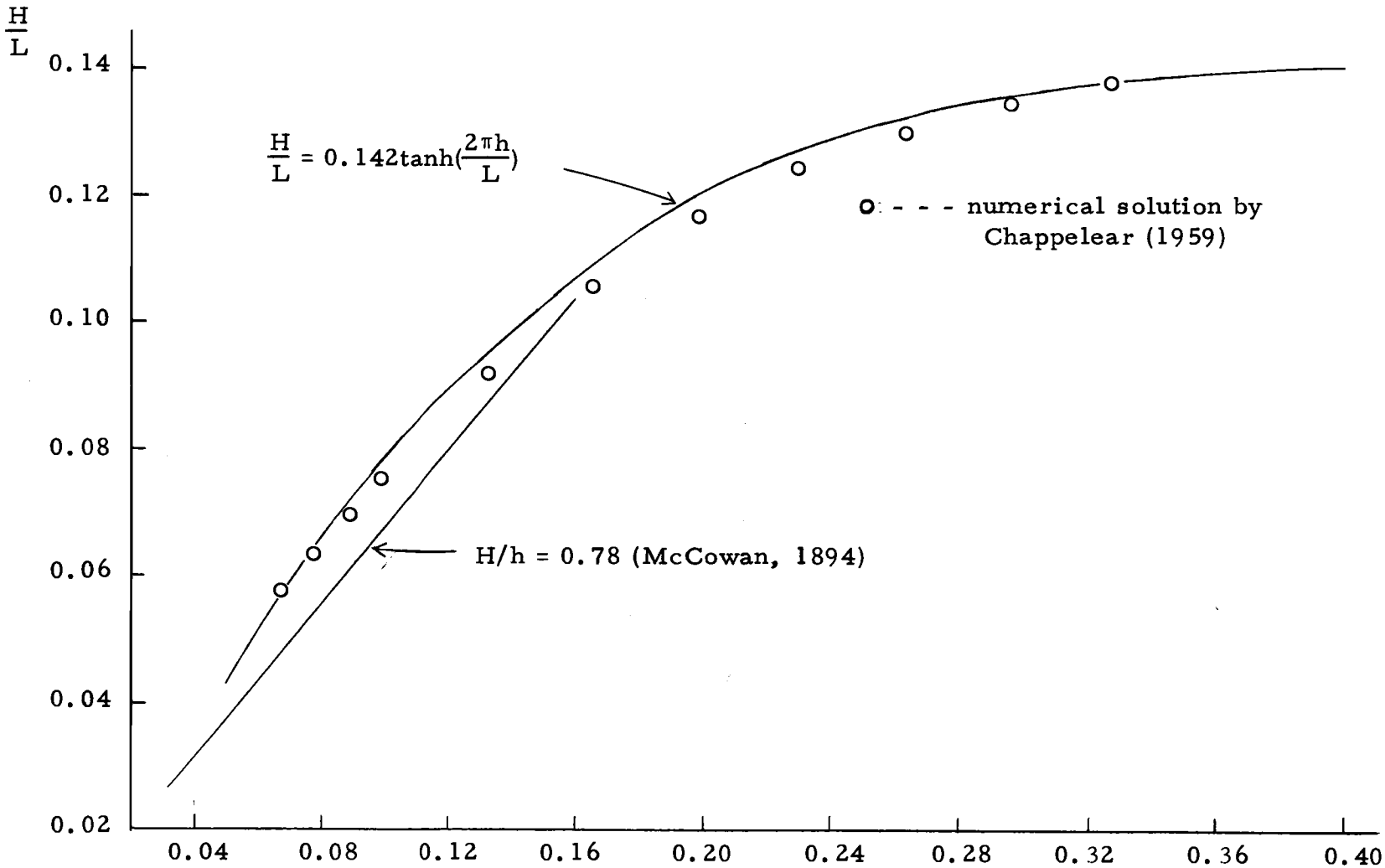

Figure 4-4. Wave steepness for kinematically limited wave as a function of the relative depth (h/L).

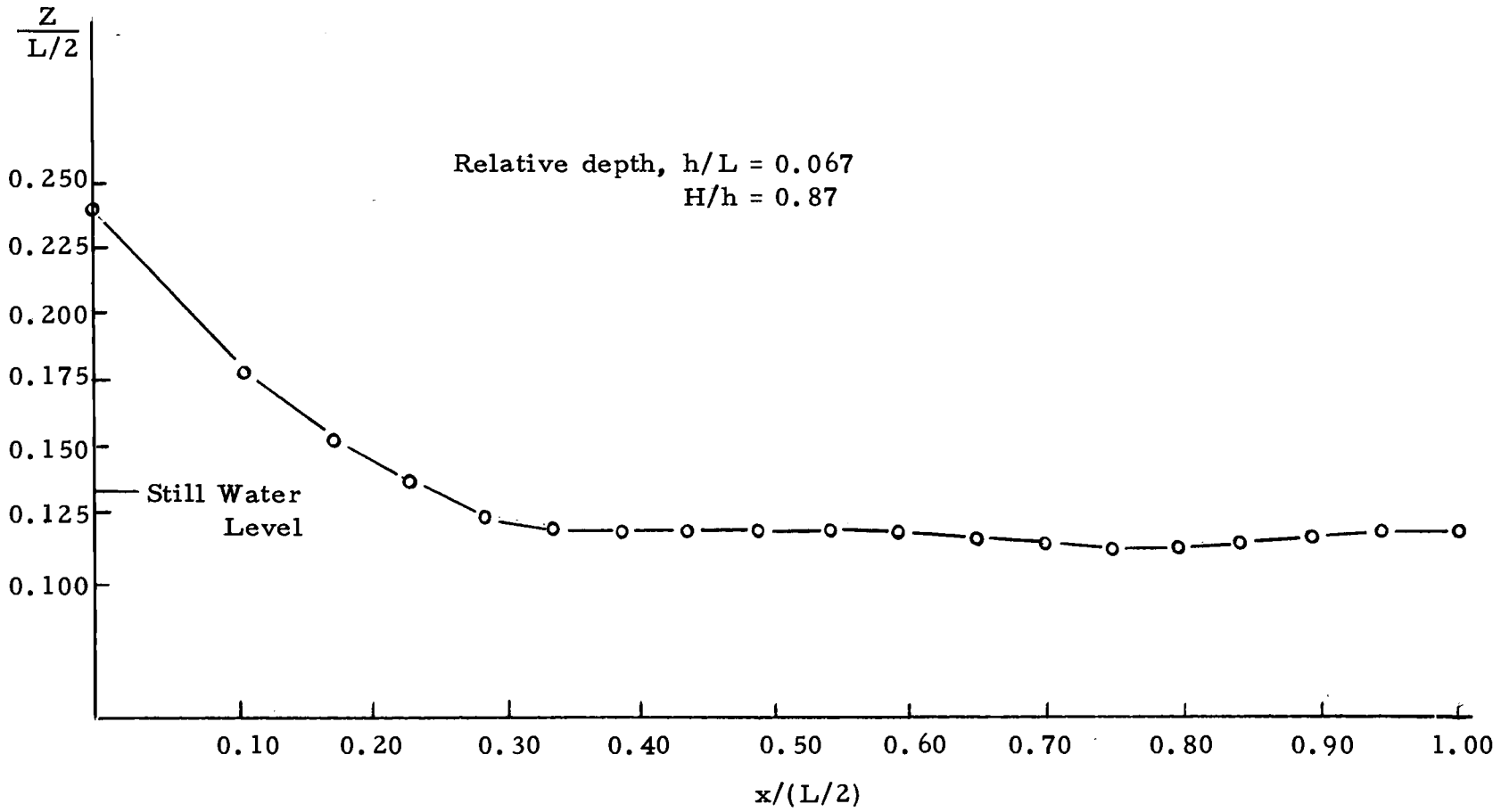

Figure 4-5. Surface profile for kinematically limited shallow water wave. (Chappelear, 1959).

from the table of numerical results given in Chappelear (1959) for the Stokes oscillatory wave theory. In contrast, Figure 4-6 shows a limiting solitary wave profile (Laitone, 1963) which does not have a sharp crest. Laitone was of the opinion that, as was first pointed out by Korteweq and deVries (1895), since a sharp crested solitary wave did not conform to the Bousinesq profile in its first order terms, it could not be steady state with respect to time in any coordinate system.

For comparison to the symmetrical steady state wave profiles described above, Figure 4-7 shows the details of a breaking wave shoaling on a constant beach slope of 0.10 (Biesel, 1952). Figure 4-7 was derived from first order wave theory using the velocity potential (see Table 2-1), and Figure 4-8 was derived from second order theory, in which particle velocity, wave height, and beach slopes squared terms were retained. In the following chapter on observations of breaking waves, it will be seen that Figure 4-7 resembles the plunging breaker type, and Figure 4-8 resembles the spilling breaker type.

Discussion and Conclusions

In this chapter we have seen that theoretical shallow water breaking criteria can be divided into two categories. One category applies to the 'highest' steady waves which can exist in water of

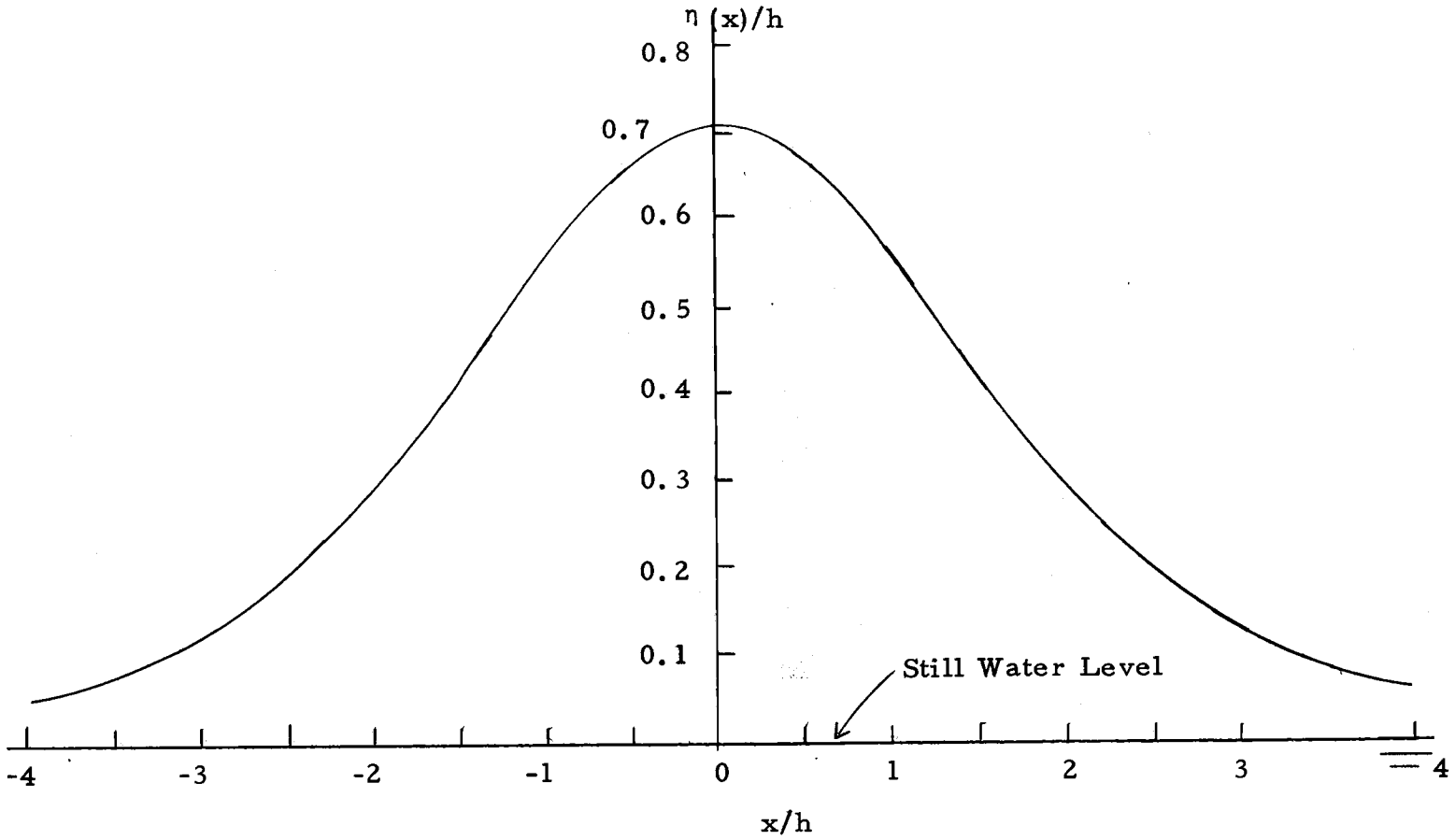

Figure 4-6. Solitary wave profile for limiting condition of 'reversal' of vertical particle velocity (Laitone, 1963).

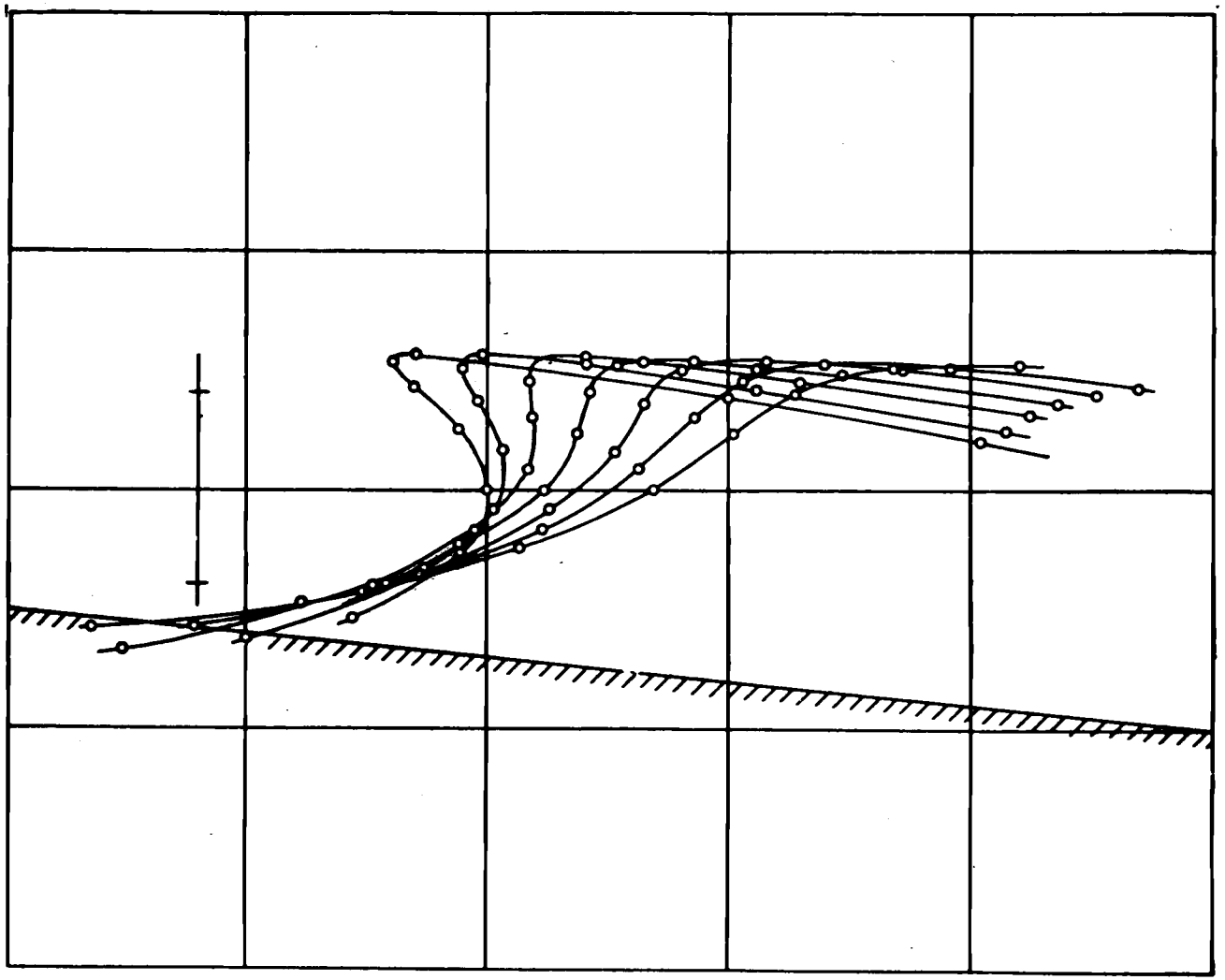

Figure 4-7. Details of breaking wave, first-order theory. (Biesel, 1952)

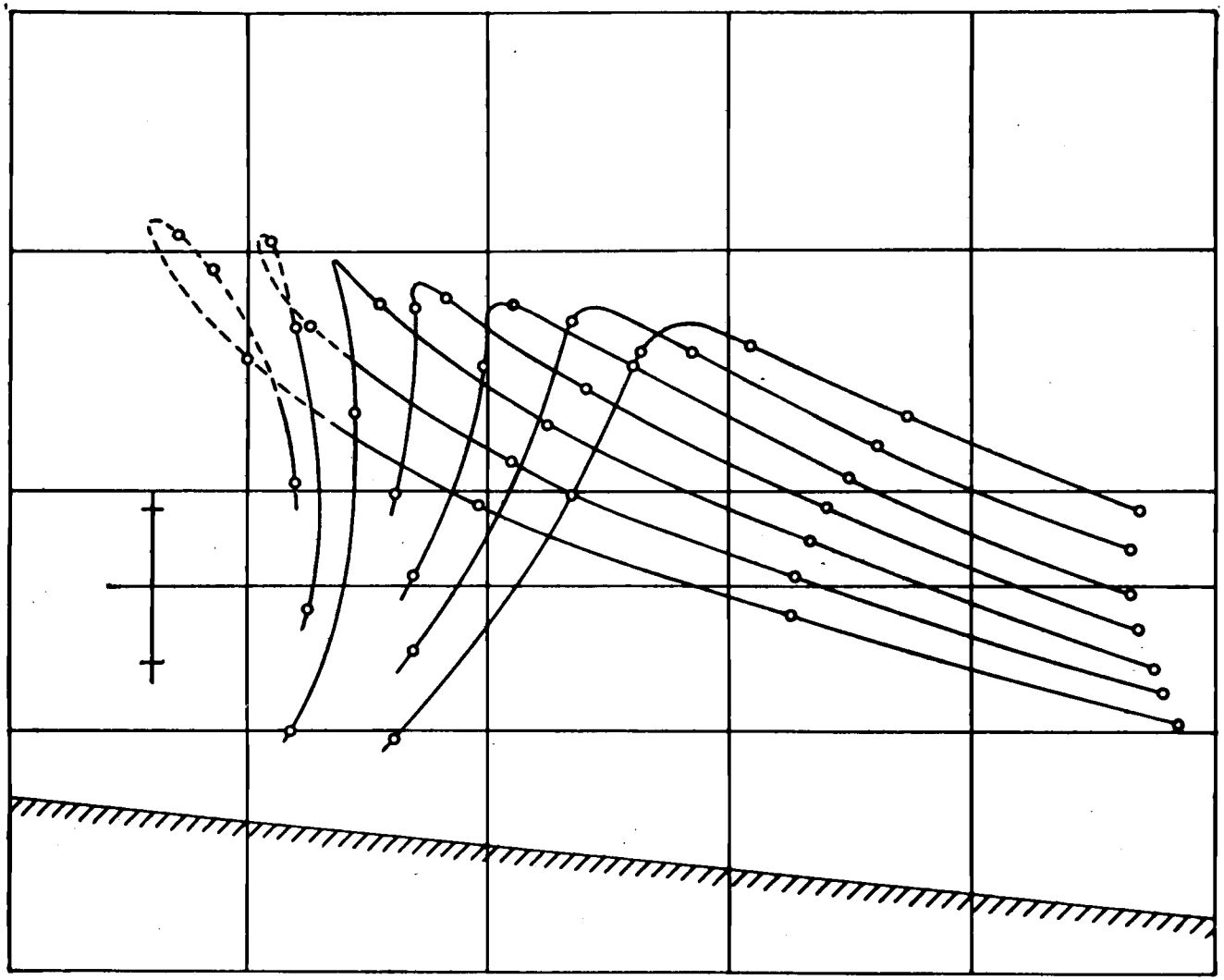

Figure 4-8. Details of breaking wave, second-order theory. (Biesel, 1952)

constant depth. These waves are assumed to be limited in their growth by a certain physical condition. The other category of breaking criteria applies to waves which are shoaling. These waves are continually changing their shape and flow properties to conform to the free surface and bottom boundary conditions.

For the highest steady wave, the theoretician is able to derive additional properties of the wave. In all but one of the studies reviewed, the kinematic criterion was assumed to limit wave growth. The exception was Laitone (1963) who demonstrated that other possible breaking criteria were the behavior of either the vertical particle velocity near the crest or the behavior of the vertical pressure gradient beneath the crest.

Although the term 'highest' steady wave has been used to denote the wave limited by these breaking criteria, the wave height (in the form of the ratio of the wave height to wave length or the ratio of wave height to water depth) was one of the derived wave properties. Table 4-1, which shows the theoretical estimates of $(H/h)_{max}$, is evidence that $(H/h)_{max}$ extends over a rather wide range (0.73 - 1.03) even if only one wave theory is considered. To obtain these estimates of $(H/h)_{max}$, the wave theories were extended to their extreme limits, and, hence, the numerical approximations required may be of the same order of magnitude as the variation between estimates. In addition, the convergence to a unique finite solution of

the infinite power series representing solutions to the wave properties has not been proven in any of the studies reviewed.

There is as yet no a priori argument that identifies which of the assumed criteria is the actual cause of limiting wave growth in shallow water. Although the kinematic breaking criterion is probably not exceeded without the water particles at the crest separating from the wave, this may be the result of flow conditions brought about in the wave by the behavior of the vertical particle velocity or the vertical pressure gradient. It is also possible that the kinematic criterion is an extreme value for the horizontal particle velocity that is never attained by even the highest wave. To determine the fundamental breaking criterion limiting the highest steady wave, careful experimental investigations of all of the flow properties within the wave are needed.

Two physical conditions which have been assumed to denote the breaking position of shoaling waves are the vertical surface and the kinematic criterion, which were both applied to long wave theory. The use of the kinematic criterion (Ayyar, 1970) seems inappropriate for long wave theory because of the assumption that the horizontal particle velocity is constant with depth. Although the choice of a vertical surface as a breaking criterion is appropriate for long waves as shown by Stoker (1957), the applicability of the long wave theory near the breaking point is doubtful due to the assumption of a

hydrostatic pressure gradient beneath the crest. Thus, the vertical surface criterion may be appropriate for actual water waves but may not be appropriate when used in conjunction with long wave theory. In addition, the introduction of the wave front concept is also a crucially limiting assumption because the possibility of prior breaking behind the wave front is ignored. Figure 4-9, which shows the profile of an actual plunging solitary breaker, points out the importance of breaking behind the wave front. The vertical surface occurs at the crest position rather than at the wave front, whose approximate location is indicated in this figure.

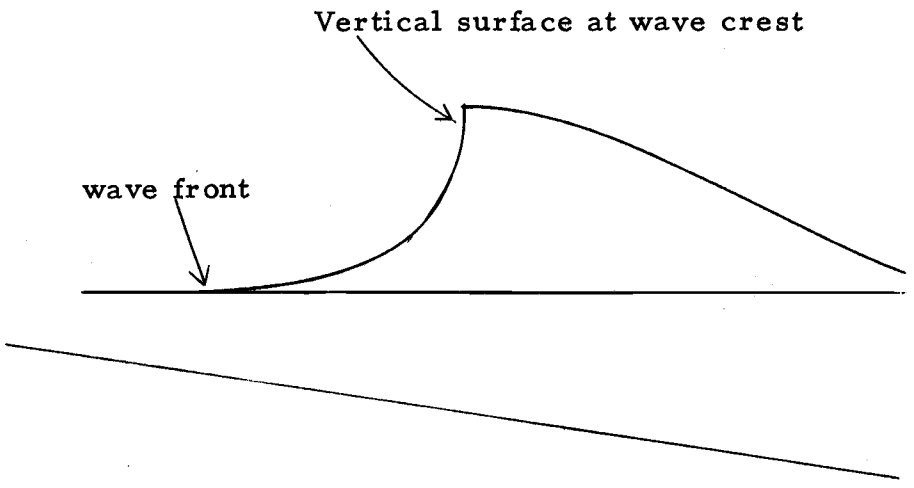

Figure 4-9. Sketch of breaking wave.

CHAPTER V

A REVIEW OF SHALLOW WATER BREAKER EXPERIMENTS

In the preceding chapter, theoretical breaking criteria for progressive surface shallow water waves were reviewed. The purpose of this chapter is to review experimental procedures, techniques, and equipment which are germane to the testing of these theoretical breaking criteria. Since attempts have been made to test only some of the theoretical breaking criteria, this review includes additional experiments which contain methods relevant to measuring breaker properties. These methods may be useful in experiments on the untested breaking criteria. A review of the results of these experiments is presented in Chapter VI.

This chapter is divided into four sections: (1) breaker types and parameters, (2) wave tank and basin studies, (3) ocean studies, and (4) problems encountered in the data reviewed.

1. Breaker Types and Parameters

Breaker Types

Laboratory studies (Galvin, 1968; Ippen and Kulin, 1955) have shown that solitary and oscillatory breakers can be classified into four principal types: (1) spilling, (2) plunging, (3) collapsing, and

(4) surging. These breaker types are described in Figure 5-1, Figure 5-2 and Table 5-1. It should be mentioned that there is really a continuum of breaker types, and these categories must therefore be somewhat artificial.

The relationship of the solitary breaker types to the initial wave height to depth ratio (H_i/h_i) and the beach slope (m) is shown in Figure 5-3 (Camfield and Street, 1966). The solitary breaker deformation can be roughly divided into four regions characterized as follows: (1) region I with spilling breakers associated with low beach slopes and steep waves; (2) region II with plunging breakers; (3) region III with shoreline-crashing plunging breakers; and (4) region IV with non-breaking waves associated with very steep beach slopes (i.e., $m \geq 0.35$).

Table 5-2 (Galvin, 1968) indicates the transition values between oscillatory breaker types for inshore and offshore parameters as determined from a laboratory study. Low beach slopes and steep initial waves also characterize oscillatory spilling breakers. The following section contains more detailed definitions of the parameters used in Figure 5-3 and Table 5-2.

Breaker Parameters

The major parameters used in the laboratory and field studies are defined in this section. Table 5-3 contains a summary of the

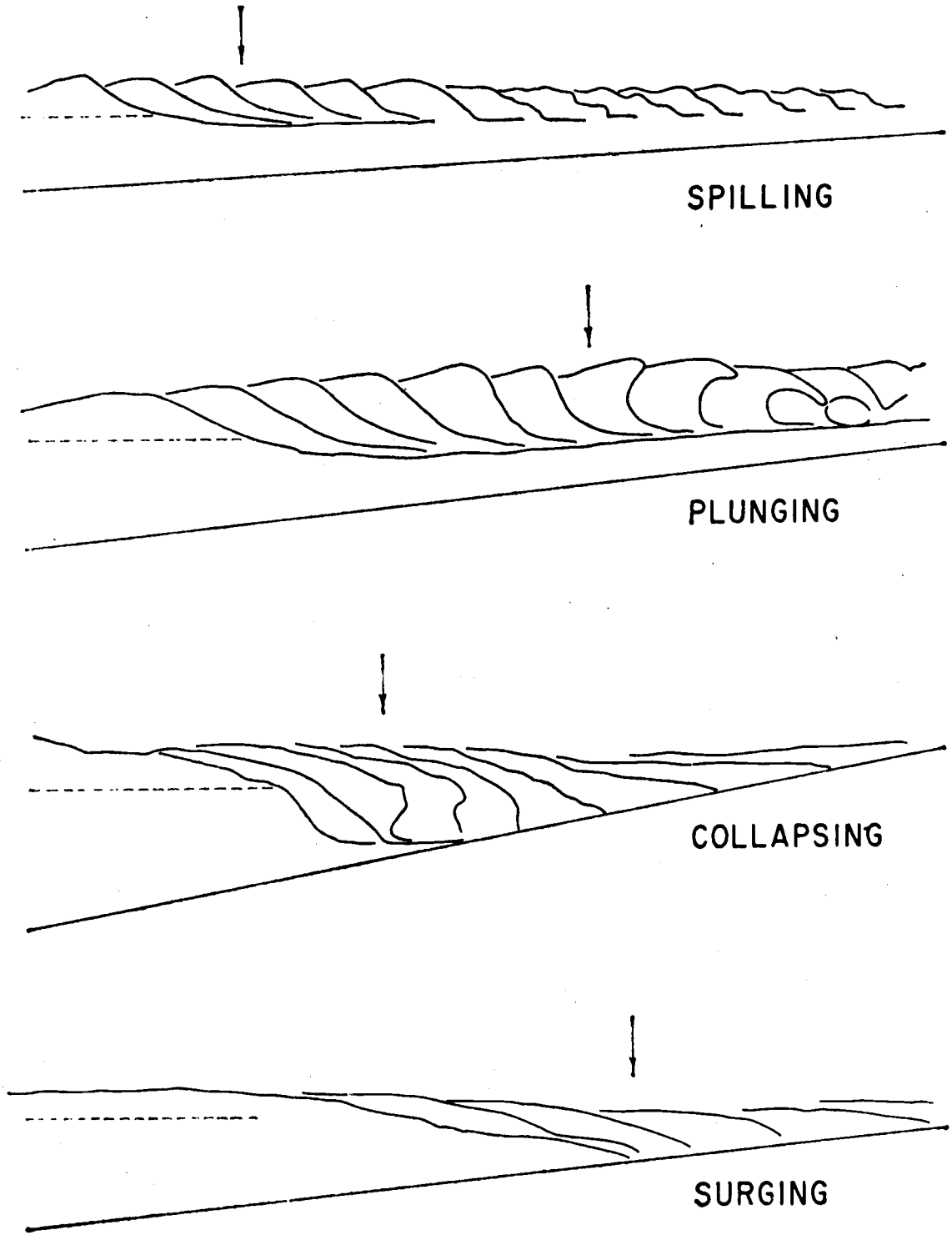

Figure 5-1. Principal oscillatory breaker types. (Galvin, 1968)

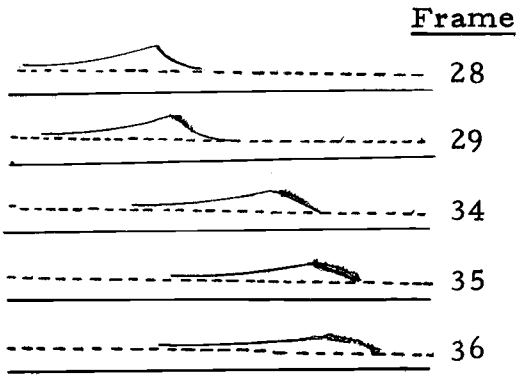

A. Spilling Breaker

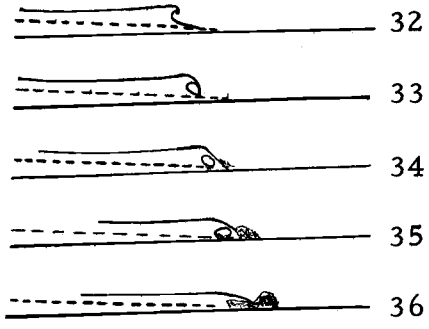

B. Plunging Breaker

Figure 5-2. Solitary breaker transformations (Ippen and Kulin, 1955).

Table 5-1. Oscillatory breaker types on laboratory beaches. (Galvin, 1968)

Code	Type of Breaking	Description
1	Spilling	Bubbles and turbulent water spill down front face of wave. The upper 25% of the front face may become vertical before breaking.
2	Well-developed plunging	Crest curls over a large air pocket. Smooth splash-up usually follows.
3	Plunging	Crest curls less and air pocket smaller than in 2.
4	Collapsing	Breaking occurs over lower half of wave. Minimal air pocket and usually no splash-up. Bubbles and foam present.
5	Surging	Wave slides up beach with little or no bubble production. Water surface remains almost plane except where ripples may be produced on the beach face during runback.
6	Plunging altered by reflected wave	Small waves reflected from the preceding wave peak up the breaking crest. Breaking otherwise unaffected.
7	Plunging altered by secondary wave	Primary may ride in on secondary immediately before it, or secondary immediately behind rides in on primary in front. First kind difficult to distinguish from 8.
8	Surging altered by secondary wave	Plunging secondary may break just in front of surging primary. Difficult to distinguish from 7.
9	Secondary wave washed out	Runback from previous primary carries the secondary wave offshore, where it may break out of field of view or just disappear.

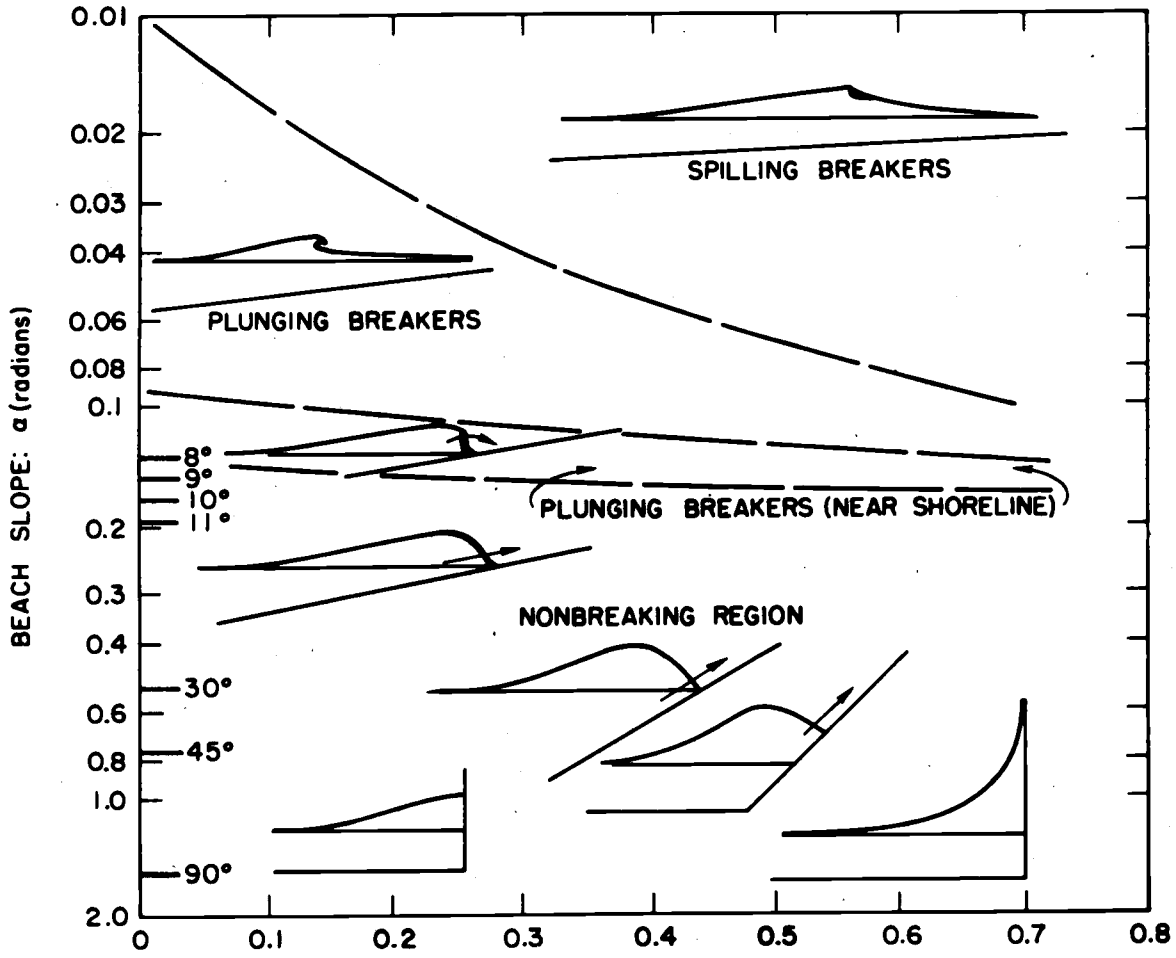

Figure 5-3. Solitary breaker types as a function of beach slope (m) and initial wave height to water depth ratio (H_i/h_i). (Camfield and Street, 1966)

Table 5-2. Transition values between oscillatory breaker types for inshore and offshore parameters. (Galvin, 1968)

Parameter	Surge-Plunge	Plunge-Spill
Offshore $H_\infty / L_\infty m^2$	0.09	4.8
Inshore $H_b / (gmT^2)$	0.003	0.068

(H_∞ = deep water wave height, L_∞ = deep water wave length, m = beach slope, H_b = breaker height, T = wave period, g = acceleration of gravity)

Table 5-3. Summarization Chart of Laboratory Investigations

	(1) Iverson 1952	(2) Komar & Simmons 1968	(3) Galvin 1968	(4) Beach Erosion Board 1949	(5) Berkeley Wave Tank 1949	(6) Nicholson 1968	(7) Morrison & Crooks 1953
Basin Size length x width	54 ft. x 1 ft.	131 ft. x 1.6 ft.	96 ft. x 1.5 ft.	85 ft. x 1.4 ft.	50 ft. x 1	90 ft. x 5 ft. 24 ft. x 2 ft.	60 ft. x 3 ft.
Measurement Techniques	motion picture 60 frames/sec.	motion picture 32 frames/sec.	motion picture 60 frames/sec.	motion picture	motion picture	point gage	motion picture
Beach Slopes	0.02, 0.033, 0.05, 0.10	0.036, 0.070, 0.086, 0.105	0.05, 0.10, 0.20	0.05, 0.03, 0.159	0.054, 0.072, 0.009	0.05, 0.10, 0.13, 0.20	0.02, 0.10
Wave Generation	double hinged flap	single hinged flap	vertical piston	?	double hinged flap	pneumatic, vertical piston	double hinged flap
Observations	67	44	43	37	16	31	6
Number of Data Points/Observation	?	10	10	?	?	?	?
Initial Wave Height (cm)	2.6 - 12.0	3.03 - 13.1	2.45 - 10.9	2.65 - 12.25	4.08 - 10.7	no	no
Initial Depth (cm)	42.6 - 71.0	30.6	61.0 - 91.5	no	no	30.0 - 77.4	?
H_{oo}/L_{oo} Range	0.0025 - 0.0907	0.0032 - 0.071	0.0028 - 0.056	0.015 - 0.067	0.007 - 0.0092	0.028 - 0.0834	0.0036 - 0.0778
Wave Period (sec)	0.74 - 2.67	0.81 - 2.37	1.0 - 8.0	0.73 - 1.08	0.86 - 1.97	0.74 - 1.21	0.78 - 2.62
Breaker Height (cm)	4.3 - 12.7	3.4 - 17.0	3.8 - 17.0	3.1 - 13.04	6.8 - 9.9	3.05 - 10.7	5.58 - 11.30
Breaker Depth (cm)	4.3 - 16.5	3.4 - 21.3	3.9 - 18.2	4.3 - 18.7	6.4 - 13.8	?	7.0 - 12.9
Breaker Type	Define, do not report		Define & Report	?	?	?	?
Initial Relative Water Depth, h/L_{oo}	0.04 - 0.68	0.03 - 0.30	0.0023 - 0.20	0.016 - 0.067	0.0007 - 0.092	0.035 - 0.40	?
Crest Height (cm)	yes	yes	no	no	no	no	no
Breaker Height Above Still Water	no	yes	no	no	no	no	no
Other Variables	yes	no	yes	yes	no	yes	no

parameters reported by each investigator.

1. Breaker point. The experimental breaker point denotes an instant in the breaking process when the breaker is of a certain, specified shape. The most accepted definitions are based on the breaker type as follows.

a. Spilling breaker point. The point of the first appearance of 'white water' at the crest (Iverson, 1952a). Also, the point of the first appearance of a break or a curling over of the water surface near the crest (Galvin, 1968).

b. Plunging and collapsing breaker points. The point where some part of the shoreward face of the breaker first becomes vertical (Galvin, 1968; Iversen, 1952a (plunging only)).

c. Surging breaker point. The point in which a major portion of the front face of the wave becomes unstable in a large scale turbulent fashion (Iversen, 1952a); also, the point when the furthest drawdown of the previous wave is halted by the advance of the next wave (Galvin, 1968).

These instants or points in the breaking process are shown by the arrows in Figure 5-1 (Galvin, 1968). Galvin reported that for plunging breakers, the vertical segment of the shoreward face is usually near the maximum elevation of the wave, and for collapsing breakers it is relatively lower. The breaker point marks the beginning of the rapid change in shape for plunging and collapsing

breakers. It is near the beginning of a gradual change toward a bore-like shape for spilling breakers, and it merely marks the reversal in water motion for surging breakers (Galvin, 1968). From the definition of the surging breaker point of Iverson (1952a), it is likely that his surging breaker is similar to Galvin's collapsing breaker.

One field study (Scripps Institute of Oceanography (SIO) Wave Report Number 1, 1944) defined the breaker point as "the point where the crest broke."

2. Breaker height, H_b. The breaker height for most oscillatory laboratory breakers and ocean breakers was the vertical distance between the crest at the breaker point and the spatially preceding trough (Figure 5-4). For solitary breakers, the breaker height was the distance between the crest at the breaker point and the still water level (Figure 5-5). One oscillatory wave study (Galvin, 1968) defined the breaker height as the difference between the maximum and minimum water surface elevations at the breaker point during one wave period. A comparison of Galvin's definition with the more common definition given above has not been made.

3. Depth of breaking, h_b. The depth of breaking for most laboratory studies was the vertical distance from the bottom to the still water level at the breaker point (Figures 5-4 and 5-5). The one exception was Galvin (1968) who defined h_b as the vertical distance from the bottom to the mean water level, where the mean water

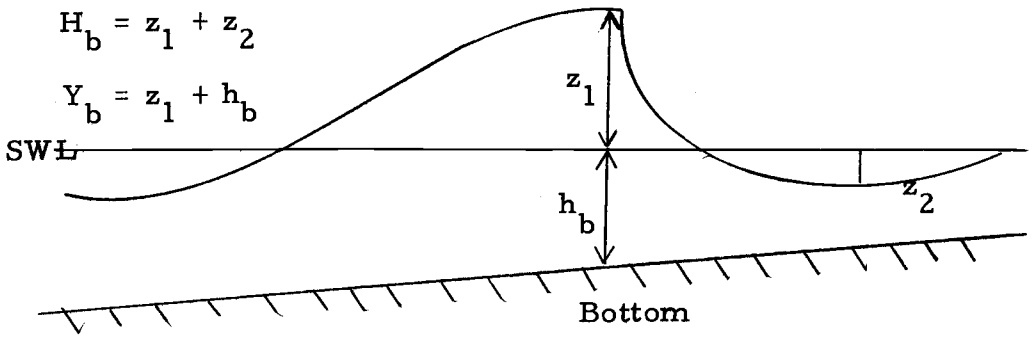

Figure 5-4. Oscillatory breaker position.

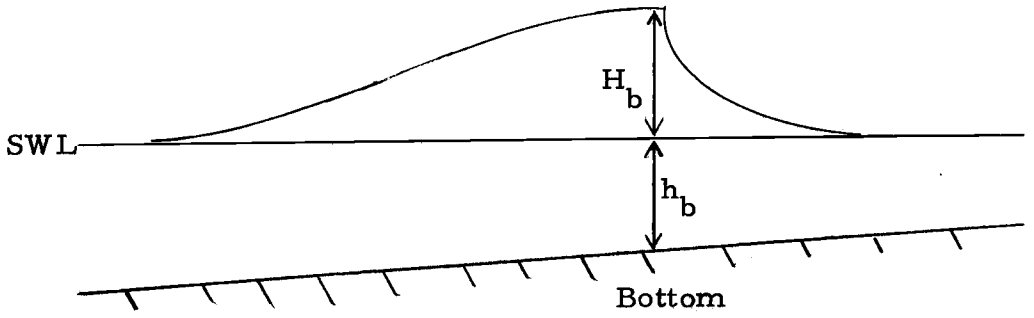

Figure 5-5. Solitary breaker position.

level was defined as the time average of the water surface elevation at the breaker point. Due to wave set-down (Bowen, Inman and Simmons, 1968), this depth of breaking is about four percent less than the depth of breaking measured to the still water level.

The SIO Wave Report Number 1 (1944) field study measured the depth of breaking as the vertical distance from the bottom to the still water level at the breaker point. Measurements of depth with reference to mean lower low water were made each day of observations and corrected with the tidal record.

4. Breaker crest elevation, Y_b. The breaker crest elevation is the vertical distance from the bottom to the crest at the breaker point (Figure 5-4).

5. Wave period, T. The wave period was equated with the period of the paddle oscillations in the laboratory studies. In an ocean study (SIO Wave Report Number 1) the wave period was the time difference between the crest under observation and the crest spatially preceding it, measured with respect to a fixed location on the adjacent pier.

6. Initial wave height, H_i, and initial water depth, h_i. For oscillatory waves, the initial wave height is the vertical distance between the crest and the spatially preceding trough in the constant depth section of the wave tank. For solitary waves, the initial wave height is the vertical distance from the crest to the still water

level in the constant depth section of the wave tank. The initial wave height and depth in the SIO Wave Report Number 1 ocean study were measured at the seaward end of a one thousand foot long pier in approximately twenty-five feet of water. In this case, the initial wave height was the vertical distance from the crest under observation to the trough spatially preceding it. In the laboratory study of Galvin (1968), the initial wave height was the wave height predicted theoretically from the linear theory for the given displacement of the wave paddle. The measured initial wave heights were "generally lower" than that predicted (Galvin and Eagleson, 1965).

7. Deep water wave height, H_∞, and deep water wave length, L_∞. The deep water wave length was computed from the wave period according to small amplitude wave theory by using the relation

$$(5\text{-}1) \qquad L_\infty = g T^2 / 2\pi \quad .$$

The deep water wave height was calculated from small amplitude wave theory by using the relations

$$(5\text{-}2) \qquad L_i / L_\infty = \tanh (2\pi\, h_i / L_i)$$

and

$$(5\text{-}3) \qquad H_i / H_\infty = ((1 + 4\pi h_i / (L_i \operatorname{Sinh}(4\pi h_i / L_i))(\tanh (2\pi\, h_i / L_i)))^{-\frac{1}{2}} \quad .$$

where L_i is the wave length in the constant depth portion of the wave tank. Alternatively, the tables of Wiegel (1964) could be used.

8. Breaker phase velocity, C_b. The wave phase velocity at the breaker point was calculated by Iverson (1952a) using motion picture film of the breaking waves. Iverson did not state how he computed C_b, but three methods were possible: (1) he divided the horizontal distance the crest moved between the frame of the crest preceding the breaker point and the frame of the breaker point by the time elapsed between frames; (2) he divided the horizontal distance the crest moved between the frame of the breaker point and the frame of the crest just following the breaker point by the time elapsed between frames; or (3) he calculated the average of C_b determined by methods (1) and (2).

9. Beach slope, m. The constant beach slope is reported throughout this thesis as the tangent of the included angle. For beach slopes up to 0.10, the tangent of the included angle is very nearly equal to the value of the angle in radians.

2. Review of Laboratory Studies

The laboratory oscillatory wave studies were not consistent in the reporting of experimental parameters (Table 5-3). The beach slope, breaker height, and wave period were the only parameters common to all seven laboratory studies. The initial wave height was used in three studies, while the remaining four studies published either the calculated deep water wave height or the calculated deep

water wave steepness. Another frequently reported parameter was the depth of breaking (five studies). Iversen (1952a) and Morison and Crooke (1953) measured the breaker phase velocity, and Galvin (1968, 1969) included the breaker types.

All of the solitary wave investigations reported the beach slope, ratio of initial wave height to still water depth, and the ratio of breaker height to depth of breaking. Ippen and Kulin (1955) published data on the breaker phase velocity and the particle velocity field at the breaker point.

Number of Observations

In each study, for constant experimental conditions, measurements were taken of the beach slope, still water depth in the constant depth section of the tank, paddle frequency and displacement, initial wave height, breaker height, and depth of breaking. This set of measurements is defined to be an observation. The number of observations in each experiment is a measure of the variety of conditions that were tested. The breaker observations of Komar and Simmons (1968), which are included in this report, and Galvin (1968, 1969) are the averages of ten consecutive waves, in which the individual measurements varied considerably in some instances. The remaining investigators did not published the number of waves which were averaged to obtain the reported breaker heights and depths of

breaking.

Table 5-3 contains a summary of the number of observations in each investigation, and Appendix I is a tabulation of these measurements. Since the solitary wave experiments presented results only in graphical form, a list of these observations could not be prepared and so is not included.

Wave Tanks

The dimensions of wave tanks ranged from 131 feet from wave generator to beach by 1.6 feet wide (Komar and Simmons, 1968) to 24 feet in length by 2.0 feet wide (Nicholsen, 1968).

Beach Slope

Beach slopes varied in magnitude and in degree of roughness of the surface. Most beach slopes were in the range 0.02 to 0.20, but some slopes were as small as 0.01 and as steep as vertical. Fig. 5-6 shows the actual slope which was identified in the Berkeley Wave Tank study (SIO Wave Report Number 47, 1945) as a 0.009 slope. The waves first encountered the short steep slope before proceeding over the 0.009 slope.

Beach slopes were commonly constructed of smooth plywood or concrete. Two exceptions were the beaches of Camfield and Street (1966, 1968) who used beaches roughened with sand glued on

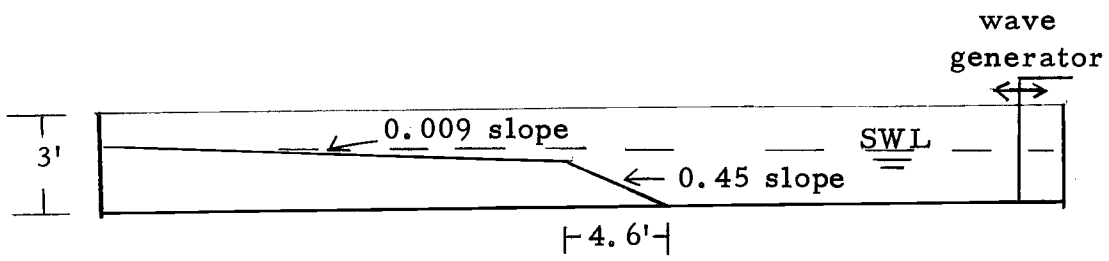

Figure 5-6. Channel arrangement for 0.009 slope in Berkeley wave tank data.
(SIO Wave Report No. 47, 1945)

them, and Nicholsen (1968) who used beaches made entirely of sand (median diameter either 0.42 or 2.00 mm).

Wave Generation

Oscillatory waves were generated by paddle devices usually driven through mechanical linkage by electrical motors. Galvin (1968, 1969) used a vertical walled piston-type generator, and Komar and Simmons (1968) employed a paddle hinged at the bottom and driven at the top. Nicholsen (1968) used a pneumatic wave generator for long period waves and a vertical plunger type for short period waves. The remaining laboratory wave studies utilized a flap which could be driven through top and bottom independently adjustable cranks to permit a "closer approximation of a shallow water wave at the wave generator" (Iversen, 1952a).

Ippen and Kulin (1955) generated solitary waves by impounding a volume of water behind a gate which could be raised suddenly. On release, this volume of water pushed a movable piston along the tank, displacing a certain amount of water in front of it within a definite time. More recently, Camfield and Street (1966; 1968) also made use of a vertical piston-type plate, but the motion of the wave plate was controlled through a hydraulic-servoelectronic system.

Measurements

Wave periods were measured by timing the oscillations of the wave paddle. Wave periods were reported to 0.01 seconds, where the smallest period was 0.80 seconds. The beach slope and the still water depth in the wave tank were also accurately measured since they are static quantities. The initial wave heights were measured using resistance gages or point gages. Either of these instruments can measure waves five centimeters high to within five percent (Beach Erosion Board Technical Memorandum 10, 1965), and most of the initial waves were higher than five centimeters. The breakers were recorded on motion picture film (32 to 60 frames per second), and the projected film image was used to measure the breaker height and the depth of breaking. Due to the high rates of change of the surface profile during the breaking process, H_b and h_b were subject to larger errors than H_i.

Water particle velocities within solitary waves were measured (Ippen and Kulin, 1955) with an open shutter camera with illumination provided by a strobe lamp. The strobe lamp was operated at twenty flashes per second. To identify individual fluid particles, droplets of colored solution with a specific gravity of unity were used for particles beneath the surface, and 1/8 inch balsa cubes were used for particles on the surface. The accuracy and precision of these

techniques are not reported, but particle velocities are given to 0.1 feet per second where 3.5 feet per second is a typical value. Comparable measurements of the kinematics of the water motion in oscillatory breakers were made by Iversen (1952a). A liquid mixture of xylene and carbontetrachloride, with zinc oxide for coloring and a specific gravity very near that of the water, were introduced near the breaker region, and the resulting motion of these particles was recorded on film. Similar values of the particle velocities were obtained.

3. Review of Ocean Breaker Studies

For the ocean experiments, an observation is defined to be a combination of measurements of beach profile, initial water depth, initial wave height (wave height at the seaward end of the SIO pier), wave period, breaker height, and depth of breaking. The ocean studies include 112 observations; 74 are of Pacific Ocean waves at the SIO pier and 38 are of Atlantic Ocean waves at Martha's Vineyard, Mass. (Munk, 1949). Since the Woods Hole reports on the Atlantic waves could not be obtained, only the SIO study is described herein.

Parameters common to all three field studies are the deep water wave steepness, the breaker height to deep water wave height ratio, and the breaker height to depth of breaking ratio. The SIO reports also included the wave period, breaker height, depth of

breaking, and the distance the wave traveled from the time it entered very shallow water until it broke (very shallow water means those depths where the ratio of the depth to the deep water wave length is less than 0.05). Each of these values (see Appendix I for list) represents a measurement of only one wave; averages were not used.

Breaker heights ranged from 4.0 to 11.4 feet, and wave periods ranged from 6.5 to 13.7 seconds. The two beach profiles are shown schematically in Figure 5-7.

Measurements were obtained from a series of still photographs of incoming waves taken near the SIO pier. Each photographic series is a pictorial record of a single wave crest from the time it passed the seaward end of the pier until it broke. The photographs were taken at five second intervals from a shore location twenty-five feet above the pier level and about eighty yards south of the pier, which projects seaward to the west-northwest. The pier pilings were scaled and referenced to mean lower low water so that water depths and surface elevations could be measured.

The initial wave height is obtained from the photograph of the wave when it is at the seaward end of the pier. From the depth of water at this location, the wave period, and the initial wave height, equation 5-3 was used to calculate the deep water wave height.

As discussed previously, the wave period is the time difference between the crest under observation and the crest spatially preceding

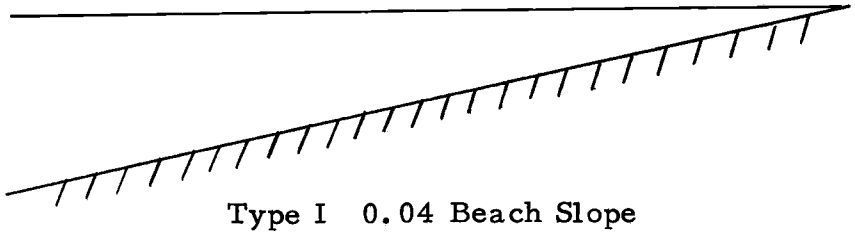

Type I 0.04 Beach Slope

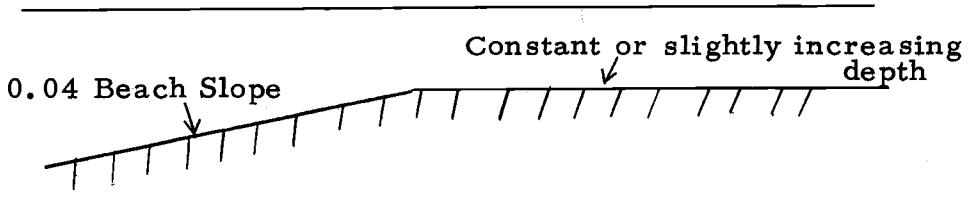

Type II

Figure 5-7. Sketch of ocean beach slope types. (SIO Wave Report No. 24, 1944)

it, as measured with reference to a fixed point on the pier. Whenever the two crests occupied exactly the same position on different photographs, the interval of time between the photographs was used as the wave period. If the two positions did not coincide a correction based on the theoretically computed wave celerity, $(gh)^{\frac{1}{2}}$, was used. This correction amounted to ten percent of the final wave period in the instances where the correction was published.

4. Problems Encountered in Analyzing the Data Reviewed

The preceding sections of this chapter have reviewed the methods and procedures used in studies on breaking waves. This section discusses possible sources of difficulties to achieving accurate and consistent breaker measurements. When considering a single experiment, the major problem is the likelihood of interferring fluid motions. Since these fluid motions may cause considerable variations in the measurements of the breaker parameters, they should be monitored to evaluate their effect. Table 5-4 describes the fluid motions which are known to occur during experiments on breakers in wave tanks. These motions arise because the energy and momentum of the generated waves are not completely dissipated in the wave breaking and run-up processes. A closely related problem is the use of complex boundary conditions, specifically a variable beach slope (Figures 5-6 and 5-7).

Table 5-4. Fluid motions encountered in breaker measurements

Fluid Motion	Definition or Explanation	Studies Effected
(1)	(2)	(3)
Friction	Due to bottom, side walls, or internal	Oscillatory, solitary, field
Backwash	The return flow down the beach slope from the previous breaker	Oscillatory, field
Solitons	Waves of temporary form that develop when steep waves travel into shallow water. The steep initial wave deforms into one large wave (primary) and one or more smaller waves (solitons) (Figure 5-8).	Oscillatory, solitary, field
Wave Reflection	Partial reflection of preceding wave may interfere with incoming wave	Oscillatory, field
Wave Set-up or Set-down	A change in the mean water level due to the presence of waves	Oscillatory, field
Edge Waves	Waves (progressive or standing) which are constrained to the edges of basins. Wave crest perpendicular to shore, wavelength parallel to shore (Figure 5-9).	Oscillatory, field
Rip Current	Narrow currents flowing seaward from the surf zone. Part of nearshore cell circulation produced by the interaction of edge waves and incoming breakers	Oscillatory, field
Seiching	Standing waves along the length of wave tank	Oscillatory

A second problem arises when it is desired to compare the results of two or more experiments. One important problem of this type is the use of different definitions for an important parameter, such as the breaker height.

Bottom and Side Wall Friction

Damping, or a decrease in wave height due to friction, is important when breaker characteristics are related to the initial wave conditions. Experimental measurements (Iversen, 1952b) of oscillatory waves over horizontal bottoms in very narrow (1-3 inches) wave tanks showed that the wave height was appreciably dampened (Table 5-5). Studies within wave tanks of the same width (1-2 feet) as those used in the breaker experiments could not be found. Fortunately, the wave tanks of the seven oscillatory wave studies were nearly of the same width (Table 5-3) so that friction probably did not vary significantly from one experiment to another.

One solitary wave investigation reported the effect of 'bottom roughness.' Ippen and Kulin (1955), using gravel 0.013 feet in diameter, found: (1) no appreciable effect on the breakers on a 0.06 beach slope, (2) a reduction of breaker height (up to ten percent) and depth of breaking on a beach slope of 0.023, and (3) a tendency to induce spilling rather than plunging breakers.

Table 5-5. Friction effects on oscillatory wave heights (Iversen, 1952b).

Wave Data	Tank Width	
	1 Inch	3 Inches
Wave period (sec.)	1.15	1.15
Still water depth (ft.)	2.04	2.04
Wave height ratios*		
H_2/H_1	0.65	0.86
H_3/H_1	0.31	0.73
H_3/H_2	0.48	0.88

---

* Subscript 1 denotes station 1 (first station encountered by wave)

Subscript 2 denotes station 2 (19.53 feet from Sta. 1)

Subscript 3 denotes station 3 (42.97 feet from Sta. 1)

Backwash

Iversen (1952a) obtained an estimate of the backwash velocity by averaging all particle velocities in the region beneath the trough spatially preceding the breaker crest. The backwash velocity was nearly constant (0.3 feet per second) with decreasing deep water wave steepness for waves on the 0.05 and 0.02 beach slopes, but the backwash velocity increased with decreasing H_∞ / L_∞ for breakers on the 0.10 beach slope. In addition, the backwash depth was nearly half of that on the 0.02 beach slope and increased with decreasing H_∞ / L_∞ on all beach slopes. Qualitatively, he found that high backwash velocities retard the base of the wave inducing plunging rather than spilling breakers.

Solitons

Solitons (Table 5-4) were first reported by Morison and Crooke (1953) who noted that extremely shallow water waves form a second wave that travels at a slower speed than that of the original wave, producing a nonpermanent wave profile. Galvin (1968) reported that solitons occurred in 53 of 75 observations of breakers (Figure 5-8). Galvin (1968) omitted wave observations if the phase difference between the primary and soliton was such that the soliton interfered with the breaking of the primary. More recently, Galvin (1972)

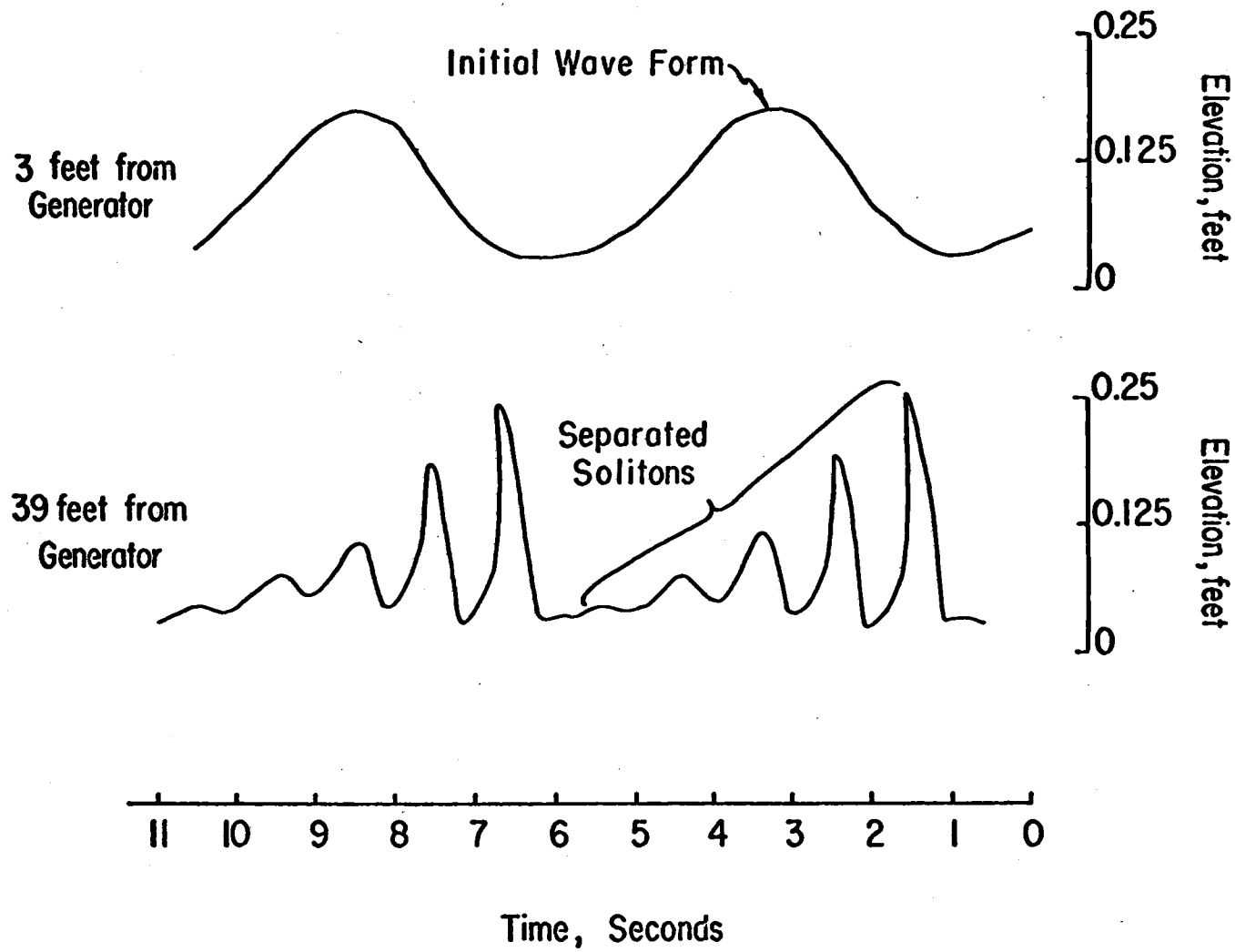

Figure 5-8. Separation of solitons from original single-crested wave. (Galvin, 1972)

published results of the breaking conditions of solitons. These results are reviewed in Chapter VI.

Wave Reflection from the Beach Slope

Galvin (1968) noted two reflected wave types, one with a shorter period than the incoming wave and one with the same period. The shorter period reflected wave was more noticeable on steeper slopes (0.20), and it effected the incoming plunging breaker by causing a sudden upward leap of the crest elevation. Although Galvin (1968) did not report any change in the breaker measurements for these plunging breakers, any variation in the breaker point on a steep beach slope would significantly change the depth of breaking.

The longer period reflected waves were more difficult to observe, and Galvin (1968) concluded that they had no noticeable effect on the breaker type. However, he found that once these waves were re-reflected from the wave generator end of the wave tank, the breaker type did change. These longer period reflected waves were more common among the surging breakers on steep slopes. By using appropriate initial wave conditions, Galvin was able to eliminate reflections on the 0.05 slope but not on the steeper slopes.

Nicholsen (1968) reported that measurable reflected waves were generated by the backwash flow of the previous breaker; the height of the reflected wave relative to the incoming wave height varied

inversely with the incident wave steepness. The ratio of the reflected wave height to the initial wave height ranged from five percent to forty percent, a considerable value.

Wave Set-Down at the Breaker Point

Wave set-down was defined in Table 5-4 as the decrease in the mean water level at the breaker point due to the presence of an incoming wave train. Table 5-6 shows the percentage of wave set-down relative to the still water depth at the breaker point for the laboratory data of Bown, Inman and Simmons (1968). This set-down, averaging 3.8% of the still water depth, was independent of the deep water wave steepness over the range tested. Since only one beach slope (0.082) was used, the dependence of this percentage on the beach slope could not be examined.

Galvin (1969) reported that the percentage of the wave set-down relative to the breaker height was 4.0% on beach slopes of 0.05 and 0.10 and 8.0% on a slope of 0.20. For comparison, this percentage was 3.1 for the data of Bowen et al. (1968).

This evidence suggests that for beach slopes less than 0.10 the mean water depth was 3.0 to 4.0% less than the still water depth at the breaker point, and that this set-down tended to increase with increasing beach slope. Because it includes the set-down at the breaker point due to the presence of waves, the depth of breaking as

Table 5-6. Wave set-down at the breaker point (Bowen et al., 1968).

Experiment	Set-down/Still Water Depth at Breaker Point (%)	Set-down/ Breaker Height (%)	H /L
71/3	4.1	3.9	0.034
71/4	3.5	3.2	0.049
51/4	3.8	2.9	0.021
51/6	4.7	3.7	0.032
51/8	4.8	4.4	0.044
35/7	3.0	2.3	0.010
35/10	3.7	2.6	0.014
35/12	2.7	2.3	0.017
35/15	4.4	3.3	0.021
24/17	3.4	2.5	0.007
24/20	4.1	3.0	0.009

Wave tank dimensions: 131 feet long, 1.64 feet wide, 2.46 feet deep

measured to the mean water level rather than the still water level may be the appropriate choice for h_b.

Edge Waves and Rip Currents

Edge waves and the associated rip currents (defined in Table 5-4) are generated from the energy and momentum of the incoming waves in a way not yet well understood. Once the edge waves are in existence, they superpose themselves on the incoming waves as shown schematically in Figure 5-9 (Bowen and Inman, 1969). Edge waves may cause significant longshore variations in breaker height, depth of breaking, and in distance of the breaker point from shore. Table 5-7 (Bowen and Inman, 1969) shows the effect of standing edge waves and rip currents on these breaker parameters in a wave basin (basins are approximately equal in width and length, while wave tanks are long and narrow). These measurements confirm the theoretical schematic of the summation of the incoming and standing edge waves shown in Figure 5-9. The antinode-rip current position has the lowest breaker height, and the antinode-no-rip position has the highest breaker height. Also, the ratio H_b/h_b was different at these two positions.

The effects of edge waves on breaker measurements will depend on the measuring techniques. For all of the studies reviewed, the breakers were filmed through the side of glass-walled wave tanks.

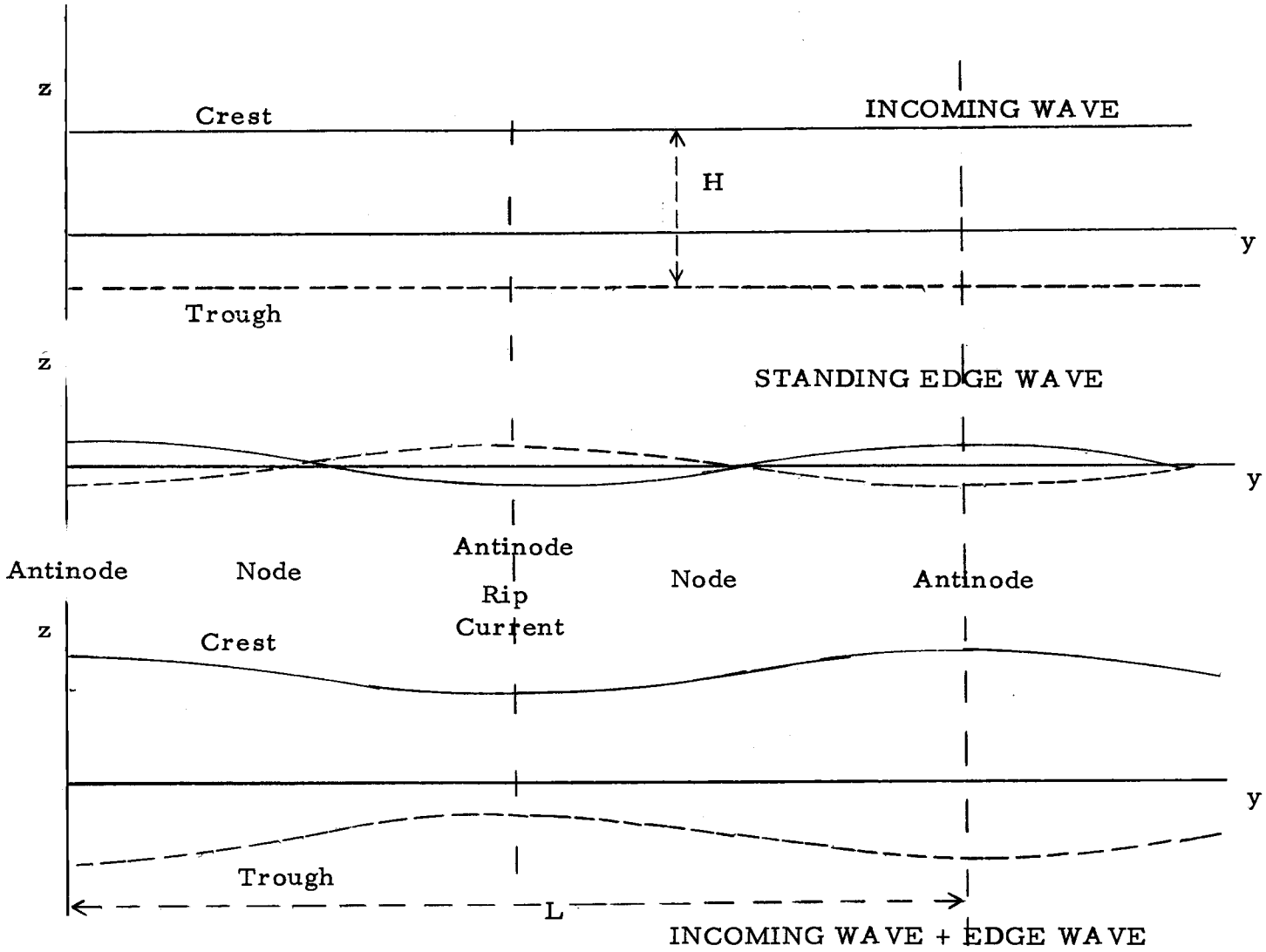

Figure 5-9. The interaction near the breaking position between the incoming wave and a standing edge wave of the same period. (Bowen and Inman, 1969).

Table 5-7. Observations of the longshore variations of breaker height, incident wave period 5.00 seconds (Bowen and Inman, 1969).

	Antinode Rip		Node		Antinode No Rip
Longshore distance * (cm)	0	72	144	216	288
Breaker Height (cm)	2.05	2.22	2.41	2.93	3.18
Distance of breaker from Still Water Level intersection with Beach Slope (cm)	34	34	34	37	40

Basin Dimensions: 50' x 60'

Working Section: 24' wide, bounded by smooth barriers that extended seaward from the top of the beach for 16'

* Distance from the right-hand barrier, facing seaward

In these cases, the measurements will contain the effects of either the antinode-rip position or the antinode-no-rip position because an antinode must be present at the wall. At the antinode-rip position, the breaker height may be decreased by the lower effective wave height, and/or premature breaking may be induced by the opposing, seaward flowing rip currents. At the antinode-no-rip position the effective breaker height is increased because the breaker and edge wave are in phase (Figure 5-9). Komar (per communication, 1973) has indicated that in the study of Komar and Simmons, edge waves found across the wave tank presented considerable difficulties at some wave periods, so much so, that the results had to be disregarded. With edge waves present a given wave crest would begin to break at one side of the tank and progressively move across the tank width. The crest may have moved 50 centimeters after the first breaking occurred and before the entire wave crest was breaking. The edge wave could also be observed in the run-up on the sloping beach, but no true distinct rip current could be seen.

The possible occurrence of standing edge waves and rip currents has not been systematically investigated. Following Bowen and Inman (1969), Table 5-8 shows the resonant periods for standing edge waves in wave tanks with dimensions characteristic of those in breaker studies. The standing edge wave period is given by

$$(5\text{-}4) \qquad T = 2(\pi b/(gm\,(2n+1)\,\tan\beta))^{\frac{1}{2}}$$

Table 5-8. Resonant periods of standing edge waves in a specified wave tank. (seconds) (After Bowen, 1969).

Tank Width (ft.) ------ 1.0	Beach Slope ------ 0.05			
Longshore Modal Number m:	1	2	3	4
Offshore Modal Number n:				
0	2.80	1.98	1.62	1.40
1	1.61	1.14	0.94	0.81
2	1.25	0.89	0.73	0.63
3	1.06	0.75		

Tank Width (ft.) ------ 1.5	Beach Slope ------ 0.10		
Longshore Modal Number m:	1	2	3
Offshore Modal Number n:			
0	1.98	1.40	1.15
1	1.14	0.81	0.60
2	0.89	0.63	0.52

where b is the wave tank width, $\tan\beta$ the beach slope, m the longshore modal number, and n the offshore modal number. The longshore modal number, m, is a result of the solid barriers which run perpendicular to the shoreline and restrict the possible longshore wave lengths of the standing edge wave (Figure 5-9). The offshore modal number, n, is one of the results of shallow water edge wave theory (Eckart, 1951) and equals the number of zeros of the surface elevation in the direction perpendicular to shore. Although the modal numbers most likely to occur cannot be theoretically predicted, Bowen and Inman found that a normally incident wave train excited a longshore mode that had a resonance period near the incident wave period. Since many of the resonant edge wave periods are nearly the same as those of the generated waves, the possibility of generating edge waves may be considerable.

Seiching

Measurements of eleven successive breakers in the Beach Erosion Board wave tank (SIO Wave Report 47, 1945) had an average breaker height of 0.275 feet with heights ranging from 0.245 feet to 0.296 feet. This variation was attributed by the investigators to seiching or surging along the length of the tank. However, since none of the more recent experiments report seiching effects, the significance of the surging on breaker parameters remains unresolved.

Variable Beach Slope

One oscillatory wave experiment contains measurements of waves that have traveled over a spatially varying beach slope in which a steep slope was seaward of a gentler slope (Figure 5-6). This change in slope with distance from the beach has been termed the 'reef effect' (SIO Wave Report 47, 1945). The Berkeley wave tank data (Munk, 1949) reported a constant beach slope of 0.009, but this slope actually followed 4.6 feet of 0.45 slope. The Type II beach slope (Figure 5-7) that was present in the study of Pacific Ocean breakers is also an example of the reef-type slope. When the depth shoreward of the discontinuity in slope increases towards shore, an offshore bar is indicated.

For the Berkeley wave tank experiment, all of the waves but one broke within one foot of the upper end of the steep slope, indicating that the reef effect may cause early breaking, and early breaking means an increase in the depth of breaking. In addition, some of these waves reformed and broke again further inshore. It may be concluded that breaker data for reef-type beach slopes are not representative of measurements which would be obtained for the gentler beach slope alone. Chapter VI reviews the results of breaker measurements taken over reef-slopes for the Pacific Ocean study at Scripps pier.

Nonuniformity of Experimental Design

One problem in comparing the results of two or more experiments is the lack of data which have identical initial wave heights, water depths, or H_i/h_i. This problem is important because of the practice of reporting the breaker measurements as a function of the theoretical deep water wave steepness. Since Iversen (1952a) has shown that the small amplitude theory does not accurately predict the change in wave height with decreasing depth for waves on constant beach slopes, this practice is not a good one.

If all of the studies had used the same initial relative depth (h_i/L_∞), then the error due to the use of the theoretical wave steepness would be constant. But a wide range of relative depths were used (Table 5-3), and each relative depth has an associated error in back-predicting the deep water wave steepness. An estimate of the error which this has on the deep water wave steepness may be obtained from Iversen (1952a), in which deep water waves were generated and followed shoreward. For a beach slope of 0.054, his results show that at a relative depth of 0.15, H/H_∞ measured was 12% less than H/H_∞ predicted by Airy wave theory. This was the largest difference for the three cases Iversen tested.

Another problem with experimental design was the use of different definitions for breaker parameters. Table 5-9 shows three

Table 5-9. Parameters with more than one definition.

Initial Wave Height

1. Measured vertical distance from crest to trough. Iversen (1952a), Komar and Simmons (1968).
2. Computed from linear theory for the given displacement of the wave generator. Galvin (1968).

Breaker Height

1. Measured vertical distance from breaker crest to trough preceding crest. Iversen (1952a), Komar and Simmons (1968).
2. Measured vertical distance between the maximum and minimum water surface elevations at the breaker point. Galvin (1968).
3. Measured vertical distance from breaker crest to still water level. Nicholson (1968).

Breaker Depth

1. Measured vertical distance from the bottom to the still water level at the breaker point. Iversen (1952a), Komar and Simmons (1968).
2. Measured vertical distance from the bottom to the mean water level. Galvin (1968).

parameters which were defined in two or more ways. Galvin (1968, 1969) reported that his definition of the initial wave height predicted higher values than Iversen's (1952a) definition, but he did not quantify this statement. Also, the three different definitions of breaker height lead to considerable confusion in comparing the studies: for example, Nicholsen's breaker height definition yields H_b values that are 25% to 40% lower than the values obtained using the Iversen definition when applied to the data of Komar and Simmons (1968).

CHAPTER VI

RESULTS OF SHALLOW WATER BREAKER EXPERIMENTS

The preceding chapter examined experimental methods of studies concerned with progressive water waves breaking in shallow water, and in Chapter IV, theoretical breaking criteria for shallow water waves were reviewed. With this information as background, the results of experiments on breaking waves are presented. Solitary and oscillatory wave investigations are reviewed separately. The measurements of ocean waves breaking on sand beaches constitute the final section.

1. Review of Solitary Breaker Measurements

Water of Constant Depth

In Chapter IV estimates of the maximum ratio of H/h for the limiting steady solitary wave were based on one of the following conditions: (1) the horizontal particle velocity at the crest just equaling the wave phase velocity, (2) the vertical particle velocity near (but not at) the crest approaching zero as the ratio H/h increases, or (3) the vertical pressure gradient beneath the crest approaching zero as H/h increases. These estimates of $(H/h)_{max}$ are listed in Table 4-1.

None of these limiting conditions has been tested experimentally for solitary waves in water of constant depth. In addition, very few studies designed to verify these $(H/h)_{max}$ values have been conducted. During an investigation whose primary purpose was to measure solitary breakers over sloping beaches, Ippen and Kulin (1955) did run some tests to determine the highest stable wave in the constant depth section of the wave tank. The largest, stable solitary wave had an $(H/h)_{max}$ value of 0.72. Confirmation of this value was reported in 1969 by Camfield and Street who found $(H/h)_{max} = 0.73$. However, neither of these studies published further details on this part of their experiment, making a discussion of the reliability of these estimates impossible.

Constant Beach Slope

Although there are no theoretical breaking criteria for solitary waves shoaling over constant beach slopes, several experiments (Ippen and Kulin, 1955; Camfield and Street, 1966, 1969; Kishi and Saeki, 1966) have measured the breaker height and depth of breaking (where both are referenced to the still water level). The results of these experiments are summarized in Figure 6-1. The curves in Figure 6-1a are visual best fits to the actual data points. General trends to these solitary breaker measurements are:

1. H_b/h_b increases with increasing beach slope.

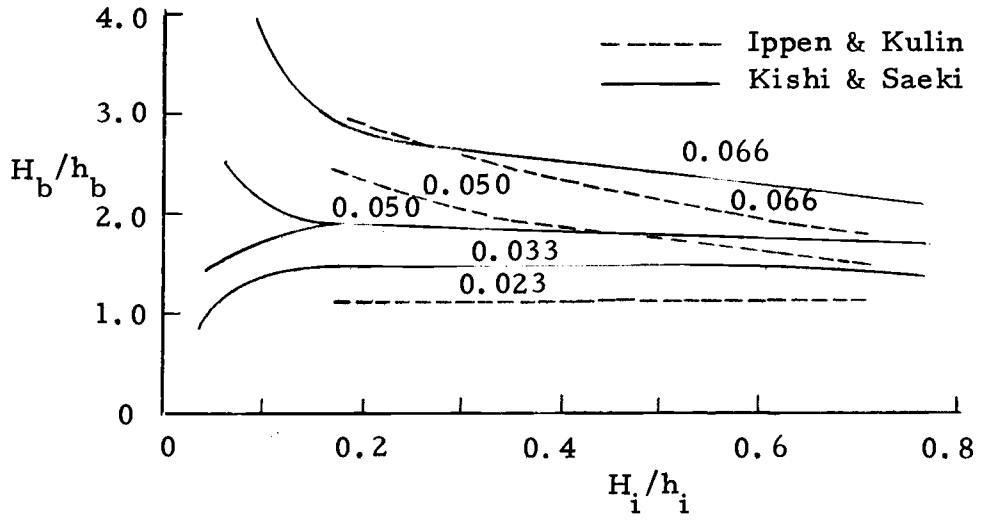

Figure 6-1a. Relation of H_b/h_b to H_i/h_i on various slopes.

(Kishi & Saeki, 1966)

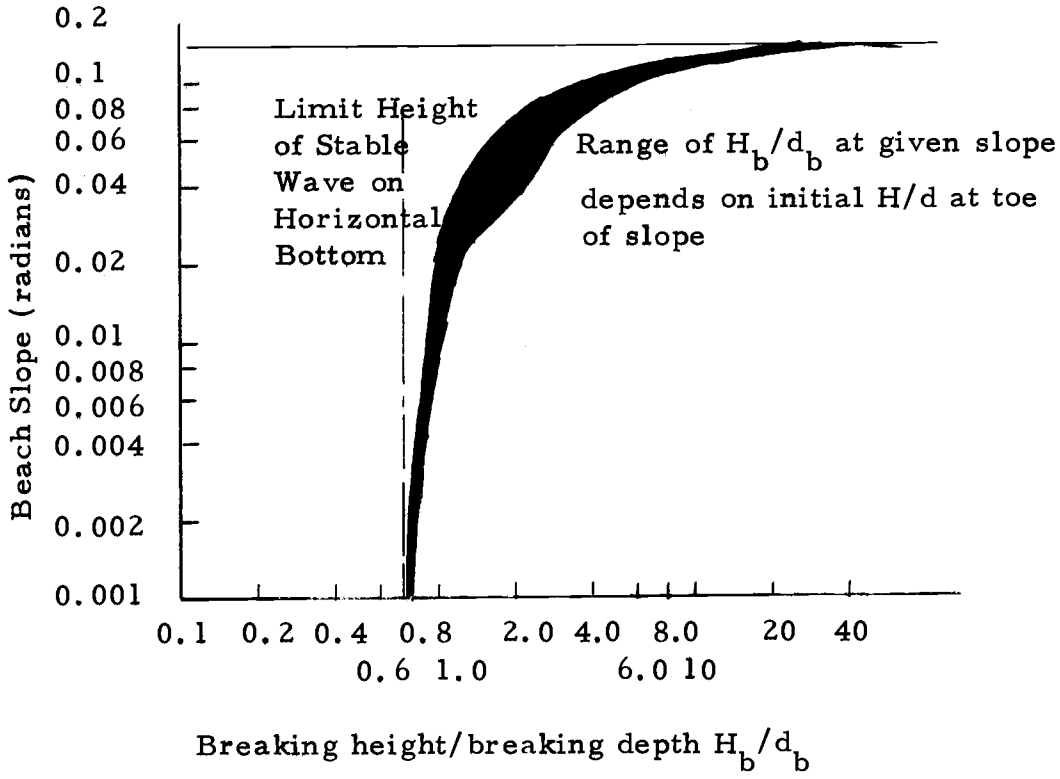

Figure 6-1b. Relation of H_b/h_b to H_i/h_i and the beach slope for solitary waves. (Camfield & Street, 1966)

2. H_b/h_b increases with decreasing H_i/h_i.

3. Breaking does not occur for beach slopes steeper than 0.15.

One exception to these general statements is that H_b/h_b behaved irregularly for H_i/h_i less than 0.15 for all beach slopes.

Since both H_b and h_b vary with beach slope and H_i/h_i, the changes in H_b/h_b depend on the relative changes in and the absolute values of the numerator (H_b) and denominator (h_b). Using the data of Ippen and Kulin (1955), Figure 6-2 was prepared to examine the changes in H_b/h_b with these two parameters. The initial water depth (h_i) was chosen as the common denominator for H_b and h_b because of the ease in visualizing the effects of a decrease in the initial wave height as the initial water depth is held constant; this is the process of generating lower and lower waves over the same initial depth. The separate curves of H_b/h_i and h_b/h_i each decrease as H_i/h_i decreases. This is to be expected since (1) lower initial waves will travel further up the beach before breaking, which decreases h_b, and (2) the lower initial wave heights result in lower H_b relative to the constant initial water depth.

These curves qualitatively explain the variation in H_b/h_b for decreasing H_i/h_i for each beach slope. The curves of H_b/h_i and h_b/h_i for the 0.023 beach slope are parallel and lie very close to one another with H_b/h_i slightly larger; H_b/h_b is approximately equal to 1.2. As the beach slope increases (Figure 6-2b and c), the h_b/h_i

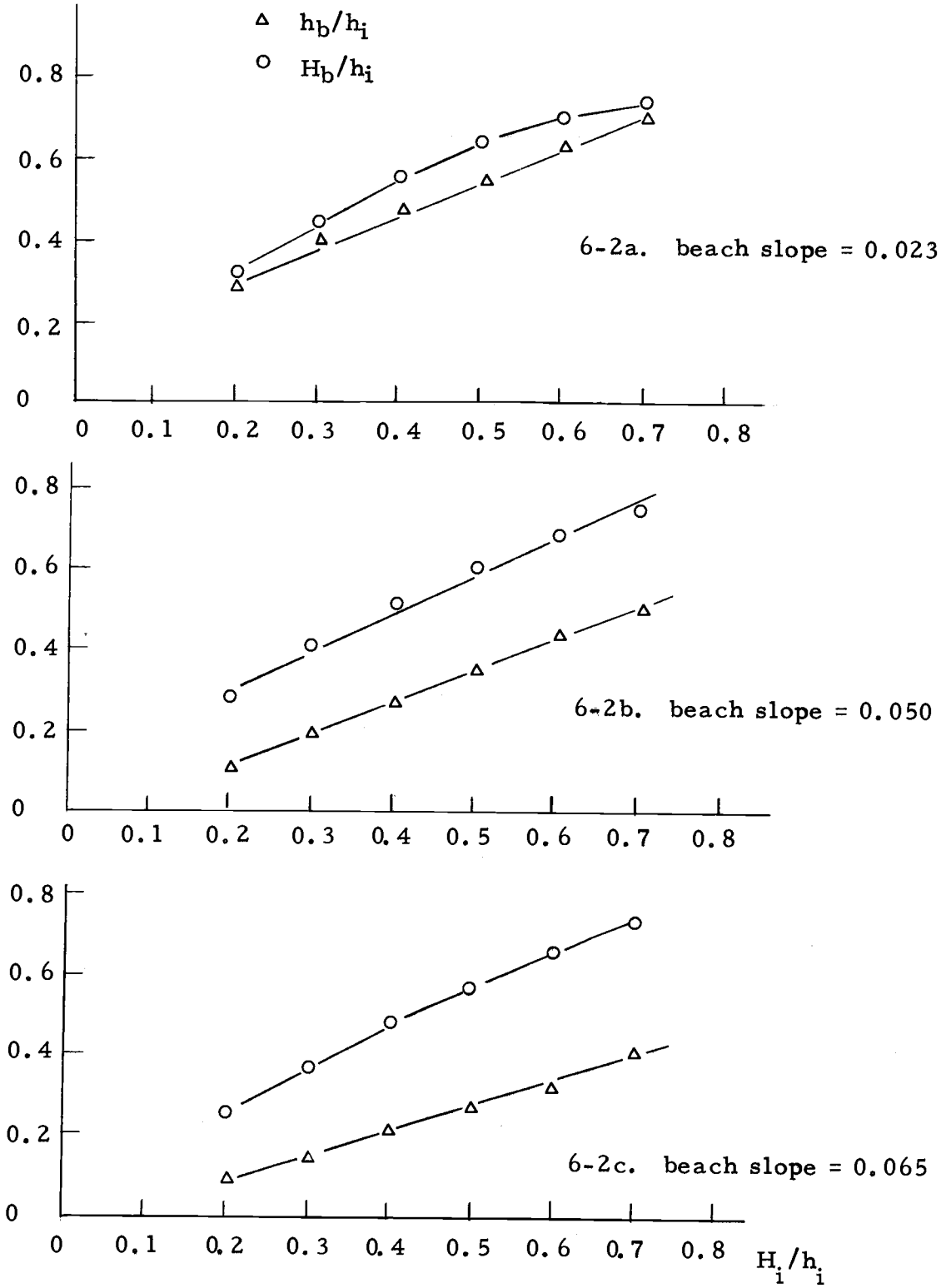

Figure 6-2. H_b/h_i and h_b/h_i dependence on H_i/h_i and beach slope for solitary breakers.

curve lies at progressively lower values; H_b/h_b increases with beach slope. The increase of H_b/h_b with increasing beach slope and decreasing H_i/h_i is primarily due to the lower depths of breaking. The lower depths of breaking are qualitatively explained by the slow rate of change of the wave deformation relative to the rate of travel of the wave up the steep beach slopes.

Although these studies were primarily concerned with the measurements of breaker heights and depths of breaking, the experiments of Ippen and Kulin (1955) did include some measurements of the breaker phase velocity and water particle velocity at the breaking position. For a beach slope of 0.023 and $H_i/h_i = 0.48$, they obtained $u_{max}/c_b = 0.85$, and for a beach slope of 0.065 and $H_i/h_i = 0.64$, $u_{max}/c_b = 0.84$.

The major results of the solitary breaker experiments are:

1. Measurements of $(H/h)_{max}$ for solitary waves in water of constant depth are in good agreement with the theoretical estimates of $(H/h)_{max}$ for solitary waves in water of constant depth limited by the conditions described above. Unfortunately, the experiments do not provide conclusive evidence determining which of the three suggested breaking criteria may be correct.

2. Marked disagreement is found between measurements of H_b/h_b for initially solitary waves which break on constant beach slopes and theoretical estimates of $(H/h)_{max}$ for solitary waves in

water of constant depth. This is clearly shown in Figure 6-1b where the disagreement is seen to increase with increasing beach slope. However, H_b/h_b does approach the theoretical $(H/h)_{max}$ value as the slope decreases.

2. Review of Oscillatory Breaker Measurements

Water of Constant Depth

Theoretical breaking criteria for oscillatory waves in water of constant depth are: (1) the horizontal particle velocity just exceeding the wave phase velocity, (2) the vertical particle velocity near (but not at) the crest approaching zero as H/h increases, and (3) the vertical pressure gradient beneath the crest approaching zero as H/h increases. Measurements of the parameters of maximum steady oscillatory waves in water of constant depth include: wave height, water depth, wave length, wave phase velocity, and the particle velocity at the crest. With these measurements, tests of u_{max}/c, $(H/h)_{max}$, $(H/L)_{max}$, and c_{max}/c_{airy} can be made.

The measurements and calculated ratios for these tests of the theoretical breaking criteria obtained by Morison and Crooke (1953) are given in Figure 6-3 and Table 6-1 and those of Danel (1952) in Figure 6-3. From this data it may be concluded that none of the theoretical breaking criteria have yet been confirmed experimentally.

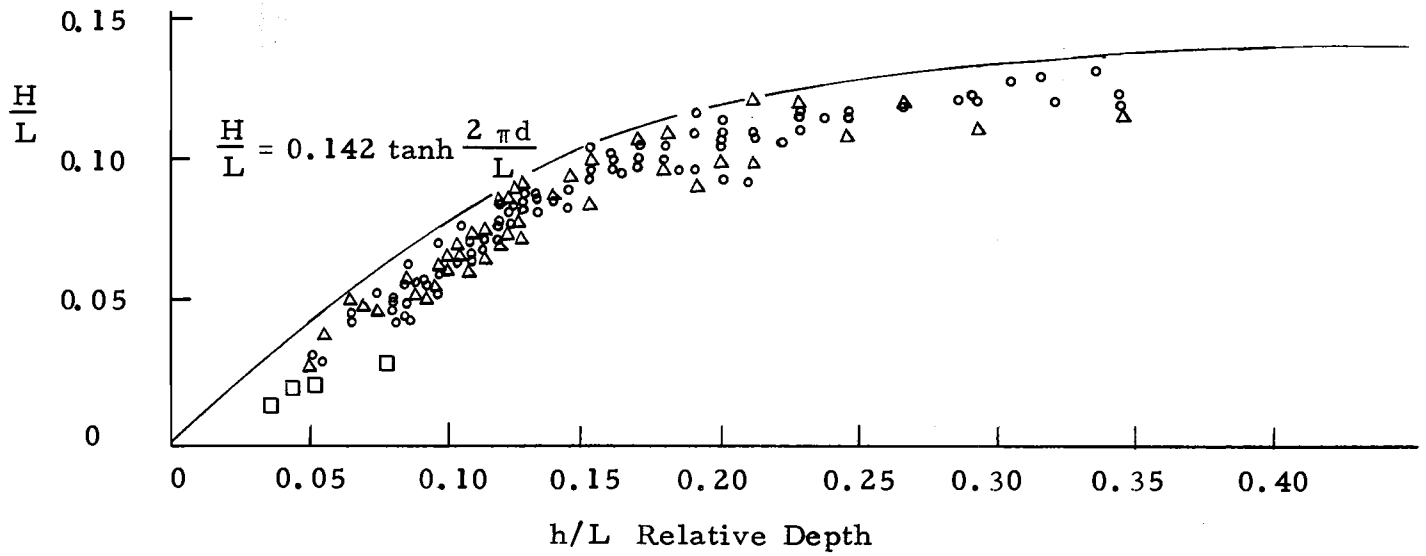

Danel (1952) ○ before breaking × after breaking

Morison & Crooke (1953) △

Figure 6-3. Limiting wave steepness for oscillatory waves over horizontal bottoms (Wiegel, 1964).

Table 6-1. Measurements of waves of maximum steepness over horizontal bottoms (Morison and Crooke, 1953)

H (ft)	L (ft)	T (sec)	h (ft)	H/L	h/L	C (ft/sec)	u_{max} (ft/s)	u_{max}/C	C_t* (ft/s)	C/C_t	H/h
0.097	2.66	0.91	0.29	0.036	0.110	2.54	--	--	3.05	0.83	0.33
0.100	2.66	0.93	0.29	0.038	0.110	2.54	--	--	3.05	0.83	0.34
0.120	3.71	1.27	0.29	0.032	0.079	2.70	0.90	0.33	3.05	0.89	0.41
0.109	3.71	1.32	0.29	0.029	0.079	3.25	1.00	0.31	3.05	1.06	0.38
0.106	5.10	1.62	0.29	0.021	0.057	2.83	0.51	0.18	3.05	0.93	0.37
0.105	5.10	1.62	0.29	0.021	0.057	3.64	0.91	0.25	3.05	1.19	0.36
0.137	6.58	2.09	0.29	0.021	0.044	2.78	0.73	0.26	3.05	0.91	0.47
0.125	6.58	2.13	0.29	0.019	0.044	3.20	0.87	0.27	3.05	1.05	0.43
0.126	6.32	2.67	0.29	0.016	0.035	3.28	--	--	3.05	1.08	0.43
0.126	6.32	2.67	0.29	0.016	0.035	4.00	1.00	0.25	3.05	1.31	0.43

0.020 0.046

---

* $C_t = (gh)^{\frac{1}{2}}$

The largest value of u_{max}/c is 0.33, and the maximum $(H/h)_{max}$ = 0.47. Figure 6-3, which compares $(H/L)_{max}$ values to the theoretical curve of Miche (1944), is evidence that the experimental points are consistently lower than the theoretical values. The limiting wave steepness data of Danel were not described in any detail in that paper, making impossible a discussion of the possible reasons for the experimental values being lower than the theoretical values. As noted by LeMehaute (1968) these wave steepness data are in better empirical agreement with the relation

$$(6\text{-}1) \qquad (H/L)_{max} = 0.12 \tanh \left(\frac{2\pi h}{L}\right) \quad .$$

Constant Beach Slope

Since there are no theoretical predictions of the breaking parameters which take into consideration the sloping beach, this section is limited to examining only empirical results. Appendix I contains a list of the breaker measurements for waves on sloping beaches.

Because the Iversen (1952a) data have been relied upon for nearly two decades as the major laboratory study of breaking waves, it is important to determine if his measurements are true representatives of breaking wave data. For this purpose, the unpublished study of Komar and Simmons (1968) is considered to be the best test for three reasons: (1) they used the same definitions for the breaker

parameters as Iversen, (2) they reported the initial wave height and initial water depth, and (3) they generally attempted to use the same methods as Iversen.

The breaker measurements of interest are H_b and h_b. These are presented in the customary format (i.e., H_b/H_∞ vs. H_∞/L_∞ and H_b/h_b vs. H_∞/L_∞) because attempts by this author to relate H_b and h_b to the measured parameters H_i, h_i, and T did not produce any additional insight (these attempts were made difficult by the failure of both studies to report the breaker type, leaving unknown the breaker shape).

Figure 6-4 is a plot of H_b/H_∞ versus H_∞/L_∞ for the data of Iversen (1952a). There appears to be a systematic relationship between H_b/H_∞ and the beach slope; H_b/H_∞ increases with increasing beach slope. Figure 6-5 is a similar plot for the data of Komar and Simmons, and, in this case, there does not appear to be a systematic trend to H_b/H_∞ with respect to changes in the beach slope.

The beach slopes used by Iversen were 0.020, 0.033, 0.050, and 0.10. Since Figure 6-4 gives only a qualitative indication of the correlation, Table 6-2 was constructed to further test this dependence. The H_b/H_∞ values in this table are averages of the individual values in each H_∞/L_∞ interval. The wave steepness range was divided into uniform intervals to avoid excessive weighting by many H_b/H_∞ values which fall within a narrow interval of H_∞/L_∞.

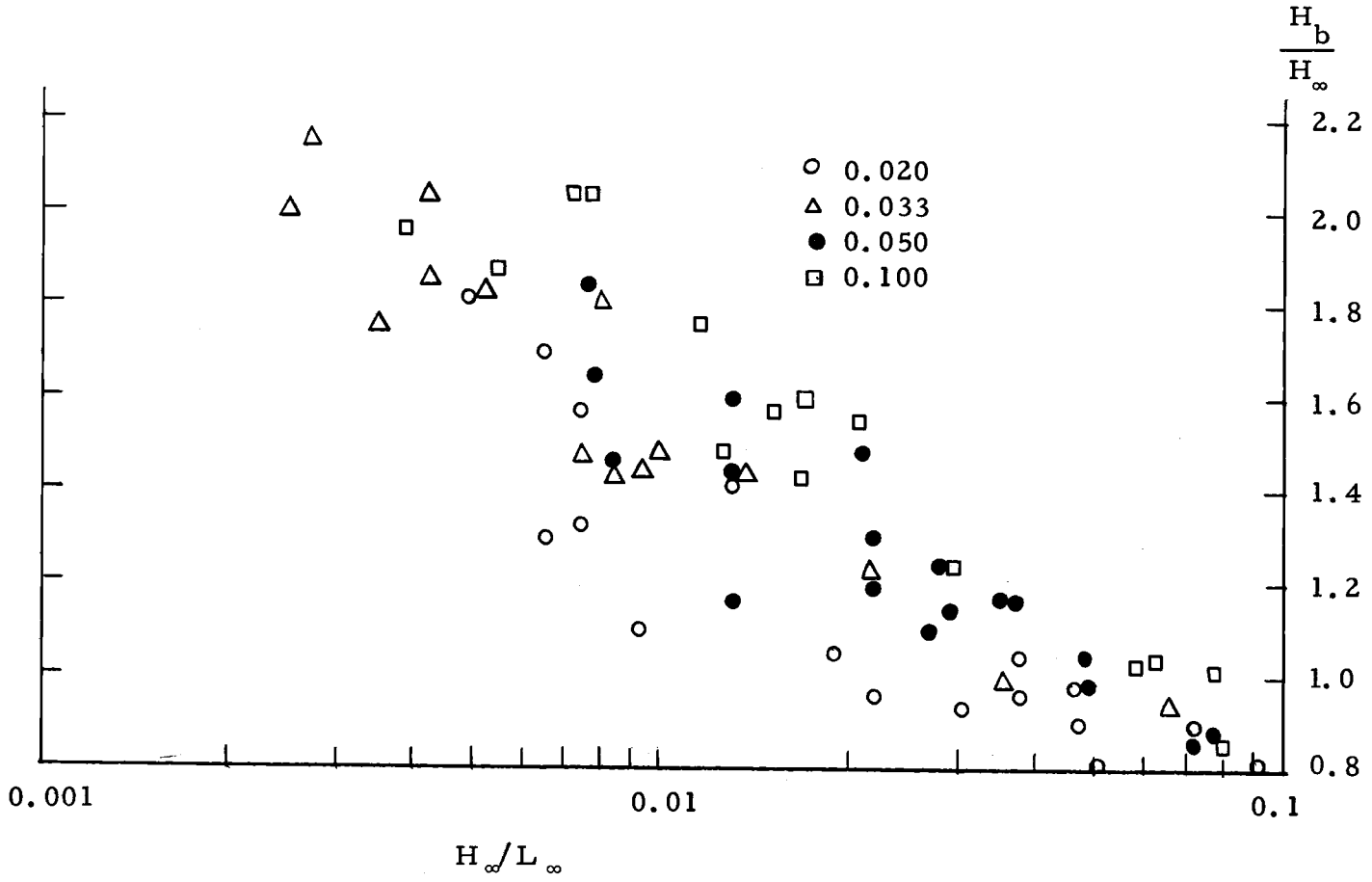

Figure 6-4. H_b/H_∞ versus H_∞/L_∞ (Iversen, 1952a).

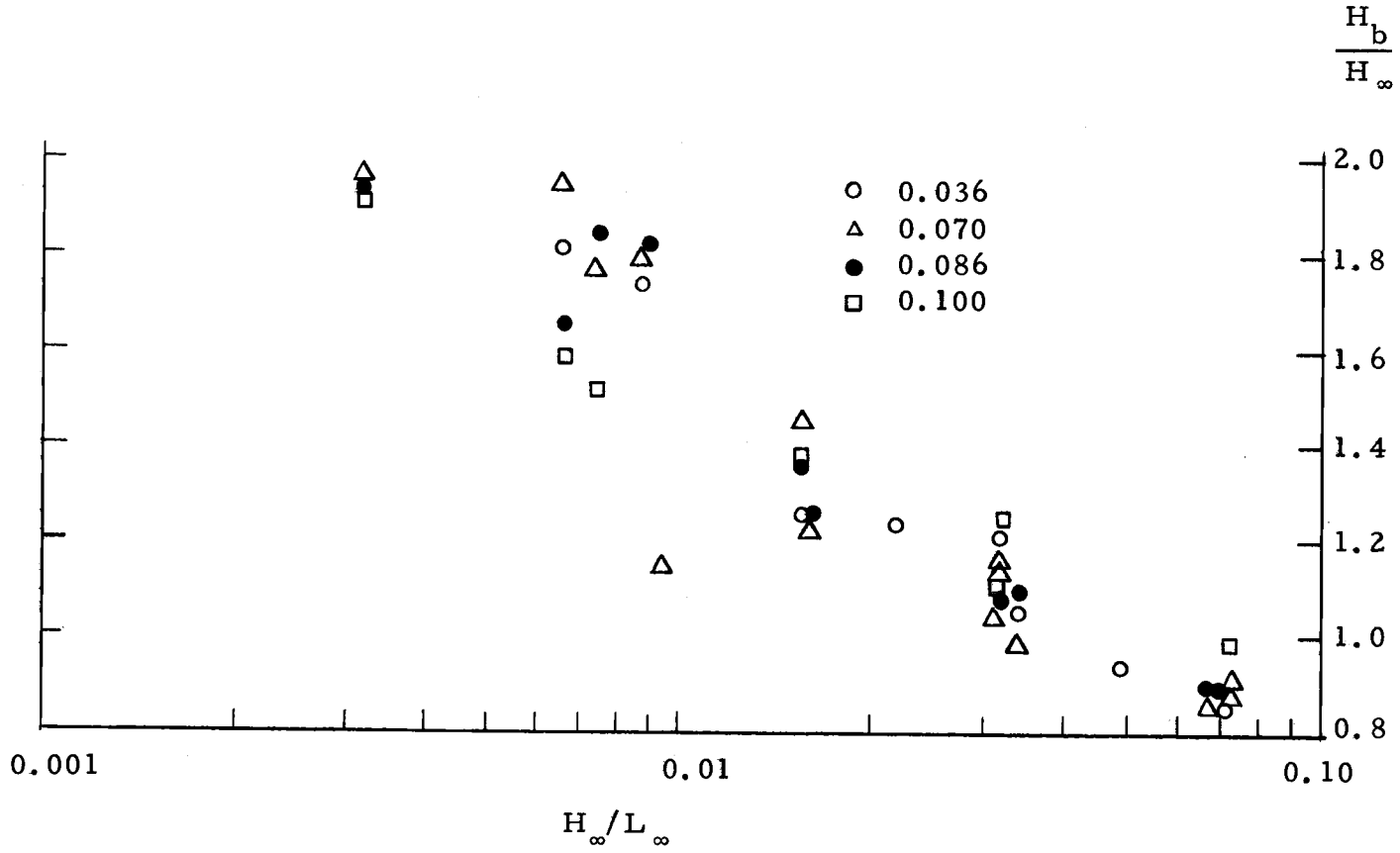

Figure 6-5. H_b/H_∞ versus H_∞/L_∞ (Komar and Simmons)

Table 6-2. Average values of H_b/h_b and H_b/H_∞ as a function of beach slope (m) and deep water wave steepness (H_∞/L_∞).

I. H_b/H (Iversen, 1952a)

H_∞/L_∞:	0.0076-0.0176	0.0177-0.0276	0.0277-0.0376	0.0377-0.0476	0.0477-0.0580
m=0.020	1.35	1.01	0.97	0.94	0.86
m=0.033	1.53	1.22	0.99	none	none
m=0.050	1.53	1.27	1.18	1.02	none
m=0.100	1.65	1.55	1.25	none	1.03

II. H_b/h_b

1. Iversen (1952a)

H_∞/L_∞:	0.0076-0.0176	0.0177-0.0276	0.0277-0.0376	0.0377-0.0476	0.0477-0.0580
m=0.020	0.88	0.87	0.81	0.85	0.84
m=0.033	0.74	0.82	0.75	none	none
m=0.050	0.90	0.86	0.90	0.79	none
m=0.100	1.13	1.23	1.00	none	0.79

2. Komar and Simmons (1968)

H_∞/L_∞:	0.0066-0.0196	0.0197-0.0326	0.0329-0.0456	0.0457-0.0586	0.0587-0.0716
m=0.036	0.83	0.82	0.80	0.93	0.69
m=0.070	1.06	0.95	0.94	none	0.78
m=0.086	1.02	0.99	0.97	none	0.79
m=0.105	0.99	0.98	0.94	none	0.88

The range of H_∞/L_∞ (i.e., 0.0076-0.058) was chosen because it is the widest range which is covered by all four beach slopes; some of the beach slopes have data beyond these limits while others do not. The results in Table 6-2 confirm the dependence for the Iversen data between H_b/H_∞ and the beach slope. Computing the average H_b/H_∞ for each of the two extreme beach slopes, we obtain $(H_b/H_\infty) = 1.05$ for $m = 0.02$ and $(H_b/H_\infty) = 1.37$ for $m = 0.10$.

The dependence of H_b/H_∞ on the deep water wave steepness was recently re-examined by Komar and Gaughan (1973). Using $H_b/h_b = \alpha_b$ as a critical similarity criterion but without reference to the solitary wave theory, applying instead Airy wave theory, and assuming conservation of energy flux, they obtained the relationship

$$(6\text{-}2) \qquad H_b = \left| \frac{(g\,\alpha_b)^{\frac{1}{2}}}{4\pi}\, T\, H_\infty^2 \right|^{2/5}$$

When H_b versus $g^{1/5}\,(H_\infty^2\,T)^{2/5}$ is plotted for the data of Komar and Simmons, the linear relationship

$$(6\text{-}3) \qquad H_b = 0.39\; g^{1/5}\; (T\,H_\infty^2)^{2/5} \quad ,$$

fits this data well, with very little scatter. The Iversen data, the field measurements presented in Munk (1949), and the Galvin (1968) data are also in good agreement with equation (6-3). By using the relationship $L_\infty = gT^2/2\pi$ between the deep water wave length L_∞ and the period T, equation (6-3) can be modified to the

dimensionless form

$$(6\text{-}4) \qquad H_b/H_\infty = 0.56/(H_\infty/L_\infty)^{1/5} \quad .$$

This relationship is similar to that obtained by Munk (1949) using solitary wave theory, the principal difference being that H_∞/L_∞ is to the -1/5 power rather than to the -1/3 power. It is also very close to the empirical equation of LeMehaute and Koh (1967) which gives H_∞/L_∞ to the -1/4 power. Figure 6-6 is the well-known graph of H_b/H_∞ versus H_∞/L_∞ from Munk (1949) showing the line from solitary wave theory fitting the data best for low H_∞/L_∞ values and a line at high wave slopes from regular Airy wave theory. Connecting the two, at intermediate values is an empirical line through the data. Superimposed on this graph is the line (solid) corresponding to equations (6-3) and (6-4). It is seen that this curve fits the data very well over the entire range of H_∞/L_∞ values, nearly lying atop the empirical curve of Munk.

Figures 6-7 and 6-8 are graphs of H_b/h_b, respectively, for the measurements of Iversen and Komar and Simmons. For the Iversen data, H_b/h_b for the steepest beach slope (0.10) is consistently larger than H_b/h_b for the other beach slopes, and, for the Komar and Simmons data, H_b/h_b for the lowest beach slope (0.036) is consistently lower than H_b/h_b for the larger beach slopes. Using the same wave steepness intervals as before, Table 6-2(II) shows the

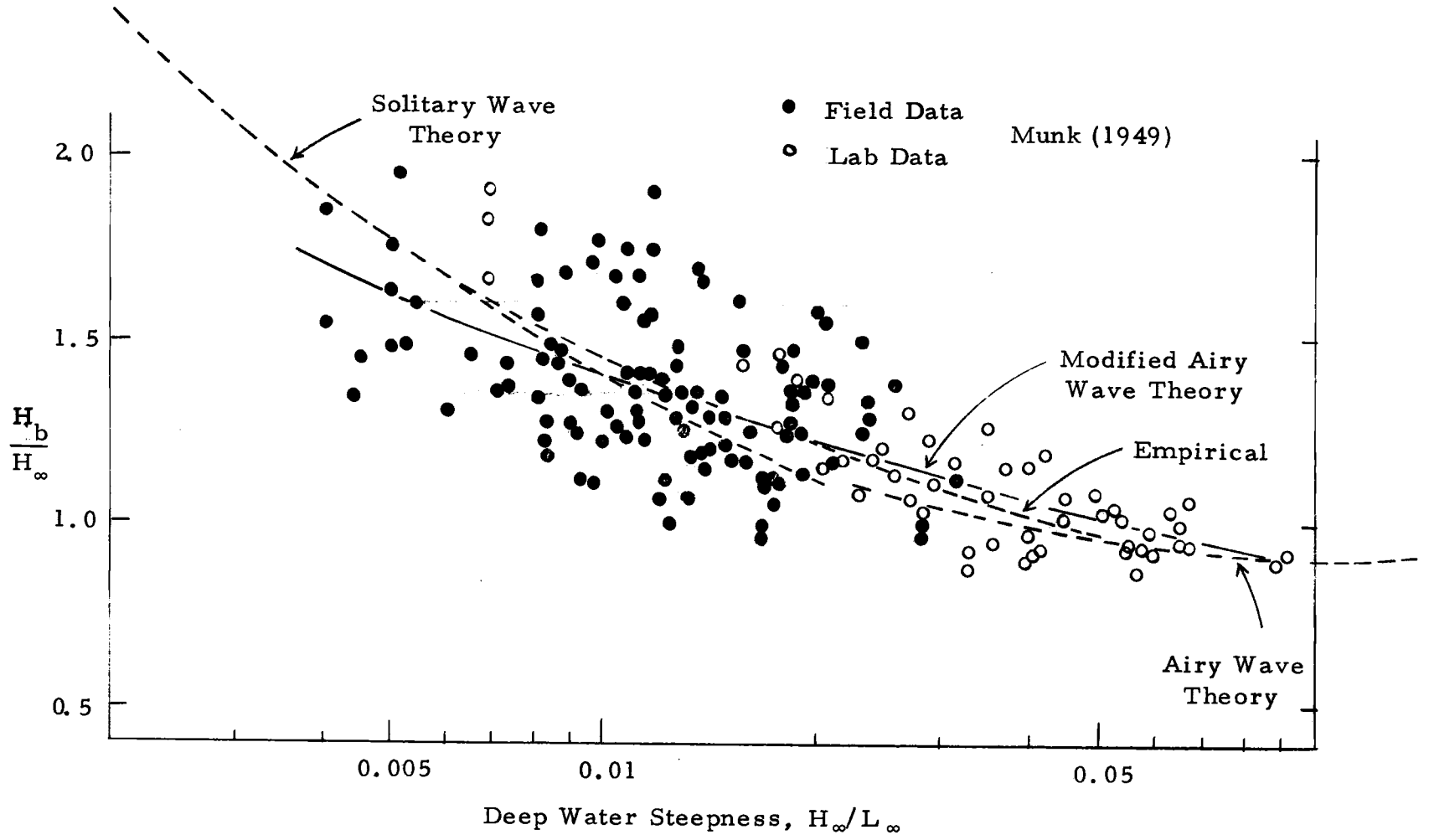

Figure 6-6. H_b/H_∞ versus H_∞/L_∞ (after Munk, 1949).

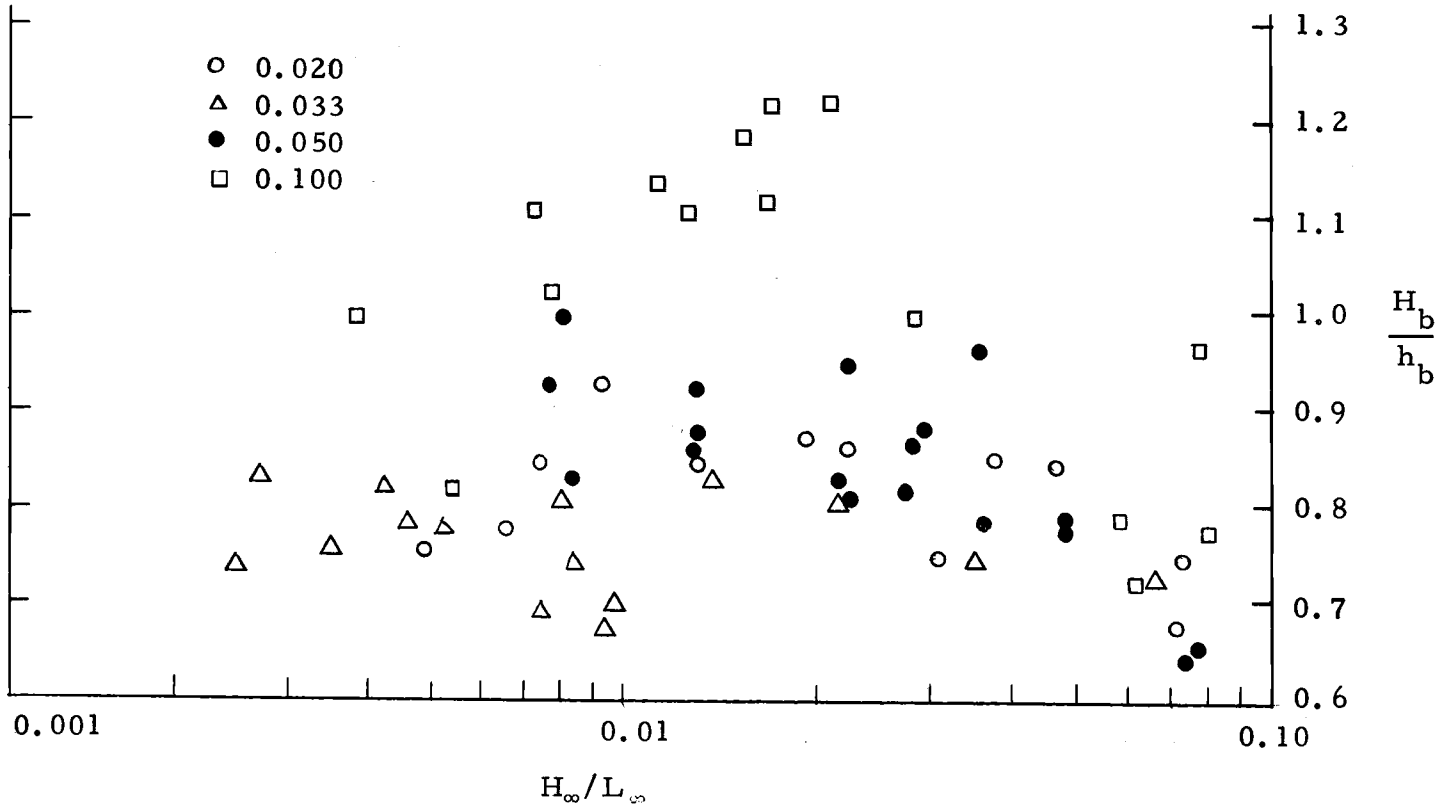

Figure 6-7. H_b/h_b versus H_∞/L_∞ (Iversen, 1952a).

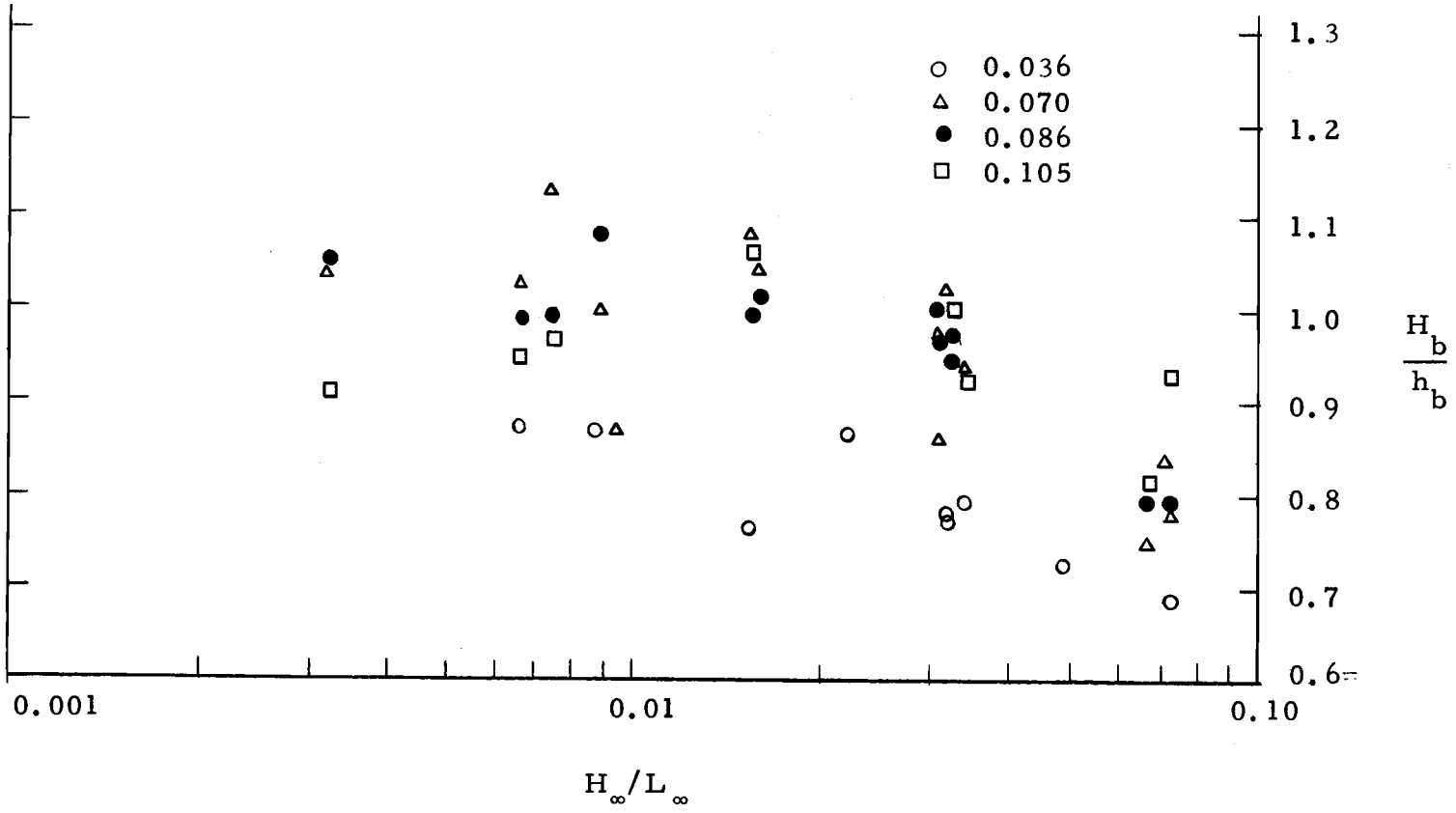

Figure 6-8. H_b/h_b versus H_∞/L_∞ (Komar and Simmons)

average H_b/h_b within these intervals for each of the beach slopes. The trend of increasing H_b/h_b with increasing beach slope is not as obvious as the trend of increasing H_b/H_∞ ; the data for the intermediate beach slopes (i.e., 0.033 and 0.050) do not substantiate the trend indicated by the data for the two extreme slopes. The average H_b/h_b for the two extreme beach slopes are 0.85 for m = 0.02 and 1.04 for m = 0.10. Table 6-2(2) constructed from the data of Komar and Simmons shows essentially the same results. Again, the results for the intermediate beach slopes do not conform to the trend exhibited by the extreme slopes.

Although these data were not from experiments designed to accurately test or determine breaking criteria, they do indicate the general trends of H_b/h_b and H_b/H_∞ as the beach slope and deep water wave steepness are varied. The omission of the reporting of breaker type hinders making any conclusions regarding the relationship between the changes in wave shape as the wave shoals and possible breaking criteria. A secondary conclusion resulting from the comparison of the Iversen and Komar and Simmons data is that the two sets of data are in general agreement although differing in some details and are therefore to be relied upon. One unexplained discrepancy is the trend of increasing H_b/H_∞ with increasing beach slope present in the Iversen measurements and not present in the Komar and Simmons measurements.

This discrepancy between Iversen and Komar and Simmons may be partially resolved by comparing their results to a third set of data. For this purpose, the data of Galvin (1968) is best suited because it has the widest range of beach slopes (0.05 - 0.20). Table 6-3 shows the average values of H_b/H_∞ within uniform intervals of deep water wave steepness for this data. Although the measurements are not uniformly spread over these intervals, the results indicate that Galvin's data, like that of Komar and Simmons, do not substantiate the slope dependence found in the Iversen data.

Since Galvin utilized different definitions for the breaker height (H_b), depth of breaking (h_b), and initial wave height (H_i) (see Chapter V), the absolute values of H_b/H_∞ are not directly comparable to either of the other two sets of data. One further point of interest is the continued increase in H_b/H_∞ with decreasing H_∞/L_∞ values at H_∞/L_∞ nearly an order of magnitude lower than the H_∞/L_∞ contained in either the Iversen or Komar and Simmons data.

A few measurements of the horizontal particle velocity and the wave phase velocity at the crest were obtained by Morison and Crooke (1953). These measurements are shown in Table 6-4. With only three measurements for each slope, the dependence of u_{max}/c_b on H_∞/L_∞ cannot be fully determined. However, an estimate of the slope dependence may be made; the average value of $u_{max}/c_b = 0.79$ is obtained for m = 0.10 and 0.63 for m = 0.02. These calculations

Table 6-3. Average values of H_b/H_∞ as a function of beach slope (m) and deep water wave steepness (H_∞/L_∞).

I. H_b/H_∞ (Galvin, 1968)

H_∞/L_∞:	0.0007-0.0117	0.0118-0.0227	0.0228-0.0337	0.0338-0.0447	0.0448-0.0557
m = 0.050	2.84	1.50	none	none	1.94
m = 0.10	2.08	1.25	none	1.07	0.89
m = 0.20	1.91	none	none	1.02	1.13

Table 6-4. Measurements of breaking waves (Morison and Crooke, 1953).

Slope	h_b ft	H/L	C_b ft/sec	C_t* ft/sec	u_{max} ft/sec	C_b/C_t	u_{max}/C_b
0.10	0.252	0.0036	3.45	2.86	2.9	1.21	0.84
0.10	0.300	0.0206	4.65	3.12	3.9	1.49	0.84
0.10	0.423	0.0797	3.55	3.69	2.4	0.99	0.68
0.02	0.297	0.0037	3.80	3.08	2.6	1.24	0.68
0.02	0.330	0.0262	4.00	3.26	2.3	1.23	0.58
0.02	0.230	0.0778	3.50	2.70	2.2	1.30	0.63

*$C_t = (gh_b)^{\frac{1}{2}}$

suggest that there may be a tendency for u_{max}/c_b to increase with increasing beach slope. Morison and Crooke did not report the size of the water particles at the crest whose velocities were measured. Since larger particles may have smaller velocities because more fluid is involved, the low values of these u_{max}/c_b calculations may be due to this reason.

3. Review of Ocean Breaker Measurements

The only ocean breaker experiments were those designed to obtain information useful to amphibious landing operations during World War II (SIO Wave Report No. 24, SIO Wave Report No. 47, 1944). As a result the data contain considerable scatter which was attributed to the measuring techniques in the original reports. Appendix I contains a list of these measurements.

When H_b/H_∞ (or H_b/h_b) is plotted as function of H_∞/L_∞ the amount of scatter present for a given wave steepness is very great (Figure 6-6). For this reason, the data are presented without the wave steepness dependence (Figure 6-9). Since the WHOI data were only reported in terms of the ratio H_b/h_b, they are not shown in this plot. In Figure 6-9, the Type I symbol refers to waves breaking over an approximately uniform 0.04 beach slope, and the Type II symbol refers to waves breaking after they have traveled past the abrupt transition between the 0.04 beach slope and the

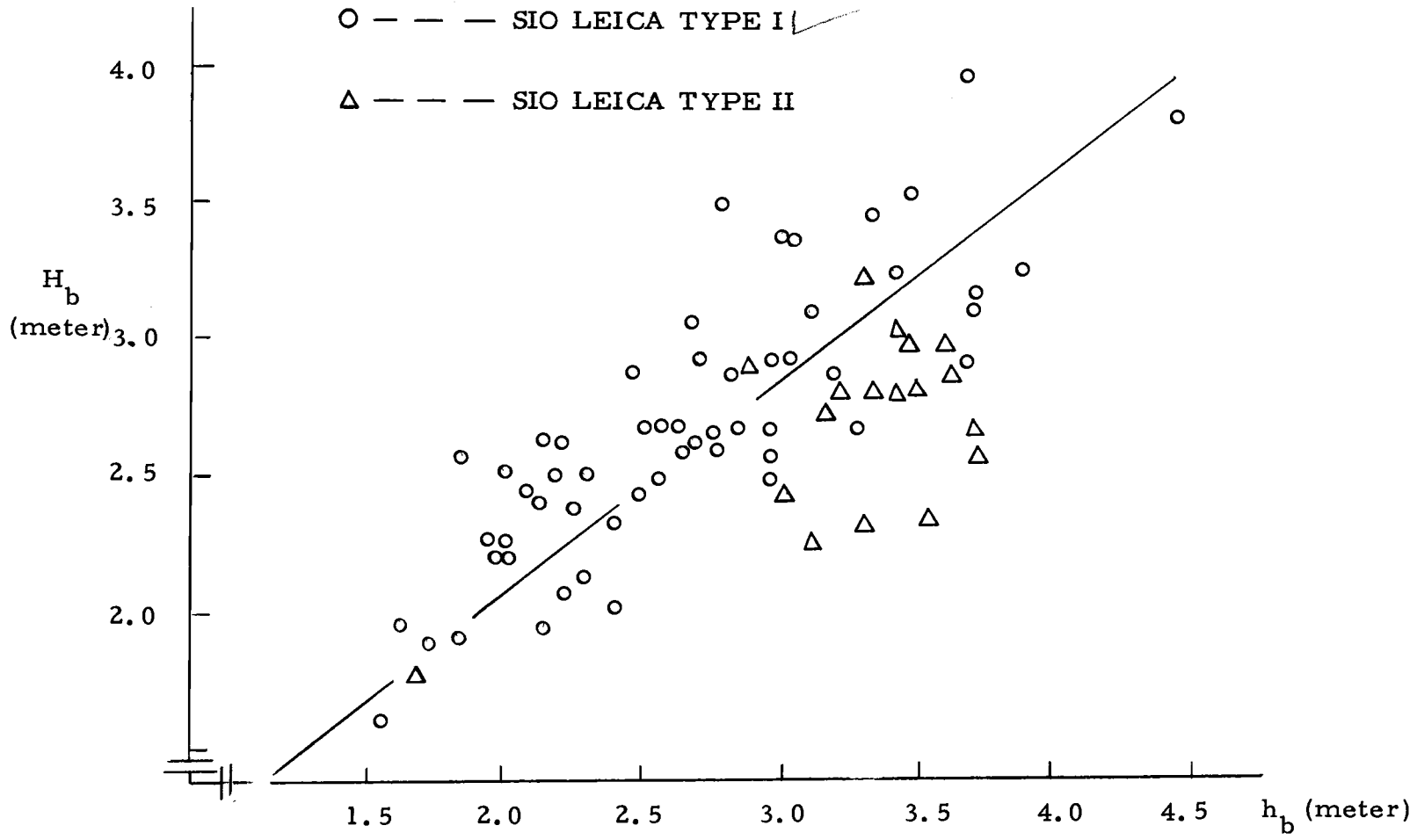

Figure 6-9. H_b versus h_b for ocean breaker data.

flatter slope inshore (see Chapter V). To provide a convenient reference, a line with a slope of 0.78 is drawn in Figure 6-9. This line represents the theoretical $(H/h)_{max}$ value derived by McCowan for a solitary wave in water of constant depth limited by the kinematic criterion.

Although the ocean breaker measurements are approximately uniformly scattered about the theoretical line, the Type II data fall primarily below the line and the Type I data fall mostly above the line. The average values of H_b/h_b for Types I and II are, respectively, 0.82 and 0.67. The lower H_b/h_b value for the Type II breakers has been shown (SIO Wave Report No. 47) to be due to the increase in h_b. Because the wave apparently deforms past an irreversible shape on the outer steep beach, it continues to deform and eventually break even though the beach suddenly flattens. If the steep beach slope was continuous, then the same initial wave would travel into much shallower water before reaching the breaking position since the spatial rate of depth decrease would be greater.

The average H_b/h_b for the WHOI data of Atlantic Ocean breakers is 0.96. Since no information is available on the experimental methods of this study, it is impossible to determine why H_b/h_b is larger than the Pacific Ocean H_b/h_b values.

These ocean breaker studies are not adequate for determining the applicability of theoretical breaking criteria to ocean waves.

Experiments which are both more accurate and more detailed are needed. In addition, laboratory experiments designed to measure the effect of variable beach slopes on breaker characteristics would be helpful.

CHAPTER VII

CONCLUSIONS

The purpose of this thesis was to evaluate the present state of knowledge of breaking criteria for progressive surface gravity waves. The conclusions below are meant to be an appraisal of this knowledge based on the review of theory and measurements given in the previous chapters.

Deep Water Wave Breaking Criteria

Only one limiting condition has been applied to deep water waves as a breaking criterion, the kinematic breaking criterion, in which the horizontal particle velocity at the crest just equals the wave phase velocity. In addition, relatively simple wave theories (based on the motion being inviscid, irrotational, incompressible, surface tension free, and two-dimensional) have been employed. Even utilizing these simple wave theories, the studies disagree on some of the derived wave properties; for example, theoretical estimates of the vertical particle acceleration at the wave crest range from zero to g, the gravitational acceleration. Measurements of maximum height waves in deep water may resolve some of these discrepancies. No such measurements have been obtained to date. Important to the advancement of knowledge of ocean waves is the theory and measurement of

wave breaking in the presence of other waves, particularly wave breaking in a random sea.

Shallow Water Wave Breaking Criteria

The conclusions regarding shallow water breaking criteria are divided into three sections: (1) theoretical shallow water wave breaking criteria (Chapter IV), (2) experimental methods of measuring shallow water breaking waves (Chapter V), and (3) measurements of shallow water breaking waves (Chapter VI).

1. Theoretical shallow water wave breaking criteria. Three breaking criteria have been suggested for maximum height steady waves in shallow water of constant depth: (1) the kinematic breaking criterion, (2) the reversal of the vertical water particle velocity near the crest as the ratio of wave height to water depth, H/h, increases, and (3) the reversal of the vertical pressure gradient beneath the crest as H/h increases. Cnoidal, stokes, and solitary wave theories were employed. Again, as was true for deep water waves, there are disagreements between the values of the derived wave properties from the numerical stream function approach (Dean, 1968) and the 'classical' approach (Rankine, 1864; Stokes, 1880; Chappelear, 1959). Somewhat better agreement is found between the several theoretical estimates of $(H/h)_{max}$ for maximum height solitary waves; these values range from 0.73 to 1.03. There

is as yet no apriori argument that identifies whether any of the breaking criteria listed above is the actual cause of limiting wave growth.

There are two breaking criteria which have been utilized for shoaling waves; the kinematic breaking criterion and the presence of a vertical surface. Unfortunately, the emphasis of these theoretical studies has been placed on the unrealistic concept of a wave front (defined on page 31) used in conjunction with the long wave theory that is not considered adequate near the breaking position.

2. Experimental methods. Methods, procedures, and reporting of experiments on shallow water breaking waves must be improved. A first step would be to standardize definitions of important parameters such as the breaking position, initial wave height (H_i), breaker height (H_b), and depth of breaking (h_b) so that results from different experiments may be compared. Since the breaking phenomenon cannot be completely isolated from other fluid motions (such as backwash, solitons, reflected waves, and edge waves & rip currents), a second step would be to monitor these possible interferences to determine their effect on the breaker measurements. Two important improvements in the reporting of breaker measurements would be to include the breaker type, which is a measure of the breaker shape, and the individual breaker measurements. The individual measurements are important

because they indicate the variability in relation to the time sequence of breakers. Finally, more accurate and precise measuring techniques need to be developed if the fundamental breaking criterion are to be determined. In particular, a technique to measure water particle velocities and accelerations accurately is required.

3. Measurements of shallow water breaking waves. Measurements of the breaker height, H_b, and the depth of breaking, h_b, for solitary waves in water of constant depth yield H_b/h_b values that are in agreement with the range of theoretical estimates of $(H/h)_{max}$. Experiments on shoaling solitary waves show that: (1) H_b/h_b increases as the beach slope increases, the ratio being higher than the theoretical $(H/h)_{max}$, (2) H_b/h_b increases as the ratio of the initial wave height to water depth, H_i/h_i, decreases, and (3) breaking does not occur on beach slopes steeper than 0.15. However, H_b/h_b does smoothly approach the theoretical $(H/h)_{max}$ as the beach slope decreases.

Measurements of oscillatory waves in water of constant depth do not confirm any of the theoretical breaking criteria; the largest value of the ratio of the horizontal particle velocity at the crest to the wave phase velocity is 0.33. The derived wave properties are, in general, greater than the values obtained from laboratory experiments. Much needed improvements in the measuring techniques may require a revision of these conclusions.

Since there are no theoretical breaking criteria for shoaling oscillatory waves, measurements have concentrated on describing the general trends of the ratio of the breaker height to the small amplitude deep water wave height, H_b/H_∞, as a function of the deep water wave steepness, H_∞/L_∞, and the beach slope (Chapter VI). The measurements of Iversen (1952a), Komar and Simmons, and Galvin (1968) are considered adequate for this purpose. Once theoretical breaking criteria and derived wave properties have been developed for shoaling oscillatory waves, further experimentation will be necessary to test the new theories.

Past measurements of ocean breakers are not sufficient to determine the applicability of present theoretical breaking criteria to shoaling ocean waves. More accurate and complete measurements of all the breaking parameters are needed.

BIBLIOGRAPHY

Ayyar, H. R. 1970. Periodic waves shoaling in water over steeply sloping beaches. In: Proceedings Twelfth Conference Coastal Engr. 1:363-376.

Biesel, F. 1952. Study of wave propagation in water of gradually varying depth. In: Gravity Waves, U. S. National Bureau of Standards Circular No. 521. p. 243-253.

Boussinesq, J. 1872. Theorie des ondes et de Remous qui se porpagent le Long d'un Canal Rectangulaire Horizontal, en Communiquant au Liquide Contenu dans ce Canal des Vitesses Sensiblement Paralleles de la Surface au Fond. Jour. Math. Pures Appliquees, Vol. 17, p. 55-108, Lionvilles, France.

Bowen, A. J., Inman, D. L., and V. P. Simmons. 1968. Wave set-down and set-up. Jour. Geophysical Res. 73(8):2569-2577.

Bowen, A. J. 1969. Rip Currents, theoretical investigations. Jour. Geophysical Res. 74(23):5467-5478.

Bowen, A. J. and D. L. Inman. 1969. Rip currents, laboratory and field observations. Jour. Geophysical Res. 74(23):5479-5490.

Burger, W. 1967. A note on the breaking of waves on non-uniformly sloping beaches. Jour. Mathematics & Mechanics 16(10):1131-1142.

Camfield, F. E. and R. L. Street. 1966. Observations and experiments on solitary wave deformation. In: Proceedings Tenth Conference Coastal Engr. 1:284-301.

Camfield, F. E. and R. L. Street. 1968. The effects of bottom configuration on the deformation, breaking, and run-up of solitary waves. In: Proceedings Eleventh Conference Coastal Engr. 1:173-189.

Camfield, F. E. and R. L. Street. 1969. Shoaling of solitary waves on small slopes. Jour. Waterways & Harbors Div., Proc. A.S.C.E., WW1, p. 1-21.

Carrier, G. F. and H. P. Greenspan. 1958. Water waves of finite amplitude on a sloping beach. Jour. Fluid Mech. 4:97-109.

Chappelear, J. E. 1959. On the theory of the highest waves. Beach Erosion Board Tech. Memo. Number 116. 28 p.

Daily, J. W. and S. C. Stephan. 1952. The solitary wave. In: Proceedings Third Conference Coastal Engr. p. 13-30.

Danel, P. 1952. On the limiting clapotis. In: Gravity Waves, U.S. National Bureau of Standards Circular No. 521. p. 35-38.

Davies, T. V. 1952. The theory of symmetrical gravity waves of finite amplitude. In: U.S. National Bureau of Standards Circular No. 521. p. 55-60.

Dean, R. G. 1968. Breaking wave criteria: a study employing numerical wave theory. In: Proceedings Eleventh Conference Coastal Engr. 1:108-123.

Eckart, C. 1951. Surface waves in water of variable depth. Univ. California Scripps Institute Oceanography Wave Report 100. 99 p.

Galvin, C. J. and P. S. Eagleson. 1965. Experimental study of longshore currents on a plane beach, U.S. Army Coastal Engr. Research Center Tech. Memo. 10, p. 1-80.

Galvin, C. J., Jr. 1968. Breaker type classification on three laboratory beaches. Jour. Geophysical Res. 73(12):3651-3659.

Galvin, C. J., Jr. 1969. Breaker travel and choice of design wave height. Jour. Waterways & Harbors Div., Proc. A.S.C.E., WW2, 95:175-200.

Galvin, C. J., Jr. and N. J. Zabusky. 1970. Shallow-water waves, the Korteweq-de Vries equation and solitons. Jour. Fluid Mech. 47:811-824.

Galvin, C. J., Jr. 1972. Waves breaking in shallow water. In: Waves on beaches and resulting sediment transport. Ed. R. E. Meyer. London, Academic Press, p. 413-456.

Greenspan, H. P. 1958. On the breaking of water waves of finite amplitude on a sloping beach. Jour. Fluid Mech. 4:330-334.

Grimshaw, R. 1971. The solitary wave in water of variable depth. Part 2. Jour. Fluid Mech. 46:611-622.

Gwythery, R. F. 1900. The classes of long progressive waves. Phil. Mag. 50(5):213-216.

Havelock, E. T. 1918. Periodic irrotational waves of finite height. Proc. Royal Society (London), Serial A, 95:38-51.

Ippen, A. T. Editor. 1966. Estuary and Coastline Hydrodynamics. New York, McGraw-Hill. 744 p.

Ippen. A. T. and G. Kulin. 1955. The shoaling and breaking of the solitary wave. In: Proceedings Fifth Conference Coastal Engr. 1:27-49.

Iversen, H. W. 1951. Laboratory study of breakers. In: Gravity Waves, U.S. National Bureau of Standards Circular No. 521. p. 9-32.

Iversen, H. W. 1952a. Discussion of results from studies of wave transformation in shoaling water including breaking. Institute Engr. Res., Univ. Calif. Tech. Report Series 3, No. 331, p. 1-16.

Iversen, H. W. 1952b. Laboratory study of wave transformation in shoaling water, including an analysis of channel boundary friction. Instit. Engr. Res., Univ. Calif., Berkeley, Tech. Report, Series 29, Issue 53. 8 p.

Kinsman, Blair. 1965. Wind Waves. New Jersey, Prentice-Hall. 676 p.

Kishi, T. and H. Saeki. 1966. The shoaling, breaking, and run-up of the solitary wave on impermeable rough slopes. In: Proceedings Tenth Conference Coastal Engr. 1:322-348.

Komar, P. D. 1973. Assistant Professor, Oregon State University, School of Oceanography. Personal communcation. Corvallis, Oregon. April 10, 1973.

Komar, P. D. and M. K. Gaughan. 1973. Airy wave theory and breaker height prediction. In: Proceedings Thirteenth Conference Coastal Engr. 1:405-418.

Korteweq, D. J. and G. deVries. 1895. On the change of form of long waves advancing in a rectangular canal and on a new type of long stationary wave. Phil. Mag., Serial 5. 39:422-443.

Laitone, E. V. 1963. Higher approximations to nonlinear water waves and the limiting heights of cnoidal, solitary, and Stokes wave. Beach Erosion Board Tech. Memo. No. 133. 106 p.

Lamb, H. 1932. Hydrodynamics. Cambridge Univ. Press., London, 738 p.

Le Mehaute, B. and R. C. Koh. 1967. On the breaking of waves arriving at an angle to the shore. Jour. Hydraulic Res. 5(1):67-88.

Le Mehaute, B. 1968. A synthesis on wave run-up. Jour. Waterways & Harbors Div., Proc. A.S.C.E., WW1. p. 77-92.

Le Mehaute, B. 1968. An introduction to hydrodynamics and water waves. U.S. E.S.S.A. Tech. Report Nos. ERL 118 - POL 3-1, 3-2. 766 p.

Lenau, C. W. 1966. The solitary wave of maximum amplitude. Jour. Fluid Mech. 26;309-320.

Longuet-Higgins, M. S. 1963. The generation of capillary waves by steep gravity waves. Jour. Fluid Mech. 16:138-159.

McCowan, J. 1891. On the solitary wave. Phil. Mag., Serial 5. 32:45-58.

McCowan. J. 1894. On the highest wave of permanent type. Phil. Mag., Serial 5. 38:351-357.

Madsen, O. S. 1971. The breaking criteria of Miche. Unpublished Memorandum for Record, U.S. Army Coastal Engr. Research Center, Wash., D. C. 2 p.

Mason, M. A. 1952. Some observations of breaking waves. In: Gravity waves, U.S. National Bureau of Standards Circular No. 521. p. 215-221.

Mei, C. C. and B. Le Mehaute. 1966. Note on the equations of long waves over an uneven bottom. Jour. Geophysical Res. 71(2): 393-400.

Miche, M. 1944. Undulatory movements of the sea in constant or decreasing depth. Inst. Engr. Res. Wave Res. Lab. Univ. Calif. Berkeley, Series 3, Issue 363. 96 p. (Translated by M. Lincoln, 1954).

Michell, J. H. 1893. On the highest waves in water. Phil. Mag., Serial 5, 38:351-357.

Morison, J. R. and R. C. Crooke. 1953. The mechanics of deep water, shallow water, and breaking waves. Beach Erosion Board Tech. Memo. No. 40, 14 p.

Munk, W. H. 1949. Solitary wave theory and its application to surf problems. In: Annals of the New York Academy of Sciences 51:376-424.

Nicholson, J. 1968. A laboratory study of the relationship between waves and beach profiles. In: Third Australian Conf. on Hydraulics of Fluid Mech. The Inst. of Engr., Australia. p. 33-37.

Packham, B. A. 1952. The theory of symmetrical gravity waves of finite amplitude. Part 2. The solitary wave. Proc. Royal Society (London), Serial A, 213:238-249.

Peregrine, D. H. 1972. Equations for water waves and the approximations behind them. In: Waves on beaches and resulting sediment transport. Ed. R. E. Meyer. London, Academic Press, p. 95-122.

Perroud, P. H. 1957. The solitary wave reflection along a straight vertical wall at oblique incidence. Inst. Engr. Research, Univ. Calif. Berkeley, Tech. Report, Series 99, Issue 3.

Phillips, O. M. 1958. The equilibrium range of the spectrum of wind generated waves. Jour. Fluid Mech. 4:426-434.

Phillips. O. M. 1966. The dynamics of the upper ocean. Cambridge University Press. 261 p.

Price, R. K. 1970. Detailed structure of the breaking wave. Jour. Geophysical Res. 75(27):5276-5278.

Price, R. K. 1971. The breaking of water waves. Jour. of Geophysical Res. 76(6):1576-1581.

Rankine, W. J. 1894. Summary of properties of certain streamlines. Phil. Mag., Serial 4. 28:282-288.

Rayleigh, Lord. 1876. On waves. Phil. Mag., Serial 5. 1:257-279.

Scripps Institute of Oceanography. 1944. Waves in shallow water. Report No. 1. 9 p.

Scripps Institute of Oceanography, 1944. Effect of bottom slope on breaker characteristics as observed along the Scripps Institution pier. Report No. 24. 10 p.

Scripps Insititute of Oceanography. 1945. Height of breakers and depth of breaking. Report No. 47. 35 p.

Stoker, J. J. 1948. The formation of breakers and bores. Communications on Applied Math. 1(1):1-87.

Stoker, J. J. 1949. The breaking of waves in shallow water. In: Annals of the New York Academy of Science. 51(3):360-375.

Stoker, J. J. 1957. Water waves. New York, Interscience. 567 p.

Stokes, G. G. 1880. Appendix B, On the theory of oscillatory waves. In: Mathematical and Physical Papers, Cambridge Univ. Press.

Taylor. G. I. 1953. An experimental study of standing waves. Proc. Royal Society (London), Serial A. 218:44-59.

Toba, Y. and H. Kunishi. 1970. Breaking of wind waves and the sea surface wind stress. Jour. Oceanographic Soc. Japan. 26(2):71-80.

Wiegel, R. L. and K. E. Beebe. 1956. The design wave in shallow water. Jour. Waterways and Harbors Div., Proc. A.S.C.E., WW1, p. 910-921.

Wiegel, R. L. 1964. Oceanographical Engineering. New Jersey, Prentice-Hall. 532 p.

Yamada, H. 1957. On the highest solitary wave. Report of Res. Inst. for Applied Mech. 5(18):53-155.

Yamada, H. 1957. Highest waves of permanent type on the surface of deep water. Report of Res. Inst. for Applied Mech. 5(18):37-52.

APPENDIX

APPENDIX I

Wave Data

Contained in this appendix are the oscillatory wave tank and ocean measurements from the studies included in this review. The symbols used in the headings are defined in Chapter V of the text. The first table contains all of the wave tank experiments. The next table contains all of the data from the field experiments.

Wave parameters measured or computed

in wave tank experiments

m	T sec	h_i cm	H_i cm	H_b cm	H_b swl cm	h_b cm	H_∞/L_∞	H_b/H_∞	H_b/h_b
				1. Komar and Simmons (1968)					
0.036	1.14	30.63	6.36	7.38	5.89	9.25	0.034	1.06	0.798
0.036	1.65	30.63	6.36	8.27	7.21	10.85	0.0155	1.26	0.762
0.036	2.37	30.63	6.36	10.58	8.73	12.05	0.0066	1.82	0.878
0.036	1.14	30.63	9.00	9.14	7.15	12.46	0.049	0.93	0.734
0.036	1.14	30.63	13.1	12.24	9.31	17.73	0.071	0.86	0.690
0.036	1.65	30.63	9.0	11.59	9.54	13.33	0.022	1.24	0.869
0.036	1.65	30.63	13.1	16.51	12.75	21.30	0.032	1.22	0.775
0.036	2.37	30.63	8.5	13.65	11.38	15.78	0.0089	1.75	0.865
0.036	1.65	30.63	13.1	16.55	12.75	21.20	0.032	1.22	0.781
0.036	2.37	30.63	8.5	13.65	11.38	15.78	0.0089	1.75	0.865
0.070	1.14	30.63	13.1	12.65	9.22	16.20	0.071	0.88	0.781
0.070	1.65	30.63	13.1	15.90	12.40	16.40	0.032	1.17	0.970
0.070	2.37	30.63	8.5	14.04	10.30	14.00	0.0089	1.80	1.003
0.070	0.81	30.63	6.36	5.82	4.58	7.75	0.067	0.87	0.751
0.070	0.81	30.63	3.03	3.40	2.64	3.95	0.031	1.06	0.861
0.070	1.14	30.63	6.36	6.91	5.24	7.39	0.034	0.99	0.935
0.070	1.14	30.63	3.03	4.07	3.23	3.89	0.016	1.23	1.046
0.070	1.65	30.63	6.36	9.60	7.70	8.86	0.0155	1.46	1.084
0.070	1.65	30.63	3.03	5.50	4.30	4.85	0.0074	1.75	1.134
0.070	2.37	30.63	6.36	11.34	8.45	10.94	0.0066	1.95	1.037
0.070	2.37	30.63	3.03	5.50	3.59	5.28	0.0032	1.98	1.042
0.070	2.37	30.63	9.00	9.52	7.24	11.00	0.0094	1.16	0.865
0.070	1.14	30.63	13.1	13.24	9.60	15.80	0.071	0.92	0.838
0.070	1.65	30.63	13.1	15.60	12.20	15.10	0.032	1.15	1.033
0.086	2.37	30.63	6.36	9.64	6.67	9.77	0.0066	1.66	0.987
0.086	2.37	30.63	3.03	5.41	3.10	5.13	0.0032	1.95	1.055
0.086	2.37	30.63	8.50	14.15	10.00	13.00	0.0089	1.81	1.088
0.086	1.14	30.63	13.1	12.63	9.25	16.20	0.071	0.88	0.780
0.086	1.65	30.63	13.1	14.73	11.66	15.50	0.032	1.08	0.950
0.086	1.14	30.63	3.03	4.19	2.97	4.11	0.016	1.26	1.019
0.086	1.65	30.63	6.36	8.96	6.37	9.01	0.0155	1.36	0.994
0.086	1.65	30.63	3.03	5.78	4.08	5.80	0.0074	1.84	0.997
0.086	0.81	30.63	6.36	5.94	4.49	7.44	0.066	0.89	0.798
0.086	0.81	30.63	3.03	3.43	2.48	3.43	0.031	1.07	1.000
0.086	1.14	30.63	6.36	7.74	5.87	7.95	0.034	1.11	0.974

m	T sec	h_i cm	H_i cm	H_b cm	H_b swl cm	h_b cm	H_∞/L_∞	H_b/H_∞	H_b/h_b
			1. Komar and Simmons, continued						
0.105	1.65	30.63	6.36	8.91	6.07	8.40	0.0155	1.36	1.061
0.105	1.65	30.63	3.03	4.76	2.80	4.90	0.0074	1.52	0.971
0.105	1.14	30.63	6.36	7.56	5.34	8.03	0.034	1.09	0.941
0.105	0.81	30.63	6.36	5.03	3.67	6.11	0.0665	0.75	0.823
0.105	0.81	30.63	3.03	3.53	2.36	3.64	0.031	1.10	0.970
0.105	2.37	30.63	6.36	9.27	4.96	9.72	0.0066	1.59	0.954
0.105	2.37	30.63	3.03	5.35	2.64	5.85	0.0032	1.92	0.915
0.105	1.14	30.63	13.1	14.27	10.20	15.20	0.071	0.99	0.93
0.105	1.65	30.63	13.1	17.04	11.80	17.00	0.032	1.25	1.002
			2. Iversen (1952a)						
0.020	2.43	47.00	7.07	10.8		--	0.0074	1.58	--
0.020	2.65	47.00	7.41	12.1		15.60	0.0065	1.70	0.780
0.020	1.00	47.00	10.60	9.24		12.29	0.0718	0.91	0.752
0.020	1.13	47.00	8.60	9.06		10.70	0.0465	0.98	0.850
0.020	1.17	47.00	7.40	8.36		9.78	0.0376	1.04	0.854
0.020	1.62	47.00	6.95	8.18		9.31	0.0190	1.05	0.876
0.020	1.74	47.00	5.80	8.64		10.18	0.0130	1.41	0.847
0.020	2.65	47.00	5.66	9.76		12.86	0.0049	1.82	0.758
0.020	0.81	47.00	9.17	7.62		--	0.0907	0.82	--
0.020	0.90	47.00	8.50	6.77		9.94	0.0706	0.76	0.681
0.020	0.95	47.00	6.77	5.83		6.95	0.0504	0.82	0.839
0.020	1.00	47.00	7.01	6.65		--	0.0474	0.90	--
0.020	1.00	47.00	5.55	5.64		--	0.0376	0.96	--
0.020	1.30	47.00	7.35	7.56		10.00	0.0305	0.94	0.756
0.020	1.35	47.00	5.80	6.07		7.05	0.0223	0.96	0.861
0.020	2.00	47.00	5.49	6.34		6.76	0.0092	1.10	0.936
0.020	1.90	47.00	3.93	5.52		6.46	0.0074	1.32	0.854
0.020	2,25	47,00	5.12	6.62		--	0.0065	1.29	--
0.033	1.05	50.30	10.85	10.70		14.64	0.0665	0.94	0.729
0.033	2.37	50.0	7.00	12.70		15.55	0.0080	1.81	0.814
0.033	1.24	48.1	7.76	8.39		11.12	0.0353	0.99	0.754
0.033	1.46	47.2	6.52	8.69		10.67	0.0214	1.22	0.815
0.033	1.87	45.7	5.15	7.99		11.37	0.0099	1.48	0.703
0.033	2.03	45.4	5.27	7.71		10.20	0.0084	1.43	0.751
0.033	2.67	46.4	5.00	8.84		11.30	0.0043	1.85	0.785
0.033	1.49	43.9	4.39	6.86		8.24	0.0138	1.44	0.834
0.033	1.60	42.6	3.38	5.34		7.92	0.0093	1.44	0.674
0.033	1.79	42.6	3.50	5.49		7.92	0.0074	1.48	0.694

m	T	h_i	H_i	H_b	H_b swl	h_b	H_∞/L_∞	H_b/H_∞	H_b/h_b
	sec	cm	cm	cm	cm	cm			
				2. Iversen, continued					
0.033	2.10	43.9	3.50	6.56		8.37	0.0052	1.83	0.782
0.033	2.29	43.5	3.54	7.01		8.55	0.0042	2.04	0.822
0.033	2.52	43.5	3.57	6.10		8.07	0.0035	1.76	0.755
0.033	2.52	43.2	2.84	5.79		7.00	0.0027	2.16	0.826
0.033	2.65	43.0	2.96	5.49		7.44	0.0025	2.00	0.737
0.050	1.40	54.9	10.07	12.8		16.14	0.0360	1.16	0.792
0.050	1.50	48.8	9.08	12.2		14.00	0.0280	1.24	0.870
0.050	1.59	48.8	7.80	12.2		14.63	0.0210	1.48	0.834
0.050	1.89	47.8	6.85	11.6		13.40	0.0130	1.60	0.864
0.050	2.24	47.8	5.88	11.0		11.90	0.0076	1.85	0.925
0.050	1.04	53.3	11.68	10.7		16.50	0.0730	0.87	0.649
0.050	1.15	48.8	9.30	9.45		11.90	0.0480	1.05	0.795
0.050	1.26	47.8	7.92	10.1		10.40	0.0350	1.16	0.971
0.050	1.33	48.8	7.25	9.14		10.40	0.0290	1.14	0.884
0.050	1.41	47.5	6.15	8.24		10.05	0.0220	1.20	0.819
0.050	1.67	46.0	5.43	8.24		8.84	0.0130	1.45	0.931
0.050	1.93	45.4	4.39	7.62		7.62	0.0079	1.66	1.000
0.050	0.74	47.2	6.52	5.79		8.84	0.0767	0.88	0.660
0.050	0.93	45.7	6.29	6.40		8.25	0.0480	0.99	0.780
0.050	1.03	45.7	5.65	5.49		7.62	0.0360	--	0.720
0.050	1.12	45.7	5.03	5.79		7.02	0.0270	1.10	0.826
0.050	1.17	45.7	4.42	6.10		6.41	0.0220	1.30	0.953
0.050	1.34	45.7	3.35	4.27		4.87	0.0130	1.17	0.875
0.050	1.55	44.8	2.86	4.57		5.48	0.0083	1.47	0.834
0.100	1.00	70.1	11.90	12.20		12.50	0.0774	1.01	0.976
0.100	1.00	70.1	11.90	12.20		12.50	0.0774	1.01	0.976
0.100	1.51	68.0	6.70	11.30		9.15	0.0206	1.55	1.231
0.100	1.73	68.5	7.04	11.00		9.75	0.0165	1.43	1.124
0.100	1.00	71.0	12.20	10.70		13.72	0.0797	1.86	0.778
0.100	0.92	68.0	7.64	7.90		10.05	0.0581	1.03	0.788
0.100	1.98	68.3	4.27	9.46		9.15	0.0076	2.04	1.031
0.100	1.98	68.0	3.99	8.84		7.92	0.0071	2.03	1.118
0.100	0.80	68.0	6.10	6.40		8.84	0.0614	1.05	0.725
0.100	1.11	68.0	5.12	6.70		6.71	0.0280	1.25	1.000
0.100	1.27	66.2	3.93	6.70		5.49	0.0167	1.60	1.223
0.100	1.26	66.2	3.48	5.80		4.89	0.0150	1.56	1.189
0.100	1.45	66.2	3.75	6.10		5.49	0.0125	1.49	1.112
0.100	1.26	65.5	2.59	4.90		4.27	0.0112	1.76	1.142
0.100	2.10	67.8	3.44	7.00		8.53	0.0054	1.88	0.822
0.100	2.50	68.0	3.38	7.30		7.32	0.0038	1.97	1.000

m	T sec	h_i cm	H_i cm	H_b cm	H_b swl cm	h_b cm	H_∞/L_∞	H_b/H_∞	H_b/h_b
			3. Berkeley Wave Tank (Munk, 1949)						
0.009	1.05		10.21	9.97		14.32	0.0590	0.98	0.698
0.009	1.09		9.60	9.75		14.29	0.0510	1.03	0.680
0.009	1.35		8.23	9.84		14.51	0.0290	1.23	0.675
0.009	1.50		6.77	9.39		14.45	0.0190	1.39	0.685
0.009	1.98		4.57	8.72		11.80	0.0070	1.91	0.740
0.054	0.86		10.21	9.17		13.84	0.0880	0.89	0.685
0.054	0.96		9.69	9.11		11.06	0.0670	0.94	0.826
0.054	1.34		7.31	8.26		7.48	0.0260	1.13	1.111
0.054	1.50		6.25	7.92		7.48	0.0180	1.27	1.064
0.054	1.97		4.08	6.83		6.31	0.0070	1.67	1.088
0.072	0.09		10.70	9.88		12.56	0.0920	0.92	0.787
0.072	1.15		9.20	9.84		10.70	0.0450	1.07	0.918
0.072	1.22		8.66	9.94		9.51	0.0370	1.15	1.041
0.072	1.50		6.41	9.45		8.23	0.0180	1.46	1.124
0.072	1.54		6.06	8.72		8.32	0.0160	1.44	1.052
0.072	1.97		4.48	8.23		7.13	0.0070	1.83	1.150
			4. Beach Erosion Board (Munk, 1949)						
0.030	1.03		3.62	4.27		6.10	0.0218	1.18	0.700
0.030	1.03		4.88	5.42		7.92	0.0296	1.11	0.685
0.030	0.85		3.05	3.26		4.57	0.0273	1.07	0.715
0.030	1.03		2.65	3.44		4.66	0.0159	1.13	0.741
0.030	1.03		5.49	5.06		8.14	0.0331	0.92	0.622
0.030	0.85		3.96	3.75		5.21	0.0354	0.95	0.719
0.030	0.75		3.05	3.29		5.12	0.0350	1.08	0.645
0.030	0.85		4.42	4.05		6.31	0.0403	0.92	0.642
0.030	0.75		4.27	3.08		4.30	0.0496	0.72	0.714
0.049	1.08		4.97	6.49		5.52	0.0271	1.31	1.178
0.049	1.08		3.81	5.12		4.33	0.0209	1.35	1.190
0.049	0.96		3.57	4.30		4.48	0.0249	1.21	0.962
0.049	1.08		5.70	6.64		8.08	0.0315	1.17	0.819
0.049	0.97		4.94	6.22		6.70	0.0352	1.26	0.926
0.049	1.08		7.31	8.38		10.45	0.0400	1.15	0.800
0.049	0.95		6.52	6.89		8.84	0.0453	1.06	0.782
0.049	0.73		3.66	4.36		5.36	0.0422	1.19	0.814
0.049	1.08		9.87	10.03		13.90	0.0540	1.02	0.725
0.049	0.97		7.31	7.89		9.75	0.0500	1.08	0.806

m	T sec	h_i cm	H_i cm	H_b cm	H_b swl cm	h_b cm	H_∞/L_∞	H_b/H_∞	H_b/h_b
			4. Beach Erosion Board, continued						
0.049	0.75		5.06	4.42		5.52	0.0566	0.87	0.80
0.049	0.74		5.03	4.75		6.28	0.0554	0.95	0.757
0.049	0.75		5.18	4.85		6.43	0.0576	0.94	0.752
0.049	1.08		12.25	13.04		18.65	0.0670	1.06	0.700
0.049	0.97		9.02	9.02		11.28	0.0652	0.95	0.800
0.159	0.97		3.26	3.53		4.84	0.0230	1.08	0.730
0.159	1.08		5.02	5.18		5.82	0.0284	1.03	0.894
0.159	1.08		3.75	4.30		4.36	0.0207	1.15	0.981
0.159	1.08		7.16	6.43		10.18	0.0394	0.90	0.633
0.159	1.08		5.85	5.12		8.23	0.0331	0.88	0.622
0.159	0.97		5.88	5.45		8.23	0.0413	0.93	0.663
0.159	0.75		3.44	3.35		4.36	0.0402	0.97	0.769
0.159	0.74		3.87	3.93		5.33	0.0446	1.02	0.741
0.159	0.96		7.62	7.98		10.18	0.0529	1.05	0.787
0.159	0.74		5.18	4.85		5.82	0.0592	0.94	0.834
0.159	1.09		10.05	9.36		11.12	0.0546	0.93	0.840
0.159	0.97		9.11	9.48		12.59	0.0626	1.04	0.752
0.159	1.09		12.10	12.13		16.95	0.0651	1.00	0.714
			5. Morison and Crooke (1953)						
0.100	2.50			7.31		7.69	0.0036		0.952
0.100	1.51			11.30		9.15	0.0206		1.231
0.100	1.00			10.67		12.90	0.0797		0.827
0.020	2.62			8.05		9.05	0.0037		0.889
0.020	1.41			8.41		10.05	0.0262		0.837
0.020	0.78			5.58		7.00	0.0778		0.794
			6. Galvin (1968)						
0.050	1.00	30.5	7.44	7.2			0.0476	0.97	
0.050	2.00	30.5	5.58	9.4			0.0089	1.68	
0.050	4.00	30.5	4.01	11.3			0.0016	2.82	
0.050	5.00	30.5	3.58	11.9			0.0009	3.32	

m	T sec	h_i cm	H_i cm	H_b cm	H_b swl cm	h_b cm	H_∞/L_∞	H_b/H_∞	H_b/h_b
				6. Galvin, continued					
0.050	1.00	38.1	8.69	7.8			0.0557	0.90	
0.050	2.00	38.1	8.69	13.0			0.0139	1.50	
0.050	4.00	38.1	7.10	17.7			0.0028	2.49	
0.050	5.00	38.1	5.08	15.9			0.0013	3.13	
0.050	6.00	38.1	3.86	13.6			0.0007	3.52	
0.100	1.00	22.9	6.09	6.5			0.0390	1.07	
0.100	2.00	22.9	2.26	6.9			0.0036	3.05	
0.100	5.00	22.9	3.48	11.3			0.0008	3.25	
0.100	6.00	22.9	2.65	10.1			0.0004	3.81	
0.100	6.00	22.9	4.42	10.1			0.0007	2.28	
0.100	7.00	22.9	3.50	9.7			0.0004	2.77	
0.100	8.00	22.9	2.87	5.7			0.0002	1.99	
0.100	1.00	30.5	7.44	7.2			0.0476	0.97	
0.100	2.00	30.5	2.80	4.3			0.0044	1.54	
0.100	2.00	30.5	8.34	11.8			0.0133	1.41	
0.100	4.00	30.5	6.00	16.4			0.0024	2.73	
0.100	5.00	30.5	4.31	6.9			0.0011	1.60	
0.100	5.00	30.5	7.17	15.0			0.0018	2.09	
0.100	6.00	30.5	9.24	7.8			0.0016	0.84	
0.100	7.00	30.5	4.34	15.0			0.0005	3.47	
0.100	8.00	30.5	3.56	7.2			0.0003	2.02	
0.100	1.00	38.1	8.69	7.0			0.0557	0.80	
0.100	2.00	38.1	3.28	4.5			0.0052	1.37	
0.100	2.00	38.1	8.69	9.4			0.0139	1.08	
0.100	4.00	38.1	7.10	14.5			0.0028	2.04	
0.200	1.00	22.9	6.09	6.2			0.0390	1.02	
0.200	2.00	22.9	2.26	1.5			0.0036	0.66	
0.200	6.00	22.9	2.65	7.9			0.0004	2.98	
0.200	6.00	22.9	4.42	10.7			0.0007	2.42	
0.200	8.00	22.9	2.87	5.7			0.0002	1.99	
0.200	1.00	30.5	7.44	9.1			0.0476	1.22	
0.200	2.00	30.5	2.80	6.4			0.0044	2.28	
0.220	4.00	30.5	6.00	6.2			0.0024	1.03	
0.200	5.00	30.5	4.31	8.7			0.0011	2.01	
0.200	7.00	30.5	4.34	6.4			0.0005	1.47	
0.200	1.00	38.1	8.69	9.0			0.0557	1.04	
0.200	2.00	38.1	3.28	6.9			0.0052	2.10	
0.200	4.00	38.1	7.10	14.8			0.0028	2.08	
0.200	5.00	38.1	5.08	14.0			0.0013	2.76	

m	T sec	h_i cm	H_i cm	H_b cm	H_b swl cm	h_b cm	H_∞ / L_∞	H_b / H_∞	H_b / h_b
				7. Galvin (1969)					
0.050	2.00	30.5		9.4		10.2			0.92
0.050	4.00	30.5		11.3		10.1			1.12
0.050	5.00	30.5		11.9		10.9			1.07
0.050	4.00	38.1		17.7		16.2			1.09
0.050	5.00	38.1		15.9		14.5			1.09
0.050	6.00	38.1		13.6		13.4			1.01
0.050	6.00	35.0		14.0		18.20			0.77
0.200	1.00	22.9		6.2		6.2			1.00
0.200	1.00	30.5		9.2		8.0			1.14
0.200	1.00	38.1		9.0		8.1			1.11
0.200	2.00	38.1		6.9		6.3			1.10
0.100	1.00	22.9		6,52		6.10			1.07
0.100	2.00	22.9		3.84		3.94			0.98
0.100	5.00	22.9		14.20		8.85			1.60
0.100	6.00	22.9		10.01		7.75			1.31
0.100	1.00	30.5		7.16		6.19			1.16
0.100	2,00	30.5		4.33		4.00			1.08
0.100	2.00	30.5		11.79		9.02			1.30
0.100	5.00	30.5		14.90		10.00			1.50
0.100	2.00	38.1		4.52		4.51			1,00
0.100	2.00	38.1		9.35		11.42			0.82
0.100	4.00	38.1		14.50		10.40			1.38

Wave parameters measured or computed in field experiments (Munk, 1949)

T sec	H_∞ cm	H cm	h_b cm	H_∞/L_∞	H_b/H_∞	H_b/h_b
		Scripps Leica Type I				
13.7	123.	225.5	225.5	0.0042	1.85	1.00
12.0	94.	146.3	161.5	0.0042	1.55	0.91
13.3	124.	164.6	231.6	0.0045	1.35	0.77
12.7	128.	225.5	277.4	0.0051	1.76	0.81
12.2	118.	195.1	219.4	0.0051	1.64	0.88
10.2	83.	121.9	155.4	0.0051	1.48	0.78
11.6	109.	213.4	265.2	0.0052	1.95	0.81
12.0	119.	176.8	228.6	0.0053	1.49	0.77
11.5	136.	231.6	277.4	0.0066	1.46	0.83
10.0	128.	170.7	201.2	0.0082	1.34	0.85
10.0	128.	201.2	201.2	0.0082	1.57	1.00
10.0	131.	170.7	198.1	0.0084	1.19	0.86
11.2	164.	201.2	231.6	0.0084	1.22	0.87
9.2	111.	140.2	173.7	0.0084	1.28	0.81
9.0	107.	158.5	222.5	0.0085	1.49	0.71
10.2	141.	201.2	298.7	0.0087	1.44	0.67
10.5	155.	262.1	313.9	0.0090	1.69	0.83
10.0	147.	201.2	219.4	0.0094	1.37	0.92
9.5	132.	146.3	216.4	0.0094	1.12	0.68
9.6	141.	213.4	222.5	0.0098	1.71	0.96
9.5	144.	176.8	201.2	0.0102	1.23	0.88
9.4	130.	195.1	249.9	0.0107	1.33	0.79
9.5	154.	243.8	298.7	0.0109	1.60	0.81
9.6	157.	219.4	286.5	0.0109	1.41	0.76
10.3	187.	243.8	298.7	0.0113	1.31	0.82
10.5	196.	274.3	387.1	0.0114	1.41	0.71
10.5	200.	219.6	329.2	0.0116	1.22	0.67
9.6	171.	268.2	371.8	0.0119	1.57	0.72
9.8	183.	213.4	268.2	0.0122	1.17	0.79
8.1	127.	140.2	182.9	0.0124	1.12	0.77
10.3	206.	286.5	304.8	0.0124	1.40	0.94
9.0	167.	207.3	296.0	0.0132	1.26	0.70
9.4	190.	256.0	268.2	0.0138	1.36	0.95
9.0	191.	207.3	182.9	0.0139	1.19	1.14
7.7	130.	152.4	240.8	0.0140	1.19	0.63
9.0	178.	298.7	335.3	0.0141	1.66	0.89
8.5	159.	182.9	240.8	0.0141	1.15	0.76
8.8	180.	237.7	246.9	0.0149	1.35	0.96
8.8	182.	219.4	256.0	0.0151	1.22	0.85

T sec	H_∞ cm	H_b cm	h_b cm	H_∞/L_∞	H_b/H_∞	H_b/h_b
		Scripps Leica Type I, continued				
10.0	236.	243.8	369.0	0.0151	1.29	0.66
8.0	153.	176.8	195.1	0.0153	1.18	0.91
7.2	128.	201.2	256.0	0.0158	1.61	0.79
9.0	216.	243.8	271.3	0.0171	1.13	0.90
8.0	175.	188.9	213.4	0.0175	1.12	0.88
9.2	232.	262.1	371.8	0.0176	1.13	0.70
8.8	216.	237.7	280.4	0.0179	1.11	0.85
8.5	204.	298.7	277.4	0.0181	1.44	1.08
8.0	194.	219.4	262.1	0.0194	1.14	0.83
7.5	173.	237.7	320.0	0.0197	1.37	0.74
9.0	252.	347.5	368.8	0.0200	1.39	0.94
8.2	246.	304.8	344.4	0.0235	1.25	0.88
7.5	210.	274.3	341.4	0.0239	1.34	0.81
7.2	193.	243.8	301.8	0.0239	1.29	0.81
8.0	242.	286.5	301.8	0.0243	1.18	0.95
6.5	187.	219.4	249.9	0.0284	1.01	0.88
7.8	300.	335.3	445.0	0.0316	1.12	0.75
		Scripps Leica Type II				
13.0	121.	177.	314.	0.0046	1.45	0.56
12.5	149.	195.	302.	0.0061	1.31	0.64
12.0	166.	232.	323.	0.0074	1.38	0.72
10.5	151.	220.	372.	0.0088	1.47	0.59
11.2	178.	250.	347.	0.0091	1.39	0.72
10.0	143.	183.	354.	0.0092	1.28	0.52
10.0	145.	183.	332.	0.0093	1.25	0.55
8.8	118.	128.	168.	0.0098	1.11	0.76
9.3	135.	238.	363.	0.0100	1.77	0.65
9.6	152.	256.	344.	0.0106	1.68	0.74
10.5	184.	232.	350.	0.0107	1.27	0.66
10.0	172.	210.	372.	0.0110	1.24	0.56
9.5	166.	238.	283.	0.0118	1.41	0.84
8.9	154.	250.	360.	0.0125	1.64	0.70
9.0	163.	232.	335.	0.0129	1.43	0.72
9.0	173.	226.	317.	0.0137	1.32	0.72
8.0	191.	232.	344.	0.0191	1.25	0.67
7.0	199.	274.	332.	0.0260	1.38	0.83

H_∞/L_∞	H_b/H_∞	H_b/h_b
Woods Hole		
0.0055	1.60	1.28
0.0072	1.37	0.81
0.0074	1.44	0.57
0.0082	1.66	
0.0083	1.80	
0.0083	1.45	
0.0104	1.31	0.95
0.0110	1.77	1.19
0.0114	1.36	0.74
0.0114	1.28	1.16
0.0115	1.68	0.92
0.0116	1.55	0.98
0.0120	1.90	
0.0120	1.75	
0.0125	1.35	
0.0126	1.00	1.02
0.0130	1.49	
0.0130	1.29	
0.0132	1.36	
0.0135	1.18	0.72
0.0139	1.70	1.08
0.0144	1.30	0.78
0.0161	1.47	
0.0161	1.17	
0.0170	1.00	
0.0170	0.97	
0.0176	1.06	0.90
0.0188	1.47	
0.0188	1.37	
0.0188	1.33	
0.0188	1.28	
0.0188	1.25	
0.0204	1.58	0.94
0.0210	1.55	
0.0211	1.38	
0.0214	1.17	
0.0235	1.50	1.18
0.0284	0.97	1.00